



University of Benghazi

Faculty of Science- Department of Physics

***Dose Estimation From X-ray Exposures During
Conventional Diagnostic Medical Procedures for Paediatric and Adult
Patients In
Some Libyan Hospitals.***

Wafa Nagi Rajab Alorfi

Supervisor: Dr. Nagi .A.Hussein

Co-Supervisor: Dr.Ibrahim Elyaseery

Thesis submitted in partial fulfilment of the requirements of the degree of Master of
Science in Physics.

Spring

International Atomic Energy Agency

Calibration certificate No. LIB/2006/04

The following instruments from *SSDL, Benghazi Radiotherapy and Radiology Center*
Benghazi, Libya

have been calibrated at the IAEA Dosimetry Laboratory:

	Ionization chamber	Electrometer
Model/type:	<i>W-30010</i>	<i>UNIDOS</i>
Serial number:	<i>476</i>	<i>20653</i>
Manufacturer:	<i>PTW Freiburg</i>	<i>PTW Freiburg</i>
Calibration period:	from <i>2006-Jun-19</i>	to <i>2006-Jul-04</i>

Calibration coefficients in terms of absorbed dose to water


The calibrations have been performed following the procedure given in 3A "Ionization Chamber Calibration Procedures at the IAEA Dosimetry Laboratory-Therapy level calibrations". The IAEA reference standard chamber NE-2611 (#132) used to calibrate the instruments had been calibrated at the BIPM in June 2004 for ^{60}Co gamma radiation and x-ray qualities recommended by the CCRI.

Radiation quality	Chamber $N_{D,w}$ [mGy/nC]	Chamber + electrometer $N_{D,w}$ [mGy /scale unit]	\dot{D}_w [mGy/min]
^{60}Co γ -rays	<i>54.2 ± 0.5</i>	<i>54.2 ± 0.5</i>	<i>349</i>

Uncertainties in the calibration coefficients correspond to a coverage factor, $k=2$. The calibration coefficients are established at the reference conditions $T = 20.0$ °C, $P = 101.325$ kPa and R.H. = 50.0 %.

Settings during the calibration (see Appendix for details):

Electrometer settings at calibration:	<i>Mode "Charge", Range "High", HV-Pol.: "-"</i>
Scale unit:	<i>nC</i>
Polarizing Voltage:	<i>400 V</i>
Polarizing Voltage for chamber calibration (alone):	<i>+400 V (coll. electrode positive)</i>


Ken R. Shortt
Head, Dosimetry and Medical
Radiation Physics Section

Date of issue: *2006-07-21*

2012-2013



University of Benghazi

Faculty of Science- Department of Physics

***Dose Estimation From X-ray Exposures During Conventional
Diagnostic Medical Procedures for Paediatric and Adult Patients
In Some Libyan Hospitals.***

Wafa Nagi Rajab Alorfi

Supervisor: Dr. Nagi.A. Hussein

Co-Supervisor: Dr. Ibrahim Elyaseery

Thesis submitted in partial fulfilment of the requirements of the degree of Master of Science in Physics, 3-7-2013 at Department of Physics, Faculty of Science, University of Benghazi.



University of Benghazi

Faculty of Science- Department of Physics

***Dose Estimation From X-ray Exposures During Conventional Diagnostic
Medical Procedures for Paediatric and Adult Patients
In Some Libyan Hospitals.***

Wafa Nagi Rajab Alorfi

Examining committee:

1 -	Supervisor
2-.....	Co- Supervisor.....
2-	Internal Examiner
3-	External Examiner

Head of physics department

.....

Dean of faculty of science

.....

الأقرباء

إليمنلا يمكن للكماتانتو فيحقهما
إلي من لا يمكن للأرقام أن تحصي فضائلهما
إلي والدي العزيزين أدامهما الله لي ❀

إلي من كانوا يضيئون لي الطريق
ويساندوني ويتنازلون عن حقوقهم
لإرضائي والعيـش في هـناء
❀ إخوتي ❀
أحبكم حبا لو مر علي أرض قاحلة
لتفجرت منها ينابيع المحبة

إلي من كانوا ملاذي وملجئي بعد الله
إلي من تذوقت معهم أجمل اللحظات
❀ أصدقائي ❀

إلي من علمونا حروفا من ذهب وكلمات من درر وعبارات من أسمي وأجلي عبارات
في العلم إلي من صاغوا لنا علمهم حروفا ومن فكرهم منارة تنير لنا سير
العلم والنجاح
❀ أساتذتي الكرام ❀
إليكم جميعا أهدي هذا العمل المتواضع

Acknowledgement

As I look back into the past two years, I see precious memories, difficult moments and unforgettable people. People, who had a big impact on my life, people who were very supportive, people whom I feel very lucky to have had around me. People whom I would like to take this opportunity to thank.

I am extraordinarily grateful to the person who guided me throughout the long hard process of the preparation of this thesis; my supervisor Dr. Nagi. A. Hussein.

I thank my co supervisor Dr. Ibrahim Elyaseery for his understanding and support.

I would like to express my gratitude to staff members at Alhawari General Hospital and Benghazi Children Hospital.

Special thanks to each of Mr. Hussein Alfituri and Miss. Maha Algalle for their support and assistance.

Special thanks to each of Dr. Gabriel Shamia and Dr. Abdul Ghaffar Almnafy

I would like to thank the thesis committee members for dedicating their time and effort towards this project.

Last but not least, I don't want to forget all people in the background, especially my parents for their support, encouragement and guidance when I needed them most.

Tables of contents

Page

Chapter 1: Introduction.....	1
Chapter 2: Basics of X-ray production.....	5
2.1 Introduction.....	5
2.2 Production of X-rays	5
2.2.1 Bremsstrahlung X-rays.....	5
2.2.2 Characteristic X-rays.....	6
2.3 The X-ray spectrum.....	7
2.3.1 Continuous X-ray spectrum.....	7
2.3.2The discrete spectrum.....	8
2.4 X-ray beam quantity and quality.....	8
2.4.1 X-ray beam quality.....	9
2.4.2 X-ray beam quantity.....	10
2.4.3 Factors affecting the X-ray beam quantity and quality	10
2.5 X-ray tube	13
2.5.1 General descriptions of the components of X-ray tube	13
2.5.2 Anode and target	14
2.5.2.1 Stationary anode	15
2.5.2.2 Rotating anode	16
2.5.2.3 Target angle	17
2.5.2.4 Focal spot size	17
2.5.2.5 Line focus principle	18
2.5.2.6 Heel effect	18
2.5.3 Tube envelope and housing	19
2.5.4 Cathode assembly	20
2.5.4.1 Filament size	20
2.5.4.2 Electron focusing	21
2.5.4.3 Grid controlled X-ray tubes	21
2.5.5 Filtration	22
2.5.6 Saturation voltage	23
2.5.7 X-ray tube kilovoltage and milliamperes	23
2.5.8 Tube vacuum.....	24
2.6 Rating of X-ray tube.....	24
Chapter 3: Interaction of X-rays with matter.....	26
3.1 Types of X-ray interactions	26
3.1.1 Photoelectric effect	26
3.1.2 Compton effect	28
3.1.3 Pair production	31
3.1.4 Photodisintegration	32

3.1.5 Rayleigh scattering (coherent scatter)	32
3.2 Relative predominance of individual effects	33
3.3 Attenuation and absorption.....	34
3.4 Coefficients	36
3.4.1 Linear attenuation coefficient (μ)	36
3.4.2 Mass attenuation coefficient	38
3.4.3 Energy transfer coefficient (μ_{tr})	40
3.4.4 Energy absorption coefficient (μ_{en})	40
Chapter 4: Diagnostic imaging quantities and parameters	41
4.1 X-ray beam quantities	41
4.2 Quantities that describe deposited energy	43
4.2.1 Kerma (K)	43
4.2.2 Kerma rate(\dot{K})	45
4.2.3 Exposure (X)	45
4.2.4 Exposure rate(\dot{X})	46
4.2.5 Cema (C)	46
4.2.6 Cema rate(\dot{C})	46
4.2.7 Energy imparted.....	47
4.2.8 Absorbed dose (D)	47
4.2.9 Absorbed dose rate (\dot{D})	48
4.2.10 Entrance skin exposure (ESE)	48
4.3 Radiation protection quantities	49
4.3.1 Organ dose (D_T)	49
4.3.2 Equivalent dose (H_T)	49
4.3.3 Effective dose (E)	51
4.4 Entrance surface dose (ESD)	52
4.5 Entrance surface air kerma (ESAK)	52
4.6 Dose area product (DAP)	52
4.7 Integral dose	53
4.8 Surface integral exposure (SIE)	53
4.9 Computed tomography dose index (CTDI)	53
4.10 Dose length product (DLP)	54
4.11 Practical radiation dosimetry	54
4.11.1 Radiation dosimeter	54
4.11.2 Practical thimble chamber	57
4.12 Dose measurements methodology	59
4.13 Backscatter factor	61
Chapter 5: Radiation effects and diagnostic reference levels	62
5.1 Ionizing radiation interactions with tissue	62

5.1.1 Direct and indirect interaction	63
5.2 Classification of biological effects	65
5.2.1 Deterministic effects (non stochastic effects)	65
5.2.2 Stochastic effects	66
5.3 Radiation protection	67
5.3.1 The principles of protection	67
5.4 Quality assurance (QA)	68
5.5 Diagnostic reference level (DRL)	68
5.5.1 Objective of DRLs	69
5.5.2 Applications of DRLs	70
Chapter 6: Materials and methods	71
6.1 Materials	71
6.1.1 X-ray machines	71
6.1.2 Patient data	72
6.2 Method	74
6.3 Dosecal program	76
Chapter 7: Results and discussion.....	80
7.1 Sample distribution according to the type of examination	80
7.2 Descriptive statistics of exposure parameters and patient data for chest and abdomen X-ray examinations	81
7.3 Entrance surface dose (ESD) in mGy and effective dose (ED) in mSv obtained using dosecal software for paediatric patients.....	86
7.4 Comparison of entrance surface dose in the present study with reference doselevels recommended by international bodies and previous studies conducted in other countries.....	91
7.5 Patient diameter(d)	96
7.6 Relation between entrance surface dose (ESD) and equivalent patient diameter (d) for chest (AP, PA, Lat projections), abdomen AP, skull Lat and cervical spine AP X-ray examinations.....	97
7.7 Relation between entrance surface dose (ESD) with age and weight for chest (AP,PA, Lat projections), abdomen AP, skull Lat and cervical spine AP examinations	102
7.8 Relation between entrance surface dose (ESD) with age and weight for chest AP.....	112
7.9 Relation between entrance surface dose (ESD) with age and weight for chest PA.....	116
7.10 Relation between entrance surface dose (ESD) with age and weight for chest Lat.....	120
7.11 Relation between entrance surface dose (ESD) with age and weight for	

abdomen AP.....	122
7.12 Discussionof benghazi children hospital results	125
7.13 Sample distribution according to the type of examination	130
7.14 Descriptive statistics of exposure parameters and weights for adult patients undergoing different X-ray examinations	131
7.15The effective dose in (mSv) against age and weight for adult patients subjected to somecommon X-ray examinations	136
7.16 Discussion of alhawari general hospital results	142
Conclusion.....	145
Recommendations	146
References.....	147
Appendix A: The patient data and dose for Benghazi Children Hospital.....	156
Appendix B: The patient data and dose for Alhawari General Hospital.....	170
Appendix C: Descriptive Statistics.....	174

List of Abbreviations

AAPM	American Association of Physicists in Medicine
AP	Anterior Posterior
ALARA	As low as reasonably achievable
ARPANSA	Australian Radiation Protection and Nuclear Safety Agency
BSF	Backscatter Factor
CTDI	Computed Tomography Dose Index
Cema	Converted Energy Per Unit Mass
CEC	Council of The European Commission
DNA	Deoxyribonucleic acid
DRLs	Diagnostic Reference levels
DAP	Dose Area Product
DLP	Dose Length Product
ESE	Entrance Skin Exposure
ESAK	Entrance Surface Air Kerma
ESD	Entrance Surface Dose
EC	European Commission
HVL	Half Value Layer
IAEA	International Atomic Energy Agency
ICRP	International Commission on Radiological Protection
ICRU	International Commission on Radiation Units and Measurements
ISO	International Standardization Organization
Kerma	Kinetic Energy Released Per Unit Mass
Lat	Lateral
MOSFET	Metal Oxide Semiconductor Field Effect Transistor
NRPB	National Radiological Protection Board
PA	Posterior Anterior
QA	Quality Assurance
SIE	Surface Integral Exposure
TLDs	Thermoluminescence Dosimeters
UNSCEAR	United Nations Scientific Committee on The Effects of Atomic Radiation
WHO	World Health Organization

List of symbols

kV_p	Peak kilovoltage
mAs	Milliamperere \times Second
W_R	Radiation weighting factor
W_T	Tissue weighting factor
m	Linear attenuation coefficient
m_{tr}	Energy transfer coefficient
m_{en}	Energy absorption coefficient
	Photon fluence Φ
f	Photon flux
Ψ	Energy fluence
y	Energy flux
K	Kerma
X	Exposure
C	Cema
D_T	Mean dose for tissue or organ T
H_T	Equivalent dose

Abstract

Medical X-ray examinations play an important role in the diagnosing of many diseases; this benefit of X-ray is usually associated with different kinds of risks. These risks are heightened for paediatric patients, who are more radiosensitive than adults. Therefore, to keep radiation dose to a minimum, one must know the dose associated with each X-ray examination. The objective of this study is to give a quantitative and qualitative assessment of radiation doses during diagnostic X-ray examinations for adult and paediatric patients in two Libyan hospitals (Benghazi Children Hospital and Alhawari General Hospital).

Effective dose, ED, in mSv was calculated for 101 adult patients, while for 146 paediatric patients, in addition to effective dose, the entrance surface dose in mGy was calculated.

The radiographic examinations performed on paediatrics were chest (AP, PA, Lat projections), abdomen AP, cervical spine AP and skull lat, while for adult patients, the following examinations were employed, abdomen AP, chest PA, cervical spine AP, pelvis AP and lumbar spine AP

The most frequent examination performed on paediatric patients was chest AP (85%), while for adult patients; the most frequent examination was chest PA projection (76%).

DoseCal package was used in these calculations. This package is based on a formula that converts exposure parameters into ESD values in mGy. A calibration procedure of the X-ray tube was conducted to obtain a conversion factor that used in the calculation of ESD for paediatric patients. The technique used for calculating ED dose in adult patients was based on dose area product, DAP, in cGy cm^2 which is then converted into ED values.

The mean entrance surface dose obtained for chest AP performed on the age groups, below 1y, (1-5)y and (5-10)y were 0.228, 0.229 and 0.309 mGy respectively.

For chest PA examination, the mean entrance surface dose for the two age groups (5-10)y and (10-15)y were found to be 0.222 and 0.196 mGy respectively.

Entrance surface doses (ESDs) for paediatric patients were found to be as following:

Dose levels resulting from the calculations for paediatric patients showed higher values of ESD when compared with international surveys conducted in many "advanced" and "developing" countries with exception of few less advanced countries in addition to recommended values by international organizations.

The elevation of dose levels for children undergoing conventional X-ray examination in this hospital is unacceptable and must be looked at very carefully. This may be attributed to many factors but was mainly due to the use of improper exposure parameters.

The mean effective dose in the present study for adult patients undergoing chest PA, abdomen AP, pelvis AP, cervical spine AP and lumbar spine AP were found to be 0.025, 0.186, 0.540, 0.040 and 0.501 mSv respectively.

Adult doses results were as following:

The adult dose levels compare well with international surveys from many countries and international organizations. One of the reasons for these values to be within the acceptable levels may be due to use of the newly purchased equipment by this hospital. The other reason was the selection of good exposure parameters in the various examinations.

Body organ dose for paediatric patients during various exposures and for different projections was also calculated. The results show the most and the least effected organs during any particular examination.

Further studies were attempted, for paediatric patients, which try to relate dose to weight, thickness and age of the patients. This was done for many reasons, the important of which is the variations of paediatric patients in size and weight with age group in addition to the sensitivity of children forces us to study all possible parameters. This study is the first of its kind in Libya as far as we know and will serve as the beginning of data base in order to establish Quality Assurance and QC programmes for medical exposure in hospitals.

تقدير الجرعات الإشعاعية من التعرض للأشعة السينية أثناء عملية التشخيص الطبى التقليدى للأطفال والبالغين فى بعض المستشفيات الليبية

الخلاصه

بالرغم من الإستخدام الكثير للأشعة السينية فى المجال الطبى وما تلعبه من دور فى تشخيص الكثير من الأمراض ، إلا أنها من الممكن أن ينجم عنها مخاطر تهدد الحالة الصحية للمرضى الخاضعين لها خصوصا إذا كانوا أطفال. لذلك لا بد من التقيد بالمعايير الدولية بخصوص الجرعة المقرره لكل نوع تشخيص على حدا. الهدف من الدراسة الحالية هو التقدير الكمى والنوعى للجرعات الإشعاعية المستخدمة لغرض تشخيص الأمراض لدى المرضى الأطفال وعددهم 146 والبالغين وعددهم 101 فى مستشفىين رئيسيين بمدينة بنغازى هما مستشفى أطفال بنغازى ومستشفى الهوارى العام.

شملت الفحوصات الإشعاعية التى تم إجرائها للمرضى الأطفالى مستشفى أطفال بنغازى؛ فحص الصدر فى إتجاهات الأمامى خلفى ،خلفى أمامى وجانبي ، فحص البطن الأمامى خلفى، فحص العمود الفقريالعنقي الأمامى خلفى وفحص الجمجمة الجانبي، بينما شملت الفحوصات الإشعاعية التى تم إجرائها للمرضى البالغين؛ فى مستشفى الهوارى العام؛ فحص الصدر الخلفى أمامى، فحص البطن الأمامى خلفى، فحص العمود الفقري العنقي الأمامى خلفى ، فحص الحوض الأمامى خلفى وفحص العمود الفقري القطنى الأمامى الخلفى. النتائج التى تم التوصل إليها أوضحت أن النسبة الأكبر من عينة الأطفال المأخوذة للدراسة (85%) قد خضعت لفحص الصدر أمامى خلفى. فى مقابل فحص الصدر الخلفى أمامى (76%) بالنسبة لعينة البالغين.

لحساب الجرعة المستخدمة للتشخيص، تم إستخدام برنامج (DoseCal). يعتمد هذا البرنامج فى عمله على صيغة رياضية لمتغيرات التعرض للأشعة التى يتم من خلالها حساب الجرعة بالميلليغراى. من الضرورى قبل إستخدام هذا البرنامج لحساب الجرعة للأطفال إجراء عملية معايرة لإنبوب الأشعة السينية.

تعتمد التقنية المستخدمة لحساب الجرعة الفعالة للمرضى الكبار على ما يعرف بحاصل ضرب المساحة المعرضة للأشعة فى الجرعة الممتصة التى يتم من خلالها حساب الجرعة الفعالة. كانت النتائج المتحصل عليها بالنسبة لجرعات المرضى الأطفال السطحية عالية نسبيا عند مقارنتها مع إحصائيات تمت فى دول متقدمة وأخرى فى دول نامية وكذلك المعايير العالمية الموصى بها من قبل المنظمات العالمية.

هذا الأرتفاع في مقدار الجرعة الإشعاعية المطبقة على الأطفال لا يعد مقبولا ومن الحكمة إعادة النظر فيه. يمكن أن يرجع السبب وراء هذه القيم المرتفعة إلى إستخدام بارامترات تعرض غير صحيحة.

كانت النتائج المتحصل عليها بالنسبة للجرعات الفعالة للمرضى البالغين مرضية عند مقارنتها مع المعايير العالمية. يرجع كون النتائج مرضية إلى إستخدام الأجهزة الحديثة وبارامترات التعرض الصحيحة.

كما تم حساب الجرعة لكل عضو من أعضاء المرضى الأطفال وبالتالي تحديد العضو الأكثر تأثرا والعضو الأقل تأثر لكل نوع تشخيص تم إجرائه.

من المعروف ان الأطفال من نفس العمر عادة ما تتباين أحجامهم وأوزانهم وكذلك الحال بالنسبة لعينة الأطفال التي تمت دراستها. كذلك يتباين الأطفال فى مدى تأثرهم بالإشعاع. هناك العديد من الدراسات تجرى لتبيان العلاقة بين وزن وسمك وعمر المريض من جهة والجرعة الإشعاعية من جهة اخرى.

على حد علمنا أن هذه الدراسة كانت الأولى من نوعها فى ليبيا. لذلك نأمل أن يتم إتخاذها كقاعدة بيانات لدراسات مستقبلية لغرض تأسيس برامج مثلابرامضمان الجودة (Quality assurance) التي بدورها الفعال ممكن أن تحد من الأخطاء والرفع من مستوى الخدمات الطبية فى المستشفيات الليبية.

Chapter 1

INTRODUCTION

After the discovery of the X-ray in 1895 by W.C. Roentgen, the use of X-ray in medicine has increased fast. In diagnostic radiology, X-rays create images that help to diagnose the patient's medical condition (Seeram and Brennan, 2006) and are also useful in detecting some disease processes in soft tissue. Examples of such X-ray examinations are the common chest X-ray examinations, which can be used to identify lung cancer or pulmonary edema and abdominal X-ray examinations, which can detect (blockage of the intestine), free air (from visceral perforations) and free gall stones or kidney stones. Fluoroscopy is an image technique commonly used by physicians to obtain real time moving images of the internal structures of a patient through the use of a fluoroscope. X-ray can be used to detect any abnormalities like broken bones, cancerous growth and tooth decay (Capps, 2006). However, in light of all the benefits of this discovery, it is to be noted that a radiation excess dose of X-rays is harmful to human beings. X-rays are ionizing radiation, which can potentially damage cells within the body. High radiation doses tend to kill cells, while low radiation doses tend to damage or alter the genetic code of deoxyribonucleic acid (DNA) of irradiated cells (Andreassi, 2004). Radiation can cause cancer and there are no dose limits for patients receiving medical exposure as part of their treatment or diagnosis, because the exposure must be justified by a net benefit to the patient and hence the clinical necessity supersedes any dose limitation. Energy from ionizing radiation breaks chemical bonds, releasing free radicals and ions that can damage DNA and proteins, short term radiation damage includes burns and hair loss. A long term effect of radiation injury includes cancer induction and cataract formation (Furlow, 2004). The biological effects of radiation can be divided into two categories: stochastic effects and deterministic effects. Stochastic effects refer to effects whose probability increases with increasing dose and for which there is no threshold dose and tissue reactions are those in which the severity of the effect, rather than the probability, increases with increasing dose and for which there is a threshold dose (Seeram and Brennan, 2006).

The risk for paediatric patients of developing long term biological effects following exposure to ionizing radiation is higher than that of adults because their cells, tissues and organs have a higher radiosensitivity and they have a longer time to live, thereby enabling the effects to manifest. In addition, the chances of repeat examinations are higher with paediatric patients due to improper immobilization and less effective communication during the examinations. The European commission (EC) states “ that the radiation exposure in the first 10 years of life is estimated to have a risk about 4 times greater than exposures incurred at 30-40 years of age for some detrimental effects” (Brindhabanand Eze,2006). It is therefore important that radiation dose to children arising from diagnostic medical exposure is minimized. The Commission of European Communities (CEC) has recognized the need for the special treatment of children and has published guidelines suggesting examples of good radiographic practice and present useful image criteria with the aim of producing high quality images at the lowest possible dose to the patient (EC, 1996). Good radiographic technique includes the use of optimum kVp. Lower kilovoltages should be avoided in paediatric chest examinations. The CEC recommends the use of 60-80 kVp for children between 0-15 years of age. Reduction in patient doses can be achieved through changes in tube potential and the advantage lies in absence of cost implications (Martin et al, 1993). Using a higher tube potential has shown a 16-36% reduction in entrance surface doses in neonatal radiography without any impairment of the diagnostic image quality (Wraith et al, 1995). More recently, new technologies and modern equipments have been included as part of diagnostic resources of radiology departments. However the necessary condition and control for the use of such devices has not been taken into account in most installation accordingly. In most countries, several initiatives have been implemented in order to regulate the use of the ionizing radiation with the best image quality lowest doses and reduce the cost to the department; the most efficient initiative is the implementation of QAP. The World Health Organization (WHO) has defined quality assurance in X-ray medical diagnosis as " an organized effort by the staff operating a facility to insure that the diagnostic images produce by the facilities are of sufficient high quality so that they consistently provide adequate diagnostic information at the lowest possible cost and with the least possible exposure of the patient to radiation. Quality assurance (QA) is a program used by

management to maintain optimal diagnostic image quality with minimum hazard and suffering to patients. The program includes periodic quality control tests, preventive maintenance procedures, administrative methods and training. It also includes continuous assessment of the efficacy of the imaging service and the means to initiate corrective action, the primary goal of radiology quality assurance is to insure the consistent provision of prompt and accurate diagnosis of patients. A QA program having the following three objectives will adequately meet this goal

- To maintain the quality of diagnostic images.
- To minimize the radiation exposure to patient and staff.
- To be cost effective (Mohamadain, 2004).

According to the international organization for standardization (ISO), QA is defined as all those planned and systematic actions necessary to provide adequate confidence that a structure, system or component will perform satisfactorily in service (ISO, 1980). DRLs are an important method of minimizing radiation dose and radiation dose variation at a minimal cost to the radiology department (Seeram and Brennan, 2006). DRLs or reference levels have been proposed by the international commission on radiological protection (ICRP). Radiation protection agencies in many countries including Australia, UK, USA and New Zealand have set reference dose levels for commonly performed diagnostic X-ray examinations. These reference levels of entrance skin dose (ESD) have been arrived at based on third quartiles of distributions of dosimetric data from national wide surveys of 5 years old patients. These values are used as guidance levels regardless of the age of paediatric patients. However this may not be suitable for newborn babies and 1 year old children whose average body weight is approximately 50% of an average 5 years old child and would lead to overexposure of infants (Brindhavan and Eze, 2006). The increasing knowledge of the hazards of ionizing radiation has led to the need for radiation dose assessment of patients during diagnostic X-ray examinations (Osibote and Azevedo, 2008). Patient radiation dosimetry is an important deal in both diagnostic and therapeutic departments. The aim is to emphasize that precautions should be taken to limit radiation doses to paediatric patient, worker and co-patient as well as to members of the public (Bushra et al, 2010). The aim of this study to investigate radiation doses for commonly performed paediatric and adult X-ray examinations in two public hospit-

als in Benghazi, Libya in order to establish guidance dose levels. A dose assessment must be done to avoid unnecessary radiation during X-ray imaging or guidance must be given on dose levels. The radiation protection system for patients subjected to medical exposures in diagnostic radiology is governed by principles of justification and optimization, including the consideration of diagnostic reference levels (DRLs). Therefore, a diagnostic radiological procedure is justified if the benefits to the individual patient from the medical diagnostic obtained with the radiological image balance the individual detriment the exposure may cause. Once a medical exposure has been justified, the principle of optimization is applied that is, the radiological examination must be carried out with equipment and exposure parameters that ensure doses to patients as low as reasonably practicable, consistent with the intended diagnostic purpose (Freitas and Yoshimura, 2009).

- **Thesis outline**

This thesis is concerned about the estimation of paediatric and adult patients' doses for some diagnostic X-ray examinations. Accordingly, it is divided into the following chapters:

The second chapter includes the X-ray production mechanism, the factors affecting the X-ray spectrum emitted by an X-ray tube and X-ray tube components.

The third chapter includes the interactions of X-rays with matter.

The fourth chapter includes the radiation quantities, methods of measurement and calculation of radiation dose.

The fifth chapter includes the effects of X-rays on human beings, principles of radiation protection and diagnostic reference levels established by International Commission on Radiological Protection (ICRP) and its applications.

The sixth chapter includes the materials, methods including dose cal programme used for estimation of radiation dose.

The seventh chapter includes the results and discussion of results obtained from Benghazi Children Hospital and Alhawari General Hospital.

Chapter 2

BASICS OF X-RAY PRODUCTION

2.1. Introduction

X-rays were discovered by Roentgen in 1895 while studying cathode rays (stream of electrons) in a gas discharge tube. He observed that another type of radiation was produced (presumably by the interaction of electrons with the glass walls of the tube) that could be detected outside the tube. This radiation could penetrate opaque substances, produce fluorescence, blacken a photographic plate, and ionize a gas. He named the new radiation X-rays (Khan, 2003).

2.2. Production of X-Rays

Projectile electrons produced by thermionic emission in the cathode are accelerated by the high voltage to the anode where either bremsstrahlung or characteristic radiation is produced (Fosbinder and Orth, 2011).

2.2.1. Bremsstrahlung X-rays

Bremsstrahlung X-rays result from coulomb interactions between the incident electrons and the nuclei of the target material. During the coulomb interaction between the incident electron and the nucleus, the incident electron is decelerated and loses part of its kinetic energy in the form of bremsstrahlung photons (radiative loss) as shown in Fig. (2.1) (Podgorsak, 2005). High speed electrons may pass by the nucleus at various distances from it. The closer an electron approaches the nucleus, the greater its deceleration due to the stronger pull of the nucleus, thus the more energy will be lost and the higher the energy keV of the emitted X-ray (Carroll, 2003).

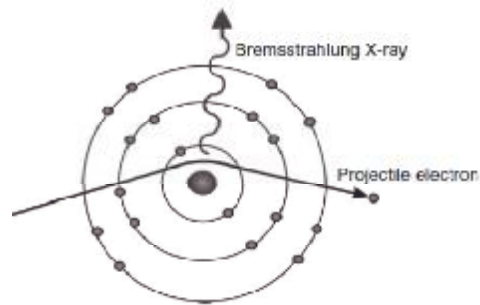


Fig.(2.1): An incoming electron changing direction, due to the atomic nucleus and giving off a bremsstrahlung X-ray (Cherry and Duxbury, 2009).

2.2.2.Characteristic X-rays

Characteristic X-rays result from coulomb interactions between the incident electrons and atomic orbital electrons of the target material (collision loss) as shown in Fig.(2.2). In a given coulomb interaction between the incident electron and an orbital electron, the orbital electron is ejected from its shell and an electron from a higher level shell fills the resulting orbital vacancy. The energy difference between the two shells may either be emitted from the atom in the form of a characteristic photon (characteristic X-ray) or transferred to an orbital electron that is ejected from the atom as an Auger electron (Podgorsak, 2005).

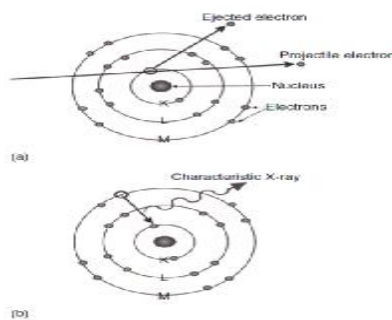


Fig.(2.2): (a) An atom being ionized when a K-shell electron is ejected by an energetic projectile electron. (b) The vacancy in the K-shell, resulting from ionization of the atom, is filled by an M-shell electron. A characteristic X-ray is given off (Cherry and Duxbury, 2009).

2.3. The X-Ray Spectrum

X-rays generated by diagnostic machines contain a spectrum of photon energies that range up to a maximum determined by the voltage applied across the X-ray tube gap. The peak tube voltage (kVp) determines the maximum photon energy (expressed in kilo electron volts (keV)) (Hirshfeld et al, 2004). There are two basic types of spectra: continuous spectrum and discrete spectrum.

2.3.1. Continuous X-ray spectrum

The emission spectrum is called a continuous emission spectrum. The energies of the photons emitted may range from zero to a maximum value. The general shape of the continuous spectrum is the same for all X-ray machines. The maximum energy that an X-ray is numerically equal to the kVp across the tube as shown in Fig. (2.3 b). The greatest number of X-ray photons is emitted with energy approximately one-third of the maximum photon energy (Nave, 2009). The continuous X-ray spectrum can be expressed in terms of wavelength of X-ray photon instead of energy as shown in Fig. (2.3 a). The continuous X-ray spectrum is also called white or bremsstrahlung spectrum.

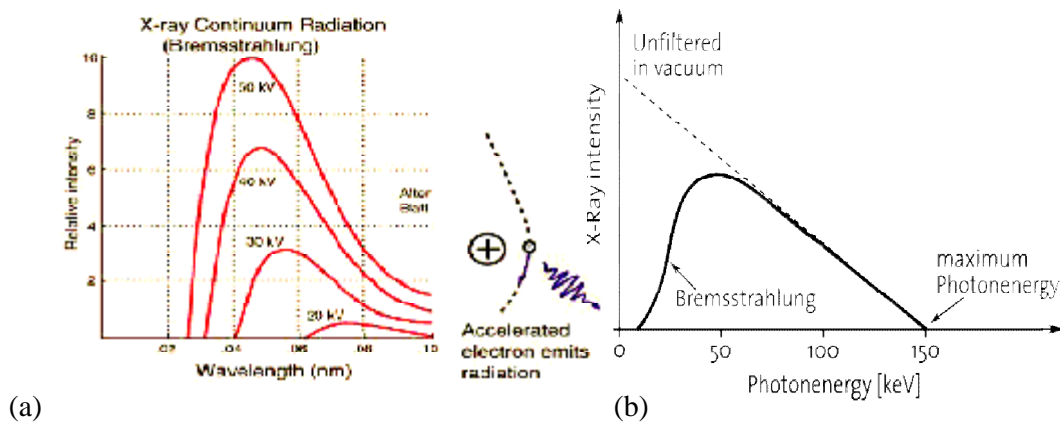


Fig.(2.3): The continuous spectrum (Nave; 2009, Cattin; 2011).

2.3.2. The discrete spectrum

Characteristic X-rays are emitted from heavy elements when their electrons make transitions between the lower atomic energy levels. The characteristic X-rays emission which is shown as two sharp peaks in Fig.(2.4) occur when vacancies are produced in the $n=1$ or K-shell of the atom and electrons drop down from above to fill the gap. The X-rays produced by transitions from the $n=2$ to $n=1$ levels are called K_{α} X-rays and those for the $n=3$ transition are called K_{β} X-rays (Nave, 2009). This spectrum is also known as line spectrum or characteristic spectrum which depends on target material therefore it determines type of target material.

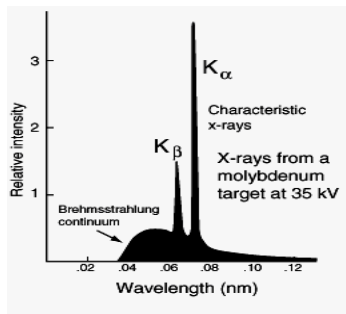


Fig.(2.4): Discrete spectrum (Nave, 2009).

2.4. X-Ray Beam Quantity and Quality

X-ray beam can be described by its quality and its quantity as shown in Fig.(2.5).

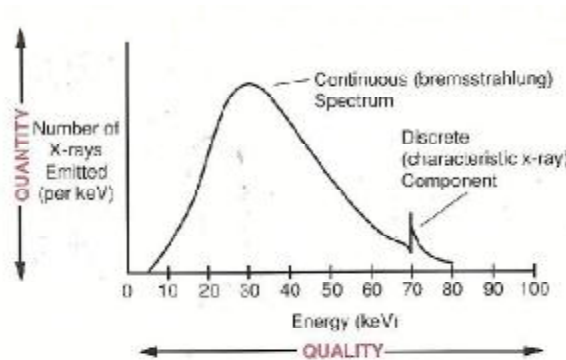


Fig.(2.5): The general form and shape of the discrete and continuous X-ray spectra (Thompson et al, 1994).

2.4.1.X-ray beam quality

Quality is an indication of X-ray beam's penetrating ability. For a given material the penetrating ability of an X-ray beam depends on the energy of the photons. For X-ray beams that contain a spectrum of photon energies, the penetration is different for each energy. The overall penetration generally corresponds to the penetration of a photon energy between the minimum and maximum energies of the spectrum (Sprawls, 1995). The beam quality is determined by half value layer (HVL) (Panichello, 1998) and is the factor that describes the penetrating ability of specific radiation and the penetration through specific objects. HVL is the thickness of material penetrated by one half of the radiation and is expressed in units of distance (mm or cm) as shown in Fig.(2.6). Increasing the penetrating ability of a radiation increases its HVL.

The HVL is given by:

$$\text{HVL} = \frac{0.693}{m} \tag{2.1}$$

Where m represents linear attenuation coefficient of that material. The equation (2.1) shows that HVL is inversely proportional to the attenuation coefficient. The number, 0.693 is the exponent value that gives a penetration of 0.5 (Sprawls, 1995).

$$(e^{-0.693} = 0.5) \tag{2.2}$$

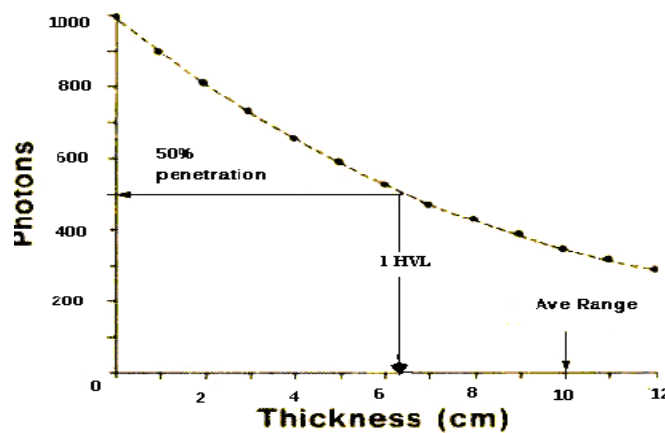


Fig.(2.6): Penetration range of individual photons (Sprawls, 1995).

2.4.2.X-ray beam quantity

Beam quantity describes the amount of X-ray photons in the X-ray beam and therefore it is related to beam intensity(Fosbinder and Orth,2011).

2.4.3.Factors affecting the X-ray beam quantity and quality

There are many factors affecting the X-ray beam quantity and quality such as X-ray tube current,tube voltage,target material and beam filtration.

- **The effect of tube current on the X-ray beam**

Changing the current of the X-ray tube (the milliamps or mA) changes the number of electrons hitting the target.If you increase the mA by a factor of 2 then the number of X-ray photons emitted at each energy will also increase by a factor of 2.The shape of the output spectrum does not change,only the area under the curve.This is illustrated in Fig.(2.7), which shows what happens when the mA are doubled and all other factors are kept constant.The intensity of the X-rays produced (I) is proportional to tube current (mA).Changing the current of the X-ray tube does not affect the quality of the beam,as the energy spread and hence effective energy stays the same (Cherry and Duxbury,2009). The tube current has no effect on characteristic spectrum.

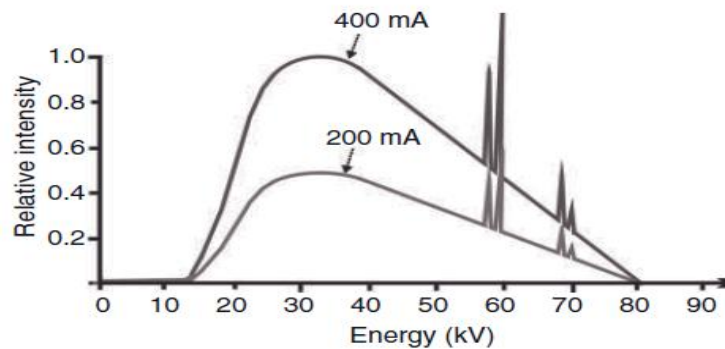


Fig.(2.7):The effect on the tube spectrum when the mA has been halved (Cherry and Duxbury,2009).

- **The effect of tube voltage on the X-ray beam**

Changing the tube voltage (kVp) across the tube increases the kinetic energy of the electrons that reach the target. This means that the amount of bremsstrahlung produced increases, as well as the average energy and the maximum energy of the X-rays produced. Fig.(2.8) shows two spectra, one with a peak tube voltage (kVp) of 70kV and another with 80 kV with other factors kept constant. The output intensity increases by a factor proportional to the kVp^2 as shown by equation:

$$\text{Intensity (I)} \propto (kVp)^2 \times mA \quad 2.3$$

The quality of the beam has also increased, because the effective energy of the beam has increased (Cherry and Duxbury, 2009).

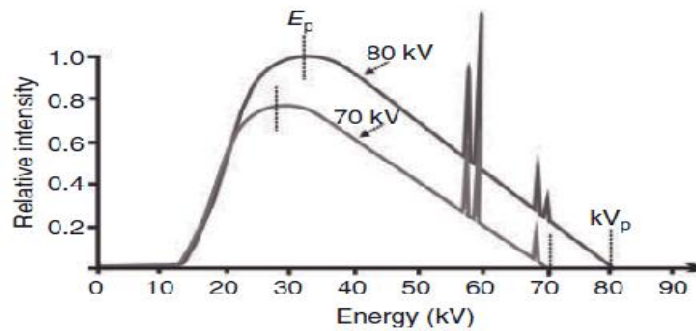


Fig.(2.8):The effect on the tube spectrum when the kV has been reduced from 80kV to 70kV (Cherry and Duxbury, 2009).

- **The effect of the target material on the X-ray beam**

The atomic number of the target material has an effect on the X-ray beam. The higher the atomic number of the target material the more positive the nucleus of the target atom and so the more it attracts the electrons from the filament which pass close to it. Thus the production of X-ray by the bremsstrahlung process is more efficient and the intensity of the beam is increased. The maximum and the minimum photon energies in the beam are not affected by the target material. The target material also affects the characteristic radiation produced as shown in Fig.(2.9). The energies of the characteristic radiations from tungsten and a n



Fig.(2.9): The effect of the target material on the X-ray spectrum (Thompson et al, 1994).

Table (2.1) Comparison of characteristic radiation energies produced from a tungsten target and molybdenum target (Graham, 1996).

	Energy of K α characteristic radiation (keV)	Energy of L α characteristic radiation (keV)
Tungsten	59.32	8.39
Molybdenum	17.48	2.22

- **The effect of filtration on the X-ray beam**

Applying a filter over the exit window will alter the number of X-rays in the useful beam and also their energy. A filter such as aluminum will filter out more of the lower energy X-rays because these are attenuated more easily by the metal, whereas the higher energy X-rays will pass through. The beam coming out of the tube will always have some effect of filtering, because the exit window and any inherent filtration will attenuate some low energy photons. Fig.(2.10) shows the effect of adding filtration into the exit beam. The highest energy of the spectrum (the kVp) stays the same, as the maximum energy of the X-rays coming out of the tube has not changed and some of these will always pass through all filtering unattenuated. The effective energy shifts to a higher kilovoltage as the number of lower energy X-rays has decreased. Filtration is used in X-ray tubes to reduce the patient dose, because lower energy X-rays will always be absorbed by the patient without giving any useful information to the medical image produced (Cherry and Duxbury, 2009).

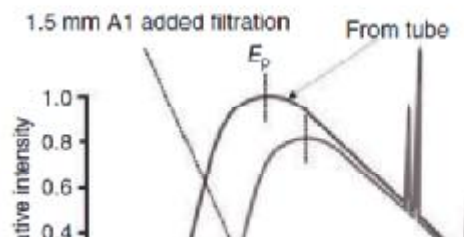


Fig.(2.10): The effect on the tube spectrum when filtration has been added to the exit beam(Cherry and Duxbury, 2009).

2.5.X-Ray Tube

An X-ray tube is an energy converter.It receives electrical energy and converts it into two other forms: X-radiation and heat.The heat is an undesirable byproduct.X-ray tubes are designed and constructed to maximize X-ray production and to dissipate heat as rapidly as possible(Sprawls,1995).

2.5.1. General descriptions of the components of X-ray tube

A simplified diagram of an X-ray tube Fig.(2.11) illustrates the minimum components. A high voltage is applied between two electrodes (the cathode and the anode) in an evacuated envelope.The cathode is negatively charged and contains a filament which is the source of electrons.The electrons are released when the filament is heated with an electric current.The anode is positively charged and is the target of electrons.As electrons from the cathode travel to the anode,they are accelerated by the electrical potential difference between these electrodes and attain kinetic energy.The kinetic energy gained by an electron is proportional to the potential difference between the cathode and the anode (Bushberg et al, 2001).When energetic electrons collide with the anode target, they lose their kinetic energies in the form of X-ray photons and heat which heats up anode and raises the temperature of anode and target.

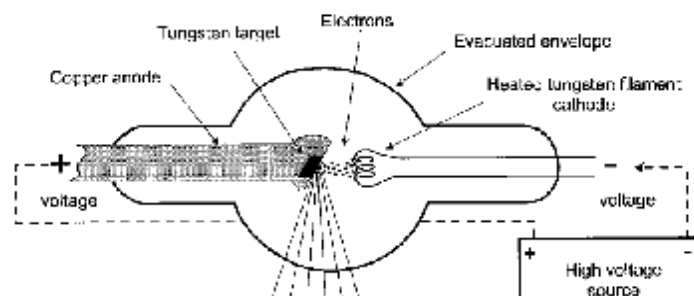


Fig.(2.11):Minimum requirements for X-ray production include a source and target of electrons, an evacuated envelope, and connection of the electrodes to a high voltage source (Bushberg et al, 2001).

A medical X-ray tubes target is usually tungsten (95%) or more the crack-resistance alloy of tungsten rhenium (5%). Tungsten is chosen as the target material because it satisfies the requirement of the anode material for the production of X-rays. It has a high atomic number 74, which makes it more efficient for the production of X-rays. It has a high melting point; it is able to withstand the high temperature produced. Tungsten melts at 3370°C. Tungsten is a good material for the absorption of heat and for the rapid dissipation away from the target area (Curry et al, 1990).

2.5.2. Anode and target

The anode and target are the components in which the X-radiation is produced. Anode is a relatively large piece of metal that connects to the positive side of the electrical circuit. The target is made of a metal located on the anode. The target and anode have two primary functions (Sprawls, 1995):

- Convert electronic energy into X-radiation.
- Dissipate the heat created in the process.

The anode and target materials used should satisfy the following requirements:

- High conversion efficiency for electrons into X-rays. High atomic number Z materials are favoured since the X-ray intensity is proportional to Z .
- High conductivity so that the heat is removed rapidly.
- High melting point so that the large amount of heat released causes minimal damage to the anode.

- Low vapour pressure, even at very high temperature, so that atoms are not boiled off from the anode.
- Suitable mechanical properties for anode construction (Dendy and Heaton, 1999).

The anodes (positive electrodes) of X-ray tubes are of two types, rotating and stationary.

2.5.2.1. Stationary anode

The anode target of a stationary anode X-ray tube consists of a small plate of tungsten, 2- or 3 mm thick that is embedded in a large mass of copper. The tungsten plate is square or rectangular in shape, with each dimension usually being greater than 1cm as shown in Fig.(2.12)(Curry et al, 1990).

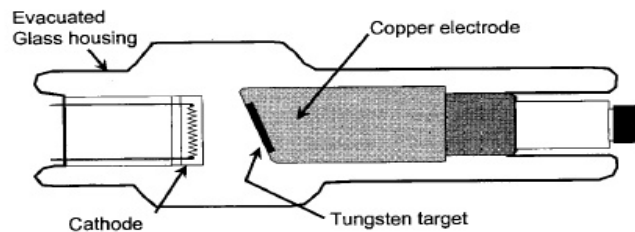


Fig.(2.12):The anode of a fixed anode X-ray tube consists of a tungsten insert mounted in a copper block. Heat is removed from the tungsten target by conduction into the copper block (Bushberg et al, 2001).

In a stationary anode the target area is pure tungsten (W) ($Z=74$, melting point 3370°C) because it satisfies the requirements of the anode material mentioned above and its ability to be shaped into many forms (Dendy and Heaton, 1999).

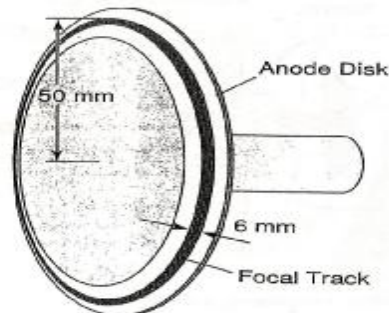
2.5.2.2. Rotating anode

Rotating anodes have a high rate at which energy deposited in the small target of an X-ray tube heats the target to a very high temperature. Rotating anodes increase the area of tungsten that absorbs energy from impinging electrons, reducing the temperature attained by the anodes. Rotating anodes are also composed of mixture of tungsten with other elements (Hendee and Ritenour, 1992).

The anode disc is connected to a motor shank which is part of the motor. When the motor is switched on, the shank spins at the same time that the filament is being heated. By spinning the anode disc, the target surface struck by the electron beam is constantly changing. The heat is distributed across a larger surface area and the anode is less likely to melt (Carroll, 2003).

Originally rotating anodes were made of pure tungsten. However, at the high temperatures generated in the rotating anode, deep cracks developed at the point of impact of the electrons. The addition of 5-10% rhenium (Rh) ($Z=75$, melting point 3170°C) greatly reduced the cracking by increasing the ductility of tungsten at the high temperature (Dendy and Heaton, 1999).

The example of the rotating anode with a larger target area can be illustrated with a simple calculation. Stationary anode, with a focal spot of 6 mm high and 1.5 mm wide has an area of 9 mm^2 . A 100 mm diameter rotating anode, with a focal track of 6 mm wide and $2\pi \cdot 50\text{ mm} = 314\text{ mm}$ long has an area of 1900 mm^2 as shown in Fig.(2.13). The area of the rotating anode is about 200 times larger than the area of the stationary tube for electrons to irradiate, with no apparent increase in the focal spot (Wolbarst, 1993).



$$\text{Area} = (6\text{ mm}) (2\pi \cdot 50\text{ mm}) = 1900\text{ mm}^2$$

Fig.(2.13): Rotating anode disk (Wolbarst, 1993).

2.5.2.3. Target angle

The anode surface of a diagnostic X-ray tube and the stream of electrons from the cathode are not perpendicular to one another. The anode surface is canted by the anode angle. The target angle is typically 10° to 20° , that is, the anode is tilted 10° to 20° away from facing the stream of electrons head-on. When high velocity electrons are incident on a target, the useful bremsstrahlung X-rays are emitted predominantly in the direction perpendicular to the electron stream and out of the target. (X-ray photons starting off in

the opposite direction are fully absorbed by the anode).The angular dependency of bremsstrahlung production is an important factor in the design of the anode.A thick target aligned perpendicularly to the electron flow would absorb most of the photons created in it.With a target that is overly canted, on the other hand,the focal spot would be too large.The target angle should be close to that which gives rise to the greatest usable X-ray beam intensity (Wolbarst, 1993).

2.5.2.4.Focal spot size

The area where the electron current hits the target is known as the focal spot.The smaller the focal spot,the greater the resolution of the image produced with the tube. However,with a small focal spot the amount of heat transferred to the target by the electrons becomes concentrated in a small area.If the heat from the target cannot be dissipated fast enough the target may become damaged and crack, causing the tube to fail.Apart from using a rotating anode a good way to reduce the focal spot size is to utilize the angle of the anode.The actual focal spot size is the area of the target that interacts with the electron beam.The angle of the anode means that the X-ray beam exiting the tube is much smaller than this area.This is called the line focus principle and is illustrated in Fig.(2.14)(Cherry and Duxbury, 2009).

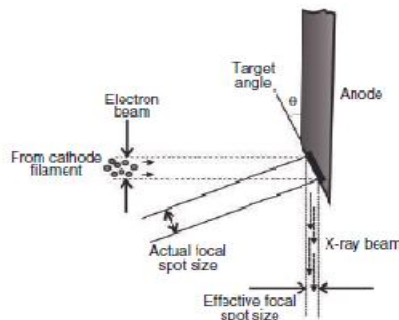


Fig.(2.14): The effective focal spot size of an X-ray tube (Cherry and Duxbury, 2009).

2.5.2.5.Line focus principle

Two approaches are used to provide a small focal spot and take advantage of the need for a large impact area to allow greater heat loading: the line focus principle and the rotating anode. X-rays emerging from the tube can be made to appear to emanate from a small area if the anode is constructed with an angle perpendicular to the incident beam. The angles are shown in Fig.(2.15), range from 10° to 20° . This construction is called the line focus principle, which causes the emitted X-rays to project an apparent focal spot that is considerably smaller than that of the actual area being bombarded. The size of the projected focal spot is directly related to the sine of the angle of the anode. Focal spot size is expressed in terms of the apparent or projected focal spot, and the sizes are typically 0.3, 0.6, 1.0, and 1.2 mm (Martin, 2006).

2.5.2.6.Heel effect

Electrons interact with target atoms at various depths into the target. The X-rays that constitute the useful beam are emitted from depth in the target toward the anode side and must transverse a greater thickness of target material than the X-rays emitted in the cathode direction of the target. The intensity of X-rays emitted through the heel of the target is reduced because they have a longer path through the target to escape and there is an increase in absorption of those rays as shown in Fig.(2.15). This is called the heel effect. Generally the smaller the anode angle, the larger the heel effect (Bushong, 1997).

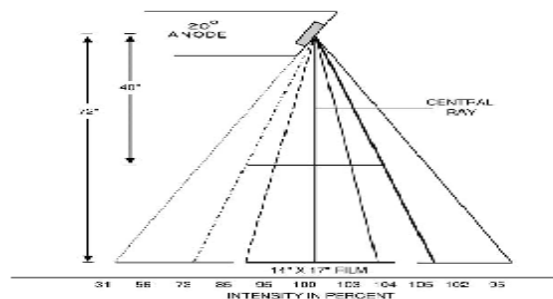


Fig.(2.15): Reduction in X-ray intensity due to the heel effect (Martin, 2006).

The heel effect can be used to advantage for radiographing body parts of different thicknesses by placing the thicker parts toward the cathode. For example, an anteroposterior (AP) film of the thoracic spine should be made such that the upper thoracic spine (i.e., thin side) is below the anode where the relative intensity is lower so that the thicker portion will receive the greater intensity (Martin, 2006).

2.5.3. Tube envelope and housing

The envelope is generally of thick walled glass and is constructed under very clean conditions to a high precision to provide adequate insulation between cathode and anode. It provides a vacuum seal to the metallic components that protrude through it. At the manufacturing stage, great care was taken to achieve a very high level of vacuum before the tube is finally sealed. If the residual gas molecules are bombarded by electrons, the electrons may be scattered and strike the walls of the glass envelope, thereby X-ray tube will have ceramic insulation between the tube and the anode and cathode connections. The presence of atoms or molecules of gas or vapour in the vacuum will have deleterious effects on the performance of the X-ray tube.

The tube housing is used to:

- Provides an X-ray window-which filters out some low energy X-rays.
- Contains the anode rotation power source.
- Provides high voltage terminals.
- Insulates the high voltage.
- Allows precise mounting of the X-ray tube envelope
- Contains the cooling oil (Dendy and Heaton, 1987; 1999).

2.5.4. Cathode assembly

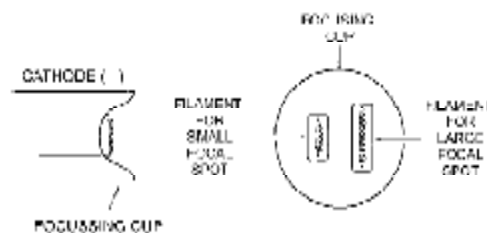


Fig.(2.16): The cathode assembly of a dual-focus tube (Wolbarst, 1993).

The basic function of the cathode is to expel the electrons from the electrical circuit and focus them into a well-defined beam aimed at the anode. The typical cathode consists of a small coil of wire (a filament) recessed within a cup-shaped region (Sprawls, 1995). The cathode assembly consists of one or more filaments in a focusing cup as shown in Fig.(2.16). The small filament is used for high resolution imaging and the larger filament is used when higher intensities are needed. It spreads the heat out over a larger focal region on the anode (Wolbarst, 1993). When the current flowing through the filament is sufficiently high, about four amperes and above, the outer-shell electrons of the filament atoms are boiled off and ejected from the filament. This is called thermionic emission. Filaments are made of tungsten. Tungsten provides higher thermionic emission than other metals because of its high melting point compared with 1500°C or less for all other metals (Bushong, 1997).

2.5.4.1. Filament size

The filament must be large enough to give a practical electron density but not too large, since this will cause focusing problems. The controlling factors are maximum operating filament temperature and filament size. In practice filament current is not switched on and off after each exposure but is kept on standby mode (about 5 mA) and increased to operating current (4.5 to 5.5 A) for exposures. When an exposure is made, a preparation switch is first depressed which starts the anode rotating and increases the filament temperature from standby mode (Dowsett et al, 1998).

2.5.4.2. Electron focusing

During the X-ray exposure, the anode of the X-ray is positively charged and the cathode is negatively charged. As a result of this, the electron space charge is emitted from the negative cathode and attracted to the positive anode. The situation which would arise if both the cathode and anode were flat plates is shown on Fig.(2.17).

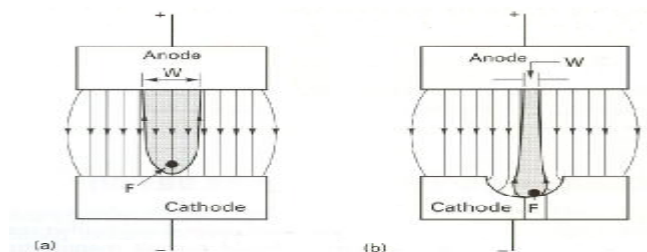


Fig.(2.17): Simplified explanation of the focusing of electrons in the X-ray tube (Graham, 1996).

Fig.(2.17 a) shows the result of no focusing cup on the cathode and in Fig.(2.17 b) the concave focusing cup directs the electrons from the thermionic emitter F towards the central axis, so that they strike a smaller area (W) on the anode. The electric force field consists of parallel lines starting at the anode and finishing at the cathode. Electrons are emitted from the filament, F , and are attracted to the positive anode and the electrons repel each other so the plume of electrons will increase in size as it travels across the X-ray tube. The area W on the anode represents an unacceptably large focal area as this would produce a large geometric bluntness on the resulting radiograph. To overcome this problem, a focusing cup is used as shown in Fig.(2.17 b). The thermionic electrons from F now experience two forces, the one towards the central axis of the beam is greater than the force of electrostatic repulsion between the electrons and the plume of electrons is focused on to a small area of the anode W in Fig.(2.17 b) (Graham, 1996).

2.5.4.3. Grid-controlled X-ray tubes

Conventional X-ray tubes contain two electrodes (anode and cathode). The switches used to initiate and to stop an exposure with these tubes must be able to withstand the large changes in voltage applied between the cathode and anode. A grid-controlled X-ray tube contains its own "switch" which allows the X-ray tube to be turned on and off rapidly. The third electrode is the focusing cup that surrounds the filament. In conventional X-ray tubes a focusing cup is electrically connected to the filament. This focusing cup helps to focus the electrons on the target (Curry et al, 1990).

2.5.5. Filtration

When a radiograph is taken, the lower energy photons in the X-ray beam are mainly absorbed by and deposit dose in the patient. Only a small fraction, if any, reaches the film and contributes to the image. The object of filtration is to remove a large proportion of

the lower energy photons before they reach the skin. This reduces the dose received by the patient while hardly affecting the radiation reaching the film, and so the resulting image. This dose reduction is achieved by interposing between the X-ray tube and patient a uniform flat sheet of metal, usually aluminum, and called the added or additional filtration. The X-ray photons produced in the target are initially filtered within the target itself, because they may be generated below its surface, and then by the window of the tube housing, the insulating oil and the glass insert. The combined effect of these disparate components is expressed as an equivalent thickness of aluminum, typically 1mm Al, and is called the inherent filtration (Allisy and Williams, 2007). Another type of filters called wedge filters which are used in diagnostic radiology to adjust for variations in patient thickness, thus achieving a beam that promotes more uniform film density after it exits the patient. The effect of a wedge filter to compensate for differences in patient thickness is shown in Fig.(2.18). Less radiation is absorbed by the thinner part of the filter so more is available to penetrate the thicker part of the patient (Martin, 2006).

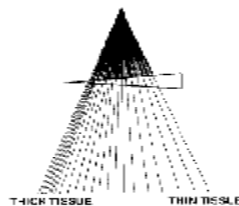


Fig.(2.18): Use of a wedge filter to shape an X-ray beam for radiography of nonuniform anatomy as may be encountered in a thoracic spine examination(Martin, 2006).

2.5.6.Saturation voltage

When the filament of an X-ray tube is heated, a space charge is produced. When a potential difference is applied between the cathode and anode, electrons flow from the filament to the anode to produce the tube current. If the potential difference applied across the tube is insufficient to cause almost all electrons to be pulled away from the filament the instant they are emitted, a residual space charge will exist about the filament. The residual space charge acts to limit the number of electrons available and thus it limits the current flowing in the X-ray tube.

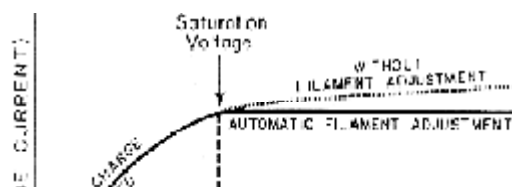


Fig.(2.19): Saturation voltage (Curry et al, 1990).

From Fig.(2.19), up to about 40 kVp, there is an increase in kilovoltage that produces a significant increase in X-ray tube current even though filament heating remains the same. Above 40 kVp (saturation voltage), further increases in kilovoltage produces very little change in tube current and space charge has no influence on current flowing in the X-ray tube. In this region the current is determined by the number of electrons made available by the heated filament and is said to be emission-limited or temperature-limited (Curry et al, 1990).

2.5.7. X-ray tube kilovoltage and milliamperage

Two sources of electrical energy are required and are derived from the alternating current (AC) mains by means of transformers. Fig.(2.20) shows:

- The filament heating voltage (about 10 V) and current (about 10 A).
- The accelerating voltage between the anode and cathode. This drives the current of electrons flowing between the anode and cathode (tube current or mA).

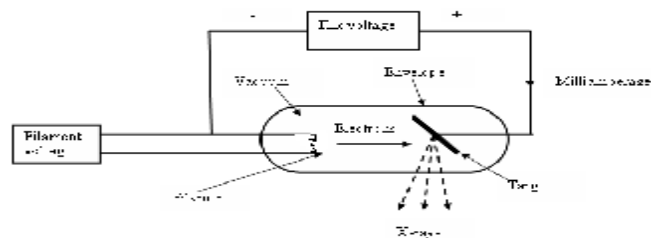


Fig.(2.20): An X-ray tube and its power supply (Farr and Allisy, 1997).

The mA is controlled by varying the filament temperature. A small increase in filament temperature, voltage or current produces a large increase in tube current (Farr and Allisy, 1997).

2.5.8. Tube vacuum

To prevent collision between molecules of air and electrons accelerated between the filament and target, X-ray tubes are evacuated to a pressure of less than 10^{-5} mm Hg. Removal of air reduces deterioration of the hot filament by oxidation. The method of evacuation includes “out gassing” procedures to remove gas occluded in components of the X-ray tube (Hendee and Ritenour, 1992).

2.6. Rating of X-ray Tube

- Heat unit

The heat unit is defined as the product of current (mA), kVp and time (sec) for the single phase power supplier (Curry et al, 1990). The high rate of energy deposited in the target of X-ray tubes heats the target to a very high temperature. The maximum-energy ratings are provided for the target, anode, and housing of an X-ray tube. These ratings are expressed in heat units, for single phase electric power.

$$\begin{aligned} \text{Number of heat units (HU)} &= (\text{Tube voltage}) (\text{Tube current}) (\text{Time}) \\ &= \text{kVp} \times \text{mA} \times \text{sec} \end{aligned} \tag{2.4}$$

If the tube voltage and current are constant, then 1 HU=1J of energy. For three phase power, the number of heat units is computed as

$$\begin{aligned} \text{Number of heat units (HU)} &= (\text{Tube voltage}) (\text{Tube current}) (\text{Time}) (1.35) \\ &= \text{kVp} \times \text{mA} \times \text{sec} \times 1.35 \end{aligned} \tag{2.5}$$

Energy ratings for the anode and the tube housing are expressed in terms of heat storage capacities which indicate the total number of heat units that may be absorbed without damage to these components. To determine whether the target of an X-ray tube might be damaged by a particular combination of the tube voltage, tube current, and the exposure time, rating charts furnished with the X-ray tube should be consulted as shown in Fig.(2.21)(Hendee and Ritenour,1992).

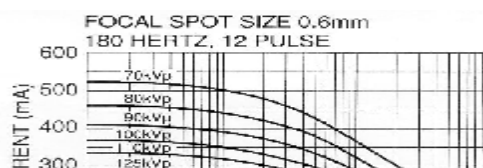


Fig.(2.21): An X-ray tube rating chart (Curry et al, 1990).

- **Cooling curves**

A cooling curve reveals the rate at which a hot anode radiates away heat. The curve can be used to determine the time required for an anode that has already absorbed a certain quantity of heat to lose any specified amount of it as shown in Fig.(2.22) (Wolbarst, 1993).

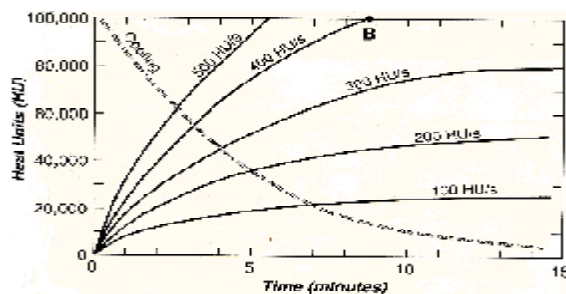


Fig.(2.22): Anode thermal characteristics chart for the tube (Wolbarst, 1993).

Chapter3

INTERACTION OF X-RAYS WITH MATTER

3.1. Types of X-Ray Interactions

There are two basic types of energy transfer that may occur when X-rays interact with matter:

- Ionization, in which the incoming radiation causes the removal of an electron from an atom or molecule leaving the material with a net positive charge.
- Excitation, in which some of the X-ray's energy is transferred to the target material leaving it in an excited (or more energetic) state.
- The important processes that occur when X-rays interact with matter are :

- The photoelectric effect
- The Compton effect
- Pair production and photodisintegration
- Coherent scatter (Connolly, 2007).

3.1.1. Photoelectric effect

A low energy photon can, by a process known as the photoelectric effect, collide with a bound orbital electron and eject it from the atom. The electron is ejected with energy equal to that of the incoming photon, $h\nu$, minus the binding energy of the electron in its particular orbit, an energy that must be overcome to free the electron from the atom. This interaction must occur with a bound electron since the entire atom is necessary to conserve momentum, and it often occurs with one of the inner shell electrons. Since a vacancy is created in the electron shell, a characteristic X-ray, typically from filling the K shell, will also be emitted. The kinetic energy of the ejected electron is almost always absorbed in the medium where photoelectric absorption occurs. Characteristic X-rays that are produced are also very likely to be absorbed in the medium, typically by another photoelectric interaction or by the ejection and absorption of Auger electrons as shown in Fig.(3.1)(Martin, 2006). The probability of photoelectric absorption per unit mass is approximately proportional to Z^3 / E^3 , where Z is the atomic number and E is the energy of the incident photon. For example, the photoelectric interaction probability in iodine ($Z= 53$) is $(53/20)^3$ or 18.6 times greater than in calcium ($Z= 20$) for photon of a particular energy. The benefit of photoelectric absorption in X-ray transmission imaging is that there are no additional nonprimary photons to degrade the image. The fact that the probability of photoelectric interaction is proportional to $1/E^3$. If the photon energies are doubled, the probability of photoelectric interaction is decreased eightfold: $(1/2)^3 = 1/8$.

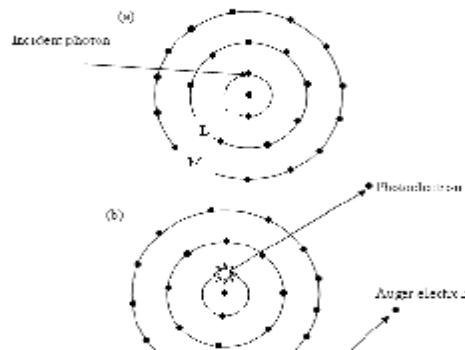


Fig.(3.1): Photoelectric absorption (Connolly, 2007).

Although the probability of the photoelectric effect decreases, in general, with increasing photon energy, there is an exception. For every element, a graph of probability of the photoelectric effect, as a function of photon energy, exhibits sharp discontinuities called absorption edges Fig.(3.2). The probability of interaction for photons of energy just above an absorption edge is much greater than that of photons of energy slightly below the edge. For example, a 33.2 keV X-ray photon is about six times as likely to have a photoelectric interaction with an iodine atom as a 33.1 keV.

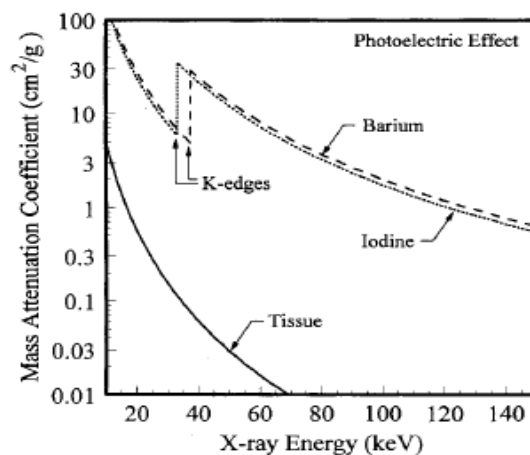


Fig.(3.2): Photoelectric mass attenuation coefficients for tissue, iodine and barium as a function of photon energy (Bushberg et al, 2001).

In the photoelectric effect, a photon cannot interact with an electron in a particular atomic shell or subshell if the photon's energy is less than the binding energy of that shell or subshell. This causes the dramatic decrease in the probability of photoelectric absorption for photons whose energies are just below the binding energy of a shell. Thus, the photon energy corresponding to an absorption edge is the binding energy of the electrons in that particular shell or subshell. The photon energy corresponding to a particular absorption edge increases with the atomic number (Z) of the element. For example, the primary elements comprising soft tissue (H, C, N, and O) have absorption edges below 1 keV. The elements iodine ($Z= 53$) and barium ($Z= 56$), commonly used in radiographic contrast agents to provide enhanced X-ray attenuation, have K- absorption edges of 33.2 and 37.4 keV, respectively. The K-edge energy of lead ($Z= 82$) is 88 keV (Bushberg et al, 2001).

3.1.2. Compton effect

Compton scattering is an elastic collision between a photon and a free electron (an electron whose binding energy to an atom is very much less than the energy of the photon), as shown diagrammatically in Fig.(3.3).

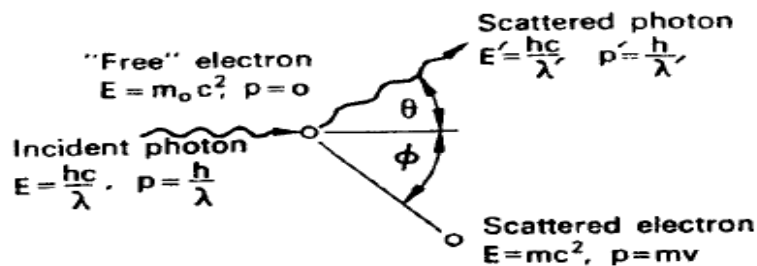


Fig.(3.3): Compton scattering: An elastic collision between a photon and an electron- (Cember and Johnson, 2009).

In a collision between a photon and a free electron, it is impossible for all the photon's energy to be transferred to the electron if momentum and energy are to be con-

served. This can be shown by assuming that such a reaction is possible. If this were true, then, according to the conservation of energy, all the energy of the photon is imparted to the electron, and we have, from equation:

$$E = mc^2 \quad 3.1$$

According to the law of conservation of momentum, all the momentum P of the photon must be transferred to the electron if the photon is to disappear:

$$P = \frac{E}{c} = mv \quad 3.2$$

Eliminating m from these two equations and solving for v , we find $v = c$, an impossible condition. The original assumption, that the photon transferred all of its energy to the electron, must therefore be false. Since all the photon's energy cannot be transferred, the photon must be scattered, and the scattered photon must have lesser energy or a longer wavelength than the incident photon, only the energy difference between the incident and scattered photons is transferred to the free electron. The amount of energy transferred in any collision can be calculated by applying the laws of conservation of energy and momentum to the situation pictured in Fig.(3.3). To conserve energy, we must have

$$\frac{hc}{l} + m_0c^2 = \frac{hc}{l'} + mc^2 \quad 3.3$$

and to conserve momentum in the horizontal and vertical directions respectively, we have

$$\frac{h}{l} = \frac{h}{l'} + mv \cos \theta \quad 3.4$$

and

$$0 = \frac{h}{l'} \sin \theta - mv \sin \theta \quad 3.5$$

The solution of these equations shows the change in wavelength of the photon to be

$$\Delta \lambda = l' - \lambda = \frac{h}{m_0c} (1 - \cos \theta) \quad 3.6$$

and the relation between the scattering angles of the photon and the electron to be

$$\frac{\theta}{2} = \left(1 + \frac{h}{m_0c\lambda} \right) \phi \quad 3.7$$

When the numerical values are substituted for the constants and centimeters are converted into angstrom units, equation reduces to

$$\Delta I = 0.0242 (1 - \cos\theta) \text{ \AA}^0 \quad 3.8$$

Equation 3.8 shows that the change in wavelength following a scattering event depends only on the scattering angle; it neither depends on the energy of the incident photon nor on the nature of the scatterer. As a consequence, a low energy photon will lose a smaller percentage of its energy than a high energy photon for the same scattering angle. Equation 3.7 shows that the electron cannot be scattered through an angle greater than 90° (Cember and Johnson, 2009).

Energy transfer to the recoiling electron is the most important consequence of Compton interactions since it will be absorbed locally to produce radiation dose. This is a variable quantity and can range from zero up to a maximum value for electrons ejected in the forward direction.

The Compton interaction coefficient σ consists of two components:

$$\sigma = \sigma_a + \sigma_s \quad 3.9$$

Where σ is the total Compton interaction coefficient, σ_a is the Compton absorption coefficient for photon energy lost by collisions with electrons, and σ_s is the loss of energy due to the scattering of photons out of the beam. The Compton interaction coefficient is determined by electron density which is directly related to Z and inversely proportional to E as follows (Martin, 2006):

$$\cong \quad \times \frac{Z}{E} \quad 3.10$$

3.1.3. Pair production

X-ray photons with energy greater than 1.02 MeV may interact with a nucleus to form an electron-positron pair. The interaction produces a pair of particles, an electron and positively charged positron. These particles have the same mass, each equivalent to rest mass energy of 0.511 MeV. The positron is eventually captured by an electron and annihilation of the two particles occurs (Sprawls, 1995). The pair production is not much important in diagnostic radiology, but it is important in mega voltage radiotherapy (Thayalan, 2001). The pair production interaction coefficient κ is proportional to the square of

the atomic number Z for photons with energy greater than 2×0.511 MeV (the energy required to form an electron-positron pair) and has the following relationship:

$$\kappa \cong \text{constant} \times Z^2(E - 1.022) \quad 3.11$$

Where Z is the atomic number and E is the photon energy in MeV (Martin, 2006).

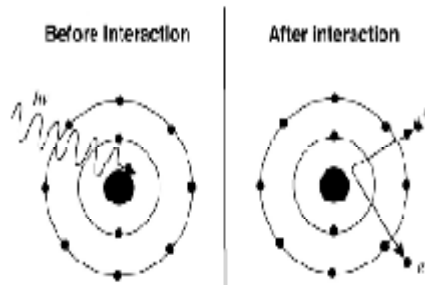


Fig.(3.4): Schematic representation of pair production in the coulomb field of a nucleus (podgorsak, 2006).

The positron created as a result of pair production process loses its energy as it traverses the matter by the same type of interactions as an electron does, namely by ionization, excitation, and bremsstrahlung. Near the end of its range, the slowly moving positron combines with one of the free electrons in its vicinity to give rise to two annihilation photons, each having 0.51 MeV energy. Because momentum is conserved in the process, the two photons are ejected in opposite directions (Khan, 2003).

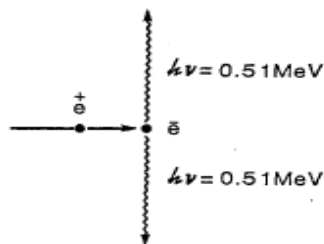


Fig.(3.5): Diagram illustrating the production of annihilation radiation (Khan, 2003).

3.1.4. Photodisintegration

Photodisintegration interactions occur when photons have enough energy to eject a nuclear particle when they are absorbed by a nucleus and can be used to measure the energy of a photon in a high-energy X-ray beam (Hendee and Ibbott, 1996).

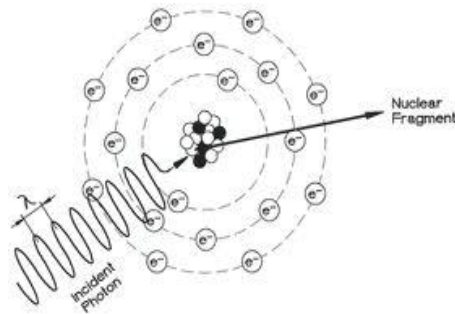


Fig.(3.6): Photodisintegration interaction.

www.zeably.com/Photodisintegration

3.1.5. Rayleigh scattering (Coherent scatter)

In Rayleigh scattering, the incident photon interacts with and excites the total atoms, as opposed to individual electrons as in Compton scattering or the photoelectric effect. This interaction occurs mainly with very low energy diagnostic X-rays, as used in mammography (15 to 30 keV).

During the Rayleigh scattering event, the electric field of the incident photon's electromagnetic wave expends energy, causing all of the electrons in the scattering atom to oscillate in phase. The atom's electron cloud immediately radiates this energy, emitting a photon of the same energy but in a slightly different direction. In this interaction, electrons are not ejected and thus ionization does not occur. In general, the scattering angle increases as the X-ray energy decreases. In medical imaging, detection of the scattered X-ray will have a deleterious effect on image quality. However, this type of interaction has a low probability of occurrence in the diagnostic energy range. In soft tissue, Rayleigh scattering accounts for less than 5% of X-ray interactions above 70 keV and at most only accounts for 12% of interactions at approximately 30 keV. Rayleigh interactions are also referred to as "coherent" or "classical" scattering (Bushberg et al, 2001).

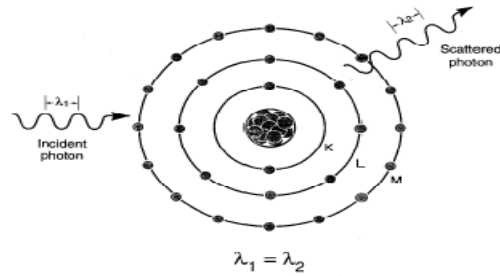


Fig.(3.7): Diagram shows the incident photon I_1 interacts with an atom and the scattered photon I_2 is being emitted with approximately the same wavelength and energy (Bushberg et al, 2001).

3.2. Relative Predominance of Individual Effects

The relative importance of Compton effect, photoelectric effect, and pair production depends on both the photon energy ($E = h\nu$) and the atomic number Z of the absorbing medium. Fig.(3.8) indicates the regions of Z and E in which each interaction predominates (Attix, 1986). From the Fig.(3.8), the photoelectric component t increases with increasing atomic number of the absorber and the photoelectric effect dominates in heavy elements, at low photon energies. The photoelectric component also increases abruptly at energies corresponding to the orbital electron binding energies of the absorber element. The Compton scatter component s decreases slowly with increasing photon energy E and with increasing absorber atomic number Z . The pair production component k is zero for energies less than the threshold energy of 1.02 MeV for this interaction, and then it increases logarithmically with increasing photon energy and with increasing atomic number of the absorber. Pair production is the dominating effect at higher photon energies in absorbers of high atomic number (Cherry et al, 2003).

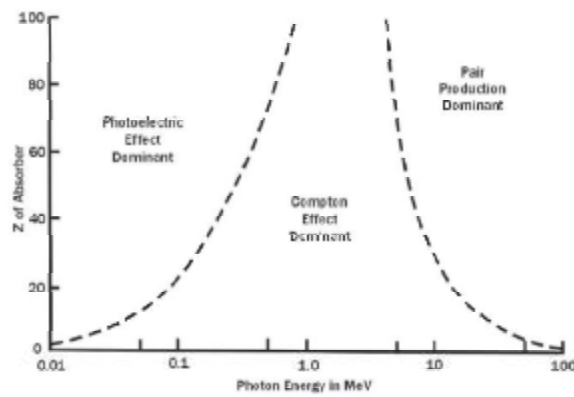


Fig.(3.8): Regions of relative predominance of the three main forms of photon interaction with matter (Connolly, 2007).

The Compton effect and the photoelectric effect are the two most important interactions in diagnostic radiology while the coherent scattering contributes < 5% in diagnostic radiology (Thayalan, 2001). For diagnostic radiology, the X-ray tube voltage range used is from roughly 20 to 150 kV.

3.3. Attenuation and Absorption

Martin (2006) derived the equation of intensity based on Fig.(3.9) as follows: The change in intensity of a photon is expressed mathematically as a decreasing function with thickness of absorber :

$$-\frac{dI}{dx} = mI \quad 3.12$$

Where the constant of proportionality m , is the total attenuation coefficient of the medium for the photons of interest. If all of the photons possess the same energy (i.e. the

beam is monoenergetic) and if the photons are attenuated under conditions of good geometry (i.e. the beam is narrow and contains no scattered photons), then the number or intensity $I(x)$ of photons penetrating an absorber of thickness x (i.e. without interaction in the medium) is found by rearranging and integrating

$$\int_{I_0}^{I(x)} \frac{dI}{I} = \int_0^x -\mu dx \tag{3.13}$$

To yield

$$\ln I(x) - \ln I_0 = -\mu x \tag{3.14}$$

or

$$\ln I(x) = -\mu x + \ln I_0 \tag{3.15}$$

Which is the equation of a straight line with a slope of $-\mu$ and a y-intercept (i.e. with no absorber) of $\ln I_0$ as shown in Fig.(3.10).

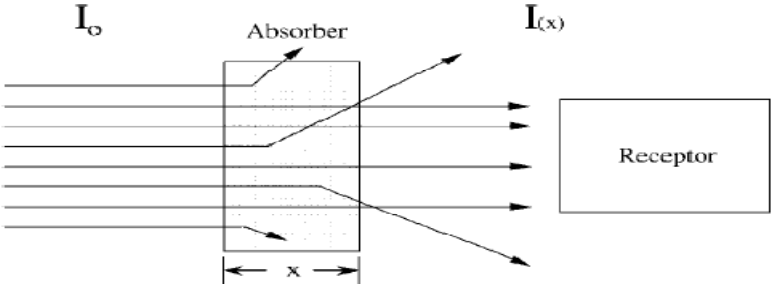


Fig.(3.9): Alteration of a beam of photons by attenuation processes (Martin, 2006).

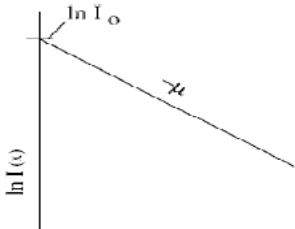


Fig.(3.10): Linear attenuation (Martin,2006).

This can be simplified by the law of logarithms to

$$\ln \frac{I(x)}{I_0} = -mx \tag{3.16}$$

and since the natural logarithm of a number of exponent to which the base e is raised to obtain the number, this expression translates to

$$\frac{I(x)}{I_0} = e^{-mx} \tag{3.17}$$

or

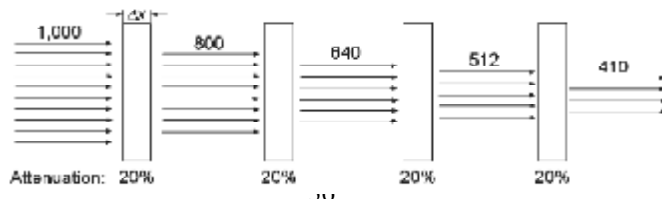
$$I(x) = I_0 e^{-mx} \tag{3.18}$$

Where I_0 is the intensity of the incident beam, $I(x)$ is the intensity after traversing a distance x through the absorbing medium, and m , the linear attenuation coefficient, is the probability of interaction per unit distance in an absorbing medium.

3.4. Coefficients

3.4.1. Linear attenuation coefficient (m)

The fraction of photons removed from a monoenergetic beam of X or gamma rays per unit thickness of material is called linear attenuation coefficient (m), typically expressed in units of inverse centimeters (cm^{-1}) (Bushberg et al, 2001).



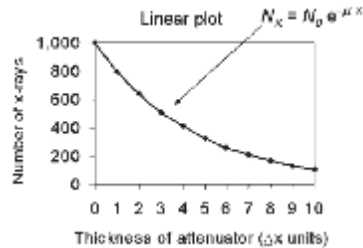


Fig.(3.11): Monoenergetic X-rays are transmitted through several layers of an attenuator with attenuation coefficient (m) of 20% per unit thickness (Seibert and Boone, 2005).

Fig.(3.11) shows the attenuation of monoenergetic beam. The factors relevant with the transition of radiation are:

- The number of photons is not halved as the thickness is doubled but decreases exponentially with thickness.
- The fraction absorbed depends on the photon energy.
- The linear attenuation coefficient is energy and atomic number Z of the material dependent (Dowsett et al, 1998).

The total linear attenuation coefficient is the sum of the linear attenuation coefficients for the individual interaction mechanisms given by

$$m = t + s_{coh} + s_c + k \tag{3.19}$$

Where s_{coh} , t , s_c and k are the attenuation coefficients for coherent scattering, photoelectric effect, Compton effect, and pair production, respectively. The individual interaction coefficients, values of m are strongly dependent on incident X-ray energy and on the physical density of the interacting medium (Seibert and Boone, 2005).

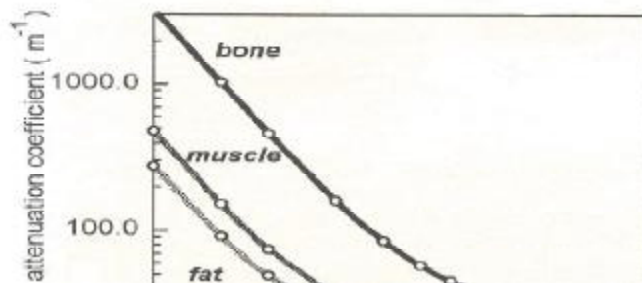


Fig.(3.12) : The linear attenuation coefficient for bone, soft tissue and fat (Dowsett et al, 1998).

When comparing muscle, bone and fat, fat has a higher concentration by weight of hydrogen (~ 11%) and carbon (~ 57%) and a lower concentration of nitrogen (~ 1%), oxygen (~30%) and high Z trace elements (< 1%). The effective atomic number of fat ($Z_{\text{eff}} = 5.9$ to 6.3) is less than that for soft tissue ($Z_{\text{eff}} = 7.4$) or bone ($Z_{\text{eff}} = 11.6$ to 13.8) and low energy photons are attenuated less rapidly in fat than in an equal mass of soft tissue or bone and attenuated more rapidly in bone than in an equal volume of soft tissue. The absorbed dose is reduced by structures beyond bone (Hendee and Ritenour, 1992).

3.4.2. Mass attenuation coefficient

For a given thickness, the probability of interaction is dependent on the number of atoms per volume. This dependency can be overcome by normalizing the linear attenuation coefficient for the density of the material. The linear attenuation coefficient, normalized to unit density, is called the mass attenuation coefficient (Bushberg et al, 2001):

$$\text{Mass attenuation coefficient } (\mu / \rho) \left[\frac{\text{cm}^2}{\text{g}} \right] = \frac{\text{Linear attenuation coefficient } (\mu) [\text{cm}^{-1}]}{\text{Density of material } (\rho) [\text{g} / \text{cm}^3]} \quad 3.20$$

For the mass attenuation coefficient, "thickness" becomes the product of the density and linear thickness of the material, or ρx . This is known as the mass thickness with unit of $\text{g}/\text{cm}^3 \times \text{cm} = \text{g}/\text{cm}^2$. The reciprocal of the mass thickness represents the units of mass

attenuation coefficient, cm^2/g , and the corresponding Lambert – Beers equation is given by:

$$I_x = N_0 e^{-rx \left(\frac{m}{r}\right)} \quad 3.21$$

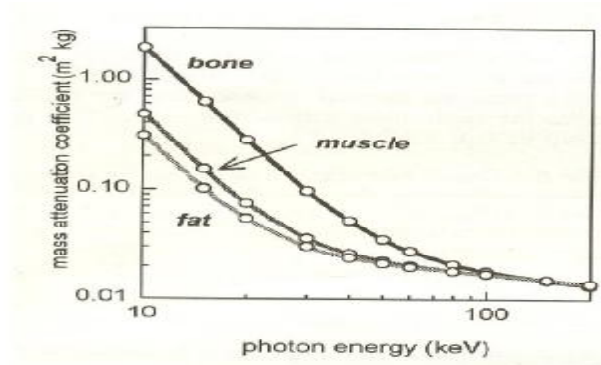


Fig.(3.13): The mass attenuation coefficients matching bone, soft tissue and fat for the attenuation coefficients in Fig.(3.12)(Dowsett et al, 1998).

The mass attenuation coefficient for a specific material is a sum of the individual interaction probabilities given by (Seibert and Boone, 2005).

$$\frac{m}{r} = \frac{t}{r} + \frac{s_{coh}}{r} + \frac{s_c}{r} + \frac{k}{r} \quad 3.22$$

Fig.(3.13) shows the mass attenuation coefficient of fat, bone and muscle as a function of the incident X-ray energy. At low incident X-ray energies, bone has by far the highest mass attenuation coefficient. As the incident X-ray energy increases, the probability of photoelectric interactions decreases greatly and the value of the mass attenuation coefficient becomes much lower. At X-ray energies greater than about 80 keV, Compton scattering is the dominant mechanism and the difference in the mass attenuation coefficients of bone and soft tissue is less than a factor of 2. At incident X-ray energies greater than around 120 keV, the mass attenuation coefficients for bone and soft tissue are very similar (Feng, 2007).

3.4.3. Energy transfer coefficient (m_{tr})

When a photon interacts with the electrons in the material, a part or all of its energy is converted into kinetic energy of electrons. If only a part of the photon energy is given to

the electron, the photon itself is scattered with reduced energy. The scattered photon may interact again with a partial or complete transfer of energy to the electrons. Thus a photon may experience one or multiple interactions in which the energy lost by the photon is converted into kinetic energy of electrons. If we consider a photon beam traversing a material, the fraction of photon energy transferred into kinetic energy of charged particles per unit thickness of absorber is given by the energy transfer coefficient (m_{tr}). This coefficient is related to m as follows:

$$m_{tr} = \frac{\bar{E}_{tr}}{h\nu} m \quad 3.23$$

Where \bar{E}_{tr} is the average energy transferred into kinetic energy of charged particles per interaction (Khan, 2003).

3.4.4. Energy absorption coefficient (m_{en})

Most of the electrons set in motion by the photons will lose their energy by inelastic collisions (ionization and excitation) with atomic electrons of the material. A few, depending on the atomic number of the material, will lose energy by bremsstrahlung interactions with the nuclei. The bremsstrahlung energy is radiated out of the local volume as X-rays and is not included in the calculation of locally absorbed energy. The energy absorption coefficient (m_{en}) is defined as the product of energy transfer coefficient and (1-g) where g is the fraction of the energy of secondary charged particles that is lost to bremsstrahlung in the material.

$$m_{en} = m_{tr}(1 - g) \quad 3.24$$

For most interactions involving soft tissues or other low Z material in which electrons lose energy almost entirely by ionization collisions, the bremsstrahlung component is negligible. Thus $m_{en} = m_{tr}$ under those conditions (Khan, 2003).

Chapter 4

DIAGNOSTIC IMAGING QUANTITIES AND PARAMETERS

4.1. X-Ray Beam Quantities

A subjective assessment of spectrum shape is given by beam quality. The quantity of X-radiation incident on a surface (e.g. patient) depends on area, time, and energy. Measurements of radiation quantity are important for estimating the sensitivity of imaging devices and dosimetry calculation. The following parameters describe intensity:

- Photon fluence
- Photon flux
- Energy fluence
- Energy flux (Dowsett et al, 1998).

Radiation is energy in transit from one location to another. The term radiation intensity is used colloquially to refer to a number of attributes of the output of a radiation source. The beam radiation is shown in Fig.(4.1).

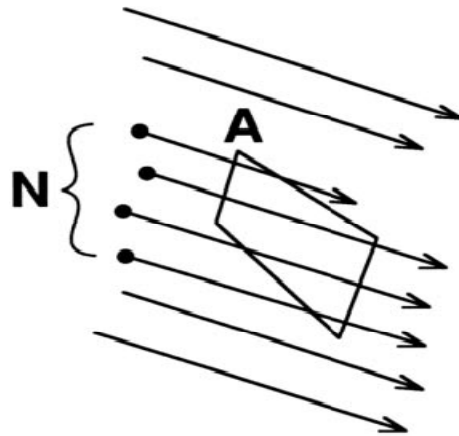


Fig.(4.1): The number of particles (N) passing through a unit area (A) that is perpendicular to the direction of the beam (Hendee and Ritenour, 1992)

The photon fluence of the beam Φ is the number N of particles or photons per area A :

$$\Phi = \frac{N}{A} \quad 4.1$$

When the beam is uniform the location or size of the area A is irrelevant because it is perpendicular to the direction of the beam. If the beam is not uniform over its entire area,

then the fluence must be averaged over a number of small areas, or specified separately for each area. The time rate of change of fluence, known as the radiation flux f , is

$$f = \frac{\Phi}{t} = \frac{N}{A \times t} \quad 4.2$$

If the fluence varies with time, then the flux must be averaged over time or specified at some instant. If all particles or photons in the radiation beam possess the same energy, the energy fluence Ψ is simply the product of the radiation fluence Φ and the energy E per particle or photon:

$$\Psi = \Phi E = \frac{NE}{A} \quad 4.3$$

The particle or photon flux f may be converted to the energy flux y , also known as the intensity I , by multiplying by the energy E per particle or photon (Hendee and Ritenour, 1992):

$$I = y = fE = \frac{NE}{At} \quad 4.4$$

Table (4.1) Fluence and Flux (Intensity) of a Beam of Radiation (Hendee and Ritenour, 1992).

Quantity	Symbol	Definition	Units
Photon fluence	Φ	$\frac{N}{A}$	$\frac{\text{photon}}{m^2}$
Photon flux	f	$\frac{N}{At}$	$\frac{\text{photon}}{m^2 \cdot \text{sec}}$
Energy fluence	Ψ	$\frac{NE}{A}$	$\frac{\text{MeV}}{m^2}$
Energy flux (intensity)	y	$\frac{NE}{At}$	$\frac{\text{MeV}}{m^2 \cdot \text{sec}}$

4.2. Quantities That Describe Deposited Energy

The amount of energy a beam deposits in matter such as tissue relates to the amount of damage caused by the beam. The transfer of energy from a radiation beam to a medium can occur in a single stage for direct ionizing radiation or in two stages for indirect ionizing radiation, such as photons. When a photon interacts with a matter, it gives all or part of its energy to an electron of the matter. The electron then gives its energy to the medium via excitation or ionization.

4.2.1. Kerma (K)

This nonstochastic quantity is relevant only for fields of indirectly ionizing radiations (photons or neutrons) or for any ionizing radiation source distributed within the absorbing medium (Attix, 1986).

The Definition

Kerma is an acronym of kinetic energy released in a medium per unit mass. It is defined the quotient of dE_{tr} by dm , where dE_{tr} is the sum of the initial kinetic energies of all the charged particles liberated by uncharged particles in a mass dm of material, thus:

$$K = \frac{dE_{tr}}{dm} \quad 4.5$$

Its unit is J/kg. The special name for the unit of kerma is the gray (Gy) (IAEA, 2007). The total kerma is usually divided into two components: the collision kerma (K_{col}) and the radiative kerma (K_{rad}). The collision kerma is that part of kerma that leads to the production of electrons that dissipate their energy as ionization in or near the electron tracks in the medium, and is the result of coulomb force interactions with atomic electrons. Thus the collision kerma is the expectation value of the net energy transferred to charged particles per unit mass at the point of interest, excluding both the radiative loss energy and energy passed from one charged particle to another. The radiative kerma is that part of kerma that leads to the production of radiative photons as the secondary charged particles slow down and interact in the medium. These interactions most prominently are bremsstrahlung as a result of coulomb field interactions between the charged particle and the atomic nuclei. The total kerma K is given by the following (Podgorsak, 2005)

$$K = K_{col} + K_{rad} \quad 4.6$$

- **Relation of kerma to energy fluence for uncharged particles**

If we consider uncharged particles of a given energy E (monoenergetic particles), and if the fluence of these uncharged particles at the position of the volume element dV is Φ , the kerma K is related to Φ according to:

$$K = \Phi E \left(\frac{m_{tr}}{r} \right) \quad 4.7$$

Where $\left(\frac{m_{tr}}{r} \right)$ is the mass energy transfer coefficient of the material for these particles of energy E . The kerma per unit fluence $\frac{K}{\Phi}$ is called the kerma coefficient for uncharged particles of energy E in a specific material. For the monoenergetic uncharged particles of energy E , the energy fluence Ψ is given by $\Psi = \Phi E$, and thus:

$$K = \Psi \left(\frac{m_{tr}}{r} \right) \quad 4.8$$

For uncharged particles of a given energy distribution, the kerma K is given according to

$$K = \int_E \Phi_E E \left(\frac{m_{tr}}{r} \right)_E dE \quad 4.9$$

or

$$K = \int_E \Psi_E \left(\frac{m_{tr}}{r} \right)_E dE \quad 4.10$$

Where Φ_E and Ψ_E are the energy distribution of fluence and energy fluence of the uncharged particles, respectively, and $\left(\frac{m_{tr}}{r} \right)_E$ is the mass energy transfer coefficient of the material under consideration for uncharged particles of energy E (Baltas et al, 2006).

4.2.2 Kerma rate (\dot{K})

Kerma rate is the quotient dK by dt , where dK is the increment of kerma in the time interval dt , thus:

$$\dot{K} = \frac{dK}{dt} \quad 4.11$$

Its unit is $J.Kg^{-1}.S^{-1}$. If the special name gray is used, the unit of kerma rate is gray per second (Gy/s) (IAEA,2007).

4.2.3.Exposure (X)

Exposure (X) is defined as the quotient of dQ by dm , where dQ is the absolute value of the total charge of the ions of one sign produced in air when all the electrons and positrons liberated or created by photons in air of mass dm are completely stopped in air, thus (Podgorsak, 2005) :

$$X = \frac{dQ}{dm} \quad 4.12$$

The SI unit of exposure is coulomb per kilogram (C/kg).The old and common unit used for exposure is the roentgen R, where $1R = 2.58 \times 10^{-4} C/kg$.

Note that, according to this definition, ionization produced by Auger electrons is included in dQ whereas ionization produced by radiative processes such as bremsstrahlung and fluorescence photons is not included in dQ (Baltas et al, 2006).

Exposure is the ionization equivalent of the collision kerma in air. It can be calculated from K_{col} by knowing the ionization charge produced per unit of energy deposited by photons.The mean energy required to produce an ion pair in dry air is almost constant for all electron energies and has a value of $\bar{W} = 33.97eV/$ ion pair.If e is the electronic charge ($= 1.60 \times 10^{-19} C$), then \bar{W}/e is the average energy required per unit charge of ionization produced. Since $1eV = 1.60 \times 10^{-19} J$, $\bar{W}/e = 33.97 J/C$. Exposure (X) is given by(Khan,2003):

$$X = \Psi_{air} \left(\frac{\bar{m}_{en}}{r} \right)_{air} \cdot \left(\frac{e}{\bar{W}} \right)_{air} = (K_{col})_{air} \cdot \left(\frac{e}{\bar{W}} \right)_{air} \quad 4.13$$

4.2.4. Exposure rate (\dot{X})

The exposure rate \dot{X} ($C\text{ kg}^{-1}\text{s}^{-1}$) is defined as the quotient of the increment of exposure dX observed in the time interval dt by this time interval (Baltas et al, 2006):

$$\dot{X} = \frac{dX}{dt} \quad 4.14$$

4.2.5. Cema (C)

The quantity cema (from converted energy per unit mass) refers to the energy lost by charged particles in electronic collisions in a specific material. This energy loss includes the charged particles energy expended against binding energy and any kinetic energy of the liberated electrons. These latest are called secondary electrons. The secondary electrons are not considered for the determination of cema. If dE_c is that energy lost by the charged particles in electronic collisions within a volume element dV of a material containing a mass $dm = r dV$ of that material, the cema C is given by

$$C = \frac{dE_c}{dm} = \frac{1}{r} \frac{dE_c}{dV} \quad 4.15$$

The special name of the SI unit for cema is gray (Gy): $1\text{Gy} = 1\text{JKg}^{-1}$ (Baltas et al, 2006).

4.2.6. Cema rate (\dot{C})

The cema rate \dot{C} is defined as the quotient of the increment of cema dC observed in the time interval dt by this time interval:

$$\dot{C} = \frac{dC}{dt} \quad 4.16$$

If the special name gray is used, the unit of cema rate is gray per second:

$1\text{Gys}^{-1} = 1\text{JKg}^{-1}\text{s}^{-1}$ (Baltas et al, 2006).

4.2.7. Energy imparted

If we consider all energy deposits E_i that take place within a given volume in matter, the energy imparted E (J) is defined as the total energy deposited in that volume expressed as the sum of all these energy deposits:

$$E = \sum_i E_i \quad 4.17$$

Given that the energy deposit is the result of a single interaction of an ionizing particle at some transfer point within the volume under consideration, we can express the mean energy imparted \bar{E} to that volume in matter in terms of radiant energy as

$$E = R_{in} - R_{out} + \sum Q \quad 4.18$$

Where R_{in} is the radiant energy of all ionizing particles entering the volume and R_{out} is the radiant energy of all ionizing particles leaving that volume. The summation term in the above equation extends over all changes Q of the rest energy of nuclei and particles occurring in the volume (Baltas et al, 2006).

4.2.8. Absorbed dose (D)

The absorbed dose is relevant to all types of ionizing radiation fields, whether directly or indirectly ionizing, as well as to any ionizing radiation source distributed within the absorbing medium (Attix, 1986).

The Definition

It is defined as the quotient of $d\bar{E}$ by dm , where $d\bar{E}$ is the mean energy imparted to matter of mass dm :

$$D = \frac{d\bar{E}}{dm} \quad 4.19$$

The SI unit for absorbed dose is J/kg and its name is the gray (Gy). The older unit of dose is the rad, representing 100erg/g (i.e. 1Gy = 100 rad) (Podgorsak, 2005).

Absorbed dose, D_t , to a material t is related to the energy fluence, Ψ by the mass energy absorption coefficient in that material, $\left(\frac{m_{en}}{r}\right)_t$, under conditions of charged particle equilibrium. For photons of a single energy, D_t is given by:

$$D_t = \Psi \left(\frac{m_{en}}{r}\right)_t \text{ (units: } \text{JKg}^{-1} \text{ or Gy)} \quad 4.20$$

In medical images where polychromatic X-ray photons are usual, the mean value of $\left(\frac{m_{en}}{r}\right)_t$, weighted according to the energy distribution of the energy fluence, is used.

If bremsstrahlung is negligible, (UNSCEAR, 2010).

$$\left(\frac{m_{en}}{r}\right)_t = \left(\frac{m_{tr}}{r}\right)_t \text{ hence } D_t = K_t \quad 4.21$$

4.2.9. Absorbed dose rate (\dot{D})

The absorbed dose rate \dot{D} is the quotient of the increment of absorbed dose dD observed in the time interval dt by this time interval:

$$\dot{D} = \frac{dD}{dt} \quad 4.22$$

As in the case of kerma rate, if the special name gray is used, the unit of absorbed dose rate is gray per second: $1\text{Gys}^{-1} = 1\text{JKg}^{-1}\text{s}^{-1}$ (Baltas et al, 2006).

4.2.10. Entrance skin exposure (ESE)

Entrance skin exposure (ESE) is the radiation exposure to the skin measured in Roentgen (R) or milliRoentgen (mR) at the point of skin entrance for the nominal patient (i.e., 30 cm from the image intensifier). The measurement is made without the contributions from scatter radiation (Racz and Noe, 2012).

4.3. Radiation Protection Quantities

The absorbed dose is the basic physical dosimetry quantity, but it is not entirely satisfactory for radiation protection purposes because the effectiveness in damaging human tissue differs for different types of ionizing radiation. In addition to the physical quantities, other dose related quantities have been introduced to account not only for the physical effects but also for the biological effects of radiation upon tissues. These quantities are organ dose, equivalent dose, effective dose, committed dose and collective dose (Podgorsak, 2005).

4.3.1. Organ dose (D_T)

The organ dose is defined as the mean dose D_T in a specified tissue or organ T of the human body, given by:

$$D_T = \frac{1}{m_T} \int_{m_T} D \, dm = \frac{E_T}{m_T} \quad 4.23$$

Where m_T is the mass of the organ or tissue under consideration; E_T is the total energy imparted by radiation to that tissue or organ (Podgorsak, 2005).

- **Biological impact**

It is sometimes desirable to express the actual or relative biological impact of radiation. It is necessary to develop a distinction between the biological impact and the physical quantity of radiation, because all types of radiation do not have the same potential for producing biological change. For example, one rad of one type of radiation might produce significantly more radiation damage than one rad of another type. In other words, the biological impact is determined by both the quantity of radiation and its ability to produce biological effects (Sprawls, 1995).

4.3.2. Equivalent dose (H_T)

The biological detriment (harm) to an organ depends not only on the physical average dose received by the organ but also on the pattern of the dose distribution that results from the radiation type and energy. For the same dose to the organ, α or neutron radiation will cause greater harm compared with g - rays or electrons. This is because the io-

nization events produced by α or neutron radiation will be much more closely spaced (densely ionizing radiations) and so there is a higher probability of irreversible damage to the chromosomes and less chance of tissue repair. Consequently, the organ dose is multiplied by a radiation weighting factor W_R to account for the effectiveness of the given radiation in inducing health effects; the resulting quantity is called the equivalent dose H_T . The equivalent dose H_T is defined as:

$$H_T = W_R D_{T,R} \quad 4.24$$

Where $D_{T,R}$ is the absorbed dose delivered by radiation type R averaged over a tissue or organ T; W_R is the radiation weighting factor for radiation type R. The SI unit of equivalent dose is J/Kg and its name is the sievert (Sv); the old unit is the rem and the relationship between two units is $1\text{Sv} = 100\text{rem}$. If an organ is irradiated by more than one type of radiation, the equivalent dose is given by the sum (Podgorsak, 2005):

$$H_T = \sum W_R D_{T,R} \quad 4.25$$

• **Radiation weighting factor (W_R)**

The probability of stochastic effects is found to depend, not only on the absorbed dose, but also on the type and energy of the radiation causing the dose. This is taken into account by weighting the absorbed dose by a factor related to the quality of the radiation (ICRP, 1991). In the past, this weighting factor has been applied to the absorbed dose at a point and called the quality factor, Q.

Table (4.2) Radiation weighting factors recommended by the International Commission on Radiological Protection (ICRP, 1991).

Type and energy range	Radiation Weighting Factors, W_R
Photons, all energies	1
Neutrons, energy < 10 keV	5
10 keV to 100 keV	10
Protons, other than recoil protons, energy > 2 MeV	5
Alpha particles, fission fragments, heavy nuclei	20

4.3.3. Effective dose (E)

The effective dose is defined as the summation of tissue equivalent doses, each multiplied by the appropriate tissue weighting factor W_T to indicate the combination of different doses to several different tissues in a way that correlates well with all stochastic effects combined (ICRP,1991):

$$E = \sum_T W_T H_T \text{ or } \sum_T W_T \sum_R W_R D_{T,R} \quad 4.26$$

Where $D_{T,R}$ is the mean absorbed dose for tissue T, W_R is the radiation weighting factor. The unit of effective dose is J/Kg and its name is the sievert (Sv). The effective dose, E, is a dosimetry parameter which takes into account the doses received by all irradiated radiosensitive organs and may be taken to be measures of the stochastic risk(ICRP,1977; ICRP, 1991).

- **Tissue weighting factors (W_T)**

The relationship between the probability of stochastic effects and equivalent dose is found also to depend on the organ or tissue irradiated. It is therefore appropriate to define a further quantity, derived from equivalent dose, to indicate the combination of different doses to several different tissues in a way which is likely to correlate well with the total of the stochastic effects. The factor by which the equivalent dose in tissue or organ T is weighted is called the tissue weighting factor, W_T which represents the relative contribution of that organ or tissue to the total detriment due to these effects resulting from uniform irradiation of the whole body (ICRP, 1991).

Table (4.3) Tissue weighting factors (W_T) recommended in ICRP publication 103 (ICRP, 2007b).

Tissue / organ	Tissue Weighting Factor (W_T)
Bone – marrow(red), colon, lung, stomach, breast, remainder tissues*	0.12
Gonads	0.08
Bladder, oesophagus, liver, thyroid	0.04
Bone surface, brain, salivaryglands, skin	0.01

*Remainder tissues;Adrenals, Extrathoracic (ET) region, Gallbladder, Heart, Kidneys, Lymphatic nodes, Muscles, Oral mucosa, Pancreas, Prostate, Small intestine, Spleen, Thymus, Uterus/cervix.

4.4.Entrance Surface Dose(ESD)

The entrance surface dose (ESD) can be defined as the absorbed dose to air at the point where the X-ray beam enters the surface of the patient stressed by the backscatter factor(Kettunen, 2004).The unit of entrance surface dose is Gy.

4.5.Entrance Surface Air Kerma (ESAK)

The Entrance surface air kerma is the air kerma on the central X-ray beam axis at the point where the X-ray beam enters the patient or phantom;it includes the effect of backscatter(UNSCEAR, 2010).

4.6.Dose Area Product (DAP)

The dose area product is the integral of the absorbed dose to air over the area, A, of the X-ray beam perpendicular to the beam axis.Thus

$$DAP = \int_A D_{air}(A)dA \quad 4.27$$

In this quantity, radiation backscattered from the patient is excluded.DAP has the convenient property of being invariant with distance from the X-ray tube focus, since the

dose is inversely related to it and the area is directly related to the square of the distance from the focus(Wall,1996).The Dose area product usually expressed in Gy cm².

4.7. Integral Dose

Integral dose is the total amount of energy absorbed in the body.It is determined not only by the absorbed dose values but also by the total mass of tissue exposed.The conventional unit for integral dose is the gram - rad, which is equivalent to 100 ergs of absorbed energy.The concept behind the use of this unit is that if we add the absorbed doses (rads) for each gram of tissue in the body, we will have an indication of total absorbed energy.Since the integral dose is quantity of energy, the SI unit used is the joule. The relationship between the two units is

$$1\text{J} = 1000 \text{ gram} - \text{rad} \quad 4.28$$

Integral dose (total absorbed radiation energy) is probably the radiation quantity that most closely correlates with potential radiation damage during a diagnostic procedure.This is because it reflects not only the concentration of the radiation absorbed in the tissue but also the amount of tissue affected by the radiation(Sprawls,1995).

4.8.Surface Integral Exposure (SIE)

Since exposure expressed in roentgens or coulombs per kilogram is a concentration, it does not express the total amount of radiation delivered to a body.The total radiation delivered, or surface integral exposure (SIE), is determined by the exposure and the dimensions of the exposed area.It is also referred to as the exposure-area product.The surface integral exposure is expressed in the conventional units of roentgens-square centimeters (R- cm²) (Sprawls, 1995).

4.9.Computed Tomography Dose Index (CTDI)

The CTDI is the primary dose measurement concept in CT

$$\text{CTDI} = \frac{1}{NT} \int_{-\infty}^{\infty} D(z)dz \quad 4.29$$

Where $D(z)$ is the radiation dose profile along the z axis, N is the number of tomographic sections imaged in a single axial scan. This is equal to the number of data channels used in a particular scan. The value of N may be less than or equal to the maximum number of data channels available on the system, and T is the width of the tomographic section along the z axis imaged by one data channel. CTDI represents the average absorbed dose, along the z axis, from a series of contiguous irradiations. It is measured from one axial CT scan (one rotation of the X-ray tube) and is calculated by dividing the integrated absorbed dose by the nominal total beam collimation (AAPM, 2008).

4.10. Dose Length Product (DLP)

The DLP is the product of the CTDI value and the length of the body area scanned. It has the units of either rad-cm or Gy-cm. It is a useful and practical quantity for comparing the total radiation to patients for various CT procedures (Sprawls, 1995).

4.11. Practical Radiation Dosimetry

4.11.1. Radiation dosimeter

A radiation dosimeter is a device, instrument or system that measures or evaluates, either directly or indirectly, the quantities exposure, kerma, absorbed dose or equivalent dose, or their time derivatives (rates), or related quantities of ionizing radiation. A dosimeter along with its reader is referred to as a dosimetry system. Measurement of a dosimetric quantity is the process of finding the value of the quantity experimentally using dosimetry systems. The result of a measurement is the value of a dosimetric quantity expressed as the product of a numerical value and an appropriate unit. To function as a radiation dosimeter, the dosimeter must possess at least one physical property that is a function of the measured dosimetric quantity and that can be used for radiation dosimetry with proper calibration. In order to be useful, radiation dosimeters must exhibit several desirable characteristics (Podgorsak, 2005).

- **Chambers and electrometers**

Ionization chambers are used in radiotherapy and in diagnostic radiology for the determination of radiation dose. The dose determination in reference irradiation conditions is also called beam calibration. Ionization chambers come in various shapes and sizes, de-

pending upon the specific requirements, but generally they all have the following properties:

- An ionization chamber is basically a gas filled cavity surrounded by a conductive outer wall and having a central collecting electrode. The wall and the collecting electrode are separated with a high quality insulator to reduce the leakage current when a polarizing voltage is applied to the chamber.
- A guard electrode is usually provided in the chamber to further reduce chamber leakage. The guard electrode intercepts the leakage current and allows it to flow to ground, bypassing the collecting electrode. It also ensures improved field uniformity in the active or sensitive volume of the chamber, with resulting advantages in charge collection.
- Measurements with open air ionization chambers require temperature and pressure correction to account for the change in the mass of air in the chamber volume, which changes with the ambient temperature and pressure.

Electrometers are devices for measuring small currents, of the order of 10^{-9} A or less. An electrometer used in conjunction with an ionization chamber is a high gain, negative feedback, operational amplifier with a standard resistor or a standard capacitor in the feedback path to measure the chamber current or charge collected over a fixed time interval, as shown schematically in Fig.(4.2)(Podgorsak, 2005)

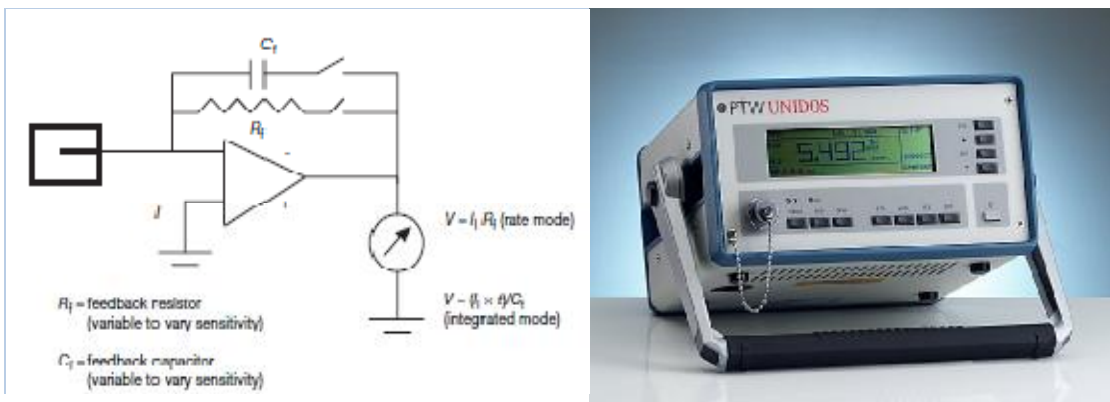


Fig.(4.2): Electrometer in feedback mode of operation (Podgorsak,2005), www.ptw.de/unidos_dosemeter_ad0.html.

- **Thimble ionization chamber**

Fig.(4.3) shows a typical thimble ionization chamber. The wall is shaped like a sewing thimble. The inner surface of the thimble wall is coated by a special material to make it electrically conducting. This forms one electrode. The other electrode is a rod of low atomic material such as graphite or aluminum held in the center of the thimble but electrically insulated from it. A suitable voltage is applied between the two electrodes to collect the ions produced in the air cavity. The principle of the thimble chamber is illustrated in Fig.(4.3 A) a spherical volume of air is shown with an air cavity at the center. Suppose this sphere of air is irradiated uniformly with a photon beam. Also, suppose that the distance between the outer sphere and the inner cavity is equal to the maximum range of electrons generated in air. If the number of electrons entering the cavity is the same as that leaving the cavity, electronic equilibrium exists. Suppose also that we are able to measure the ionization charge produced in the cavity by the electrons liberated in the air surrounding the cavity. Then by knowing the volume or mass of air inside the cavity, we can calculate the charge per unit mass or the beam exposure at the center of the cavity (Khan, 2003).

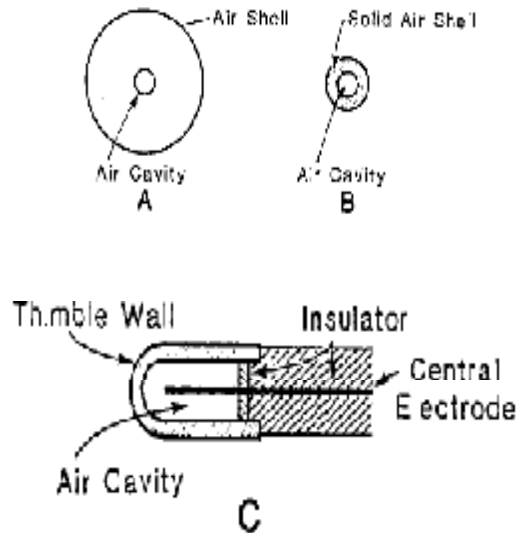


Fig.(4.3): Schematic diagram illustrating the nature of the thimble ionization chamber. A: Air shell with air cavity. B: Solid air shell with air cavity. C: The thimble chamber (Khan, 2003).

4.11.2. Practical thimble chamber

- **Farmer chamber**

This chamber is shown schematically in Fig.(4.4). Actual dimensions of the thimble and the central electrode are indicated on the diagram. The thimble wall is made of pure graphite and the central electrode is of pure aluminum. The insulator consists of polytrichlorofluorethylene. The collecting volume of the chamber is nominally 0.6 cm^3 . There are three electrodes in a well guarded ion chamber: the central electrode or the collector, the thimble wall and the guard electrode. The collector delivers the current to a charge measuring device, an electrometer. The electrometer is provided with a dual polarity HV source to hold the collector at a high bias voltage (e.g., 300V). The thimble is at ground potential and the guard is kept at the same potential as the collector. Most often the collector is operated with a positive voltage to collect negative charge although either polarity should collect the same magnitude of ionization charge, if the chamber is designed with minimal polarity effects. The guard electrode serves two different purposes. One is to prevent leakage current from the high voltage electrode (the collector and the other is to define the ion collecting volume)(Khan, 2003).

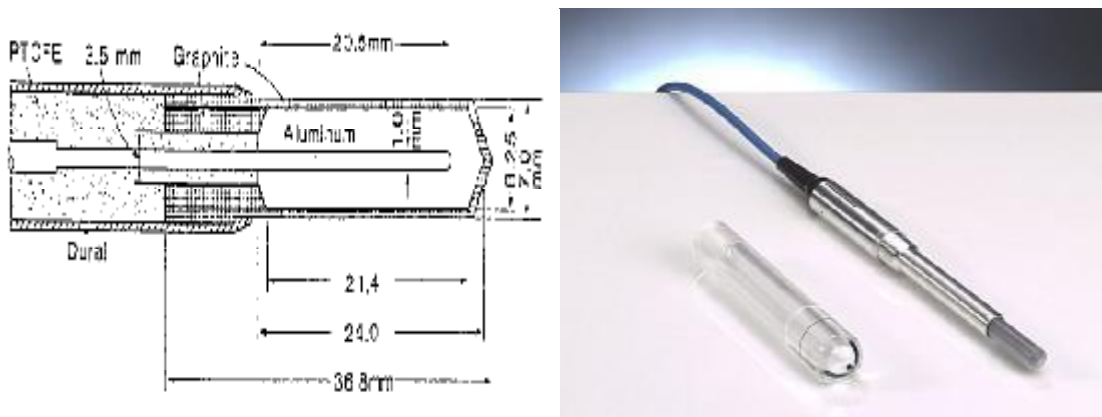


Fig.(4.4): Farmer graphite / aluminum chamber. Nominal air volume, 0.6 ml. PTCFE, polytrichlorofluorethylene (Khan, 2003), www.ptw.de/radiation_therapy.html

- **TLDs**

Many different crystals emit light if they are heated after having been exposed to radiation. This effect is called thermoluminescence, and dosimeters based on this effect are called thermoluminescent dosimeters (TLDs). Some of these TLD crystals include LiF, CaF₂: Mn (CaF₂ containing a small amount of added Mn, which functions as an activator), CaSO₄: Tm, Li₂B₄O₇: Cu, and LiF: Mg, Ti. Thermoluminescent materials are found in the form of loose powder, disks, squares, and rods (Cember and Johnson, 2009).

- **Theory of thermoluminescent dosimetry**

The chemical and physical theory of TLD is not exactly known, but simple models have been proposed to explain the phenomenon qualitatively.

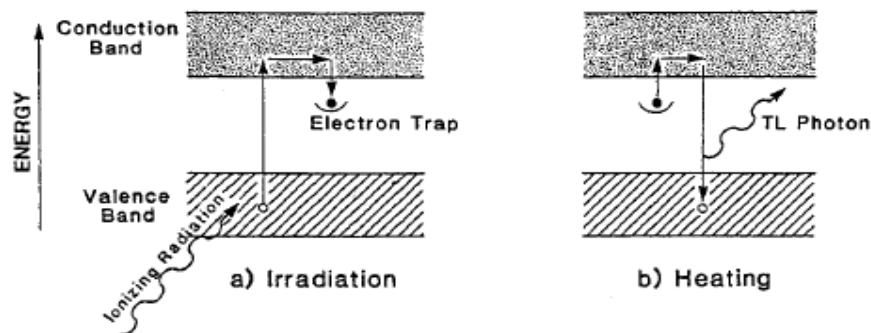


Fig.(4.5): A simplified energy level diagram to illustrate thermoluminescence (Khan, 2003).

Fig.(4.5) shows an energy level diagram of an inorganic crystal exhibiting TL by ionizing radiation. In an individual atom, electrons occupy discrete energy levels. In a crystal lattice, on the other hand, electronic energy levels are perturbed by mutual interactions between atoms and give rise to energy bands: the “allowed” energy bands and the forbidden energy bands. In addition, the presence of impurities in the crystal creates energy traps in the forbidden region, providing metastable states for the electrons. When the material is irradiated, some of the electrons in the valence band (ground state) receive sufficient energy to be raised to the conduction band. The vacancy thus created in the valence band is called a positive hole. The electron and the hole move independently through their respective bands until they recombine (electron returning to the ground state) or until they fall into a trap (metastable state). If there is instantaneous emission of light

owing to these transitions, the phenomenon is called fluorescence. If an electron in the trap requires energy to get out of the trap and fall to the valence band, the emission of light in this case is called phosphorescence (delayed fluorescence) (Khan, 2003).

4.12. Dose Measurements Methodology

- **Determination of ESD from TLD measurements**

There are currently a number of methods available by which one can estimate or measure the patient skin dose. They may be classified as direct or indirect methods.

- Direct method

The direct method of skin dose estimation involves use of small detectors placed on the patient's skin or phantom's surface at the beam entrance location. Types of detectors used for direct method are thermoluminescence dosimetry (TLD), photographic film and diodes or metal oxide semiconductor field effect transistor (MOSFET). Use of TLDs is potentially the most accurate way of determining actual skin dose and the dosimeters are taped to the patient's skin or phantom's surface (Rampado and Ropolo, 2004; Mahesh, 2001).

- **Calculation of ESD from tube output data**

ESD may be calculated in practice by means of knowledge of the tube output. The relationship between X-ray unit current time product (mAs) and the air kerma free in air is established at a reference point in the X-ray field at 80 kVp tube potential. Subsequent estimates of the ESD can be done by recording the relevant parameters (tube potential, filtration, mAs and FSD) and correcting for distances and back scattered radiation according to the following equation (Toivonen, 2001).

$$ESD = OP \times \left(\frac{KV}{80} \right)^2 \times mAs \times \left(\frac{100}{FSD} \right)^2 \times BSF \quad 4.30$$

Where OP is the tube output per mAs measured at a distance of 100 cm from the tube focus along the beam axis at 80 kVp, kV is peak tube voltage (kVp) recorded for any given examination (in many cases the output is measured at 80 kVp) and therefore this

appears in the equation as a quotient to convert the output into an estimate of that which would be expected at the operational kVp. The value of 80 kVp should be substituted with whatever kVp the actual output is recorded at in any given instance. mAs is the tube current-time product which is used in any given instant. FSD is the focus-to-patient entrance surface distance and BSF is the backscatter factor.

ESD is estimated from knowledge of the technique factors, X-ray tube output and backscatter factors (BSFs), in accordance with the following formula:

$$ESD (mGy) = \text{output} (mGymAs^{-1}) \times mAs \times BSF \times ISL \times \left[\frac{(m_{en}/r)_{tis}}{(m_{en}/r)_{air}} \right] \quad 4.31$$

Where the ISL factor is an inverse square law correction from the focus to chamber distance (100 cm) to the focus to skin distance (FSD), and $(m_{en}/r)_{tis}$ and $(m_{en}/r)_{air}$ are the mass energy absorption coefficient for tissue and air, respectively (Armpilia et al, 2002).

The Entrance surface dose (ESD) can be calculated by using following equation:

$$ESD = \frac{Y_D \cdot mAs \cdot D^2}{[L - (d + b)]^2} \cdot BSF \quad 4.32$$

Where Y_D ($\mu Gy/mAs$) is X-ray tube output at distance D normalized by mAs, mAs is the product of the tube current and the exposure time, L is the focus – film distance, b and d are film table top distance and patient equivalent diameter, respectively and BSF is backscatter factor (Ciraj et al, 2003).

- **Determination of ESD from DAP measurements**

Entrance surface doses (ESDs) are calculated using examination techniques and DAP data by the formula:

$$ESD_{DAP} = \frac{I \times DAP_{read} \times FFD^2 \times BSF}{A \times FSD^2} \quad 4.33$$

Where I is the calibration coefficient (dependent on tube potential) for DAP meter, DAP_{read} is the reading of DAP meter, BSF is the backscatter factor (dependent on radiation field size and half value layer (HVL), A is the field size measured on the film of

patient examination, FSD is the focus to skin distance, FFD is the focus to film distance (Kepler et al, 2002).

4.13.Backscatter factor

Backscatter factors are essential in the determination of radiation dose for kilovoltage X-ray beams. For radiotherapy applications, backscatter factor is defined as the ratio of the water kerma at a point on the beam axis at the surface of a sufficiently large (water) phantom to the water kerma at the same point in the primary (i.e., incident) beam, with no phantom present. In alternative definitions the ratios of air kermas or of absorbed doses, for example, IAEA (1987) are used. For the X-ray energy range typically used in radiology, the quantities water kerma and absorbed dose to water have effectively the same values. Values of backscatter factor are primarily a function of half value layer (HVL) and field size but are also dependent to a lesser extent on the anode angle, focus to surface distance (d_{FSD}) and phantom thickness and material. The influence of the anode angle on backscatter factor has been qualitatively investigated by Carlsson (1993). The smaller the anode angle the larger is the heel effect, i.e., the lower is the fluence rate at the anode side of the field. Furthermore, the smaller the anode angle the more the anode material acts as a filter. This latter effect, however, also influences the half value layer. For large beam angles and a small anode angle, the heel effect reduces the value of backscatter factor. For radiology (except mammography), it might be expected that, because of the relatively large d_{FSD} the influence of anode angle on the value of backscatter factor is most likely a few percentage at maximum. Calculations of Grosswendt (1990) demonstrate an increase in backscatter factor with increasing focus to surface distance. For values of focus to surface distance (d_{FSD}) in the range from 30 to 100 cm the variation in backscatter factor at a field size of 20 cm diameter is ~ 3% at maximum. For values of focus to surface distance ≥ 100 cm, the change in backscatter factor with d_{FSD} will be even smaller (ICRU, 2005).

Chapter 5

RADIATION EFFECTS AND DIAGNOSTIC REFERENCE LEVELS

5.1. Ionizing Radiation Interactions With Tissue

The human body consists of tissues and organs. These tissues and organs are composed of cells which consist of molecules and other biological materials. The cell is composed mainly of nucleus, a surrounding liquid known as the cytoplasm and a membrane which forms the cell wall. The cytoplasm is the factory of the cell while the nucleus contains all the information which the cell needs to carry out its function and reproduce itself. The nucleus contains the chromosomes which are small threadlike structures made of genes. The genes consist of deoxyribonucleic acid (DNA) and protein molecules and carry the information, which determine the characteristics of the daughter cell (Akhdar, 2007). The physical interactions of ionizing radiation lead to loss of energy of radiation and production of ionization and excitation of atoms and molecules which may convert into free radicals in pico to femto seconds after physical interaction with atom. These radicals react with neighbouring molecules and produce secondary DNA or lipid radicals by reaction with another neighbouring molecule. Chain reactions may also occur, particularly in lipids, and may play a role in damage to cell membranes. Free radicals are fragments of molecules having unpaired electrons, which have high reactivity with cellular molecules and therefore have a short life. Free radicals are generated in great numbers by ionizing radiation due to the process of energy absorption and breakage of chemical bonds in molecules. These are known to play a major role in radiation effects on biological tissues and organisms. Both electromagnetic and particulate radiation act on cells to cause free radicals and subsequent molecular damage through direct as well as indirect actions (IAEA, 2010). When radiation is absorbed, chemical changes are produced immediately and subsequent molecular damage follows in a short space of time (seconds to minutes). It is after this, during a much longer time span of hours to decades, which the biological damage becomes evident as shown in Fig.(5.1) (Farr, 1997).

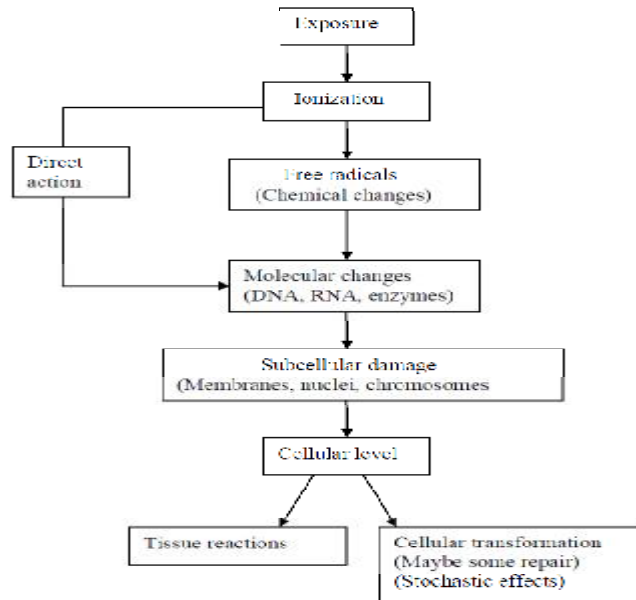


Fig.(5.1): Chain of events following exposure to ionization radiation (Farr, 1997).

If the radiation passes through the tissue without absorption, there would be no biological effects and no radiological image would be produced (Farr, 1997). When ionizing radiation energy is deposited in a macromolecule that is important for the biological effect observed (often DNA for cell killing), it is called a direct effect of radiation (IAEA, 2010).

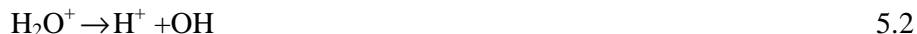
5.1.1. Direct and indirect interaction

In the case of direct interaction, the incident radiation (photons) ionize the atoms of the DNA molecules and break different bonds of the molecules as shown in Fig.(5.2). In the case of indirect interaction and since the most abundant substance in cells is water, the incident radiation break the bonds of water molecules, which produce the free radicals H^+ and OH as shown in Fig.(5.2). These radicals have unpaired electrons and are chemically highly reactive and could cause damages by chemical interaction with important molecules of the cell (Akhdar, 2007).

The process of water ionization may be written as



Where H_2O^+ is the positive ion and e^- is the negative ion. The positive ion dissociates immediately according to the equation



The negative ion e^- may also attach to a neutral water molecule and form H_2O^- ion which may then dissociate and form H and OH^- as following:



The ions H^+ and OH^- are of no consequence, since all body fluids contain significant concentrations of both these ions. The free radicals H and OH may combine with like radicals, or they may react with other molecules in solution. Their most probable fate is determined by the LET of the radiation. In the case of a high rate of LET, such as that which results from passage of an alpha particle or other particle of high specific ionization, the free OH radicals are formed close enough together to enable them to combine with each other before they can recombine with free H radicals, which leads to the production of hydrogen peroxide.



The hydrogen peroxide, which is a very powerful oxidizing agent, can thus affect molecules or cells that did not suffer radiation damage directly. If the irradiated water contains dissolved oxygen, the free hydrogen radical may combine with oxygen to form the hydroperoxyl radical as follows:



The hydroperoxyl radical is not as reactive as the free OH radical and therefore has a longer lifetime than it. This greater stability allows the hydroperoxyl radical to combine with free hydrogen radical to form hydrogen peroxide, thereby further enhancing the toxicity of the radiation (Cember and Johnson, 2009).

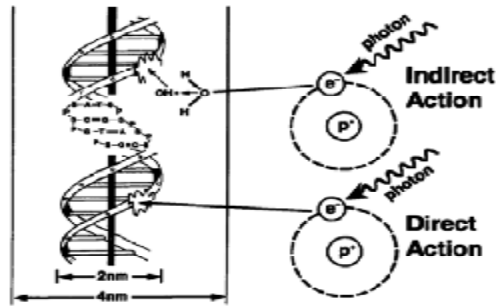


Fig.(5.2): Direct versus indirect action (Hall and Giaccia, 2006).

5.2. Classification of Biological Effects

The biological effects of radiation can be grouped into two types: deterministic effects (tissue reactions) and stochastic effects (cancer and heritable effects) (ICRP 105, 2007).

5.2.1. Deterministic effects (nonstochastic effects)

Deterministic effects are clinically observable only if the radiation dose is above a certain threshold (Kettunen, 2004). The threshold is variable, depending on the nature and condition of the exposed tissue. For doses in excess of the threshold, both the probability and the severity of deterministic effects increase with dose as shown in Fig.(5.4). Examples of deterministic effects include erythema and necrosis of the skin as shown in Fig.(5.3) (Hirshfeld, 2004). The severe deterministic injuries can extend into the subcutaneous fat and muscle (Monaco et al, 2003).



Fig.(5.3): Example of skin damage occurred as a result of exposure to a high X-ray dose during an angiographic procedures (Hirshfeld, 2004).

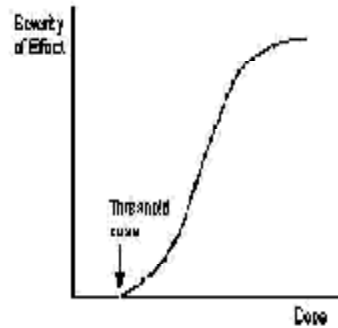


Fig.(5.4): Schematic diagram of the non- stochastic dose response curve (Alshehri, 2006).

5.2.2. Stochastic effects

Stochastic effects from radiation can result from mutational changes in cells that retain their ability to divide (unprepared or unrepaired DNA damage). These modified cells may sometimes initiate a malignant transformation of a cell, leading to the development of a malignant clone and eventually to a cancer. The period between the initiation and the manifestation of the disease may extend from a few years (leukaemia, thyroid cancer) to several decades (colon and liver cancer). In addition, genetic effects may be initiated due to the irradiation of germ cells (hereditary effects). For stochastic effects, no threshold dose is assumed (Kettunen, 2004). The likelihood of stochastic effects increases with the total radiation energy absorbed by the different organs and tissues of the patients shown in Fig.(5.5), but their severity is independent of total dose. The likelihood of stochastic effects is greater in paediatric patients, because of their increased susceptibility to radiation and longer potential life span (Miller et al, 2010). Any dose, no matter how small, has the potential to cause harm. When harm occurs and the damage becomes apparent years after exposures, it is called late effects. The Late effects may include the clouding of the eye lens, known as cataract as shown in Fig.(5.6)(Alshehri, 2006).

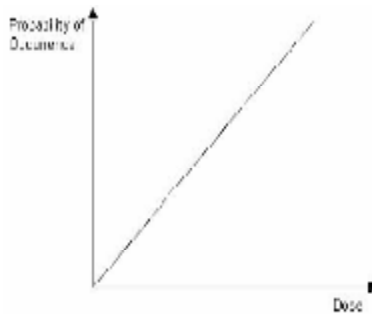


Fig.(5.5): Schematic diagram of the stochastic dose response curve (Alshehri, 2006).



Fig.(5.6): The cataract (Alshehri, 2006).

5.3. Radiation protection

The goal of radiation protection in the radiology department is to prevent tissue reactions by ensuring that radiation doses are kept well below relevant threshold doses and to minimize the probability of stochastic effects (Seeram and Brennan, 2006).

5.3.1. The principles of protection

The international commission on radiological protection (ICRP) recommends three fundamental principles of radiological protection: justification, optimization of protection, and application of dose limits. The first two are source related and apply to all radiation exposure situations. The third applies to staff, but does not apply to medical exposures of patients (ICRP 103, 2007; ICRP 105, 2007).

- **Justification principle**

The principle of justification is that, in general, any decision that alters the radiation exposure situation should do more good than harm. This means that, by introducing a new radiation source, by reducing existing exposure, or by reducing the risk of potential exposure, one should achieve sufficient individual or societal benefit to offset the detriment it causes (ICRP 103, 2007; ICRP 105, 2007).

- **optimization principle**

The likelihood of incurring exposure, the number of people exposed, and the magnitude of their individual doses should all be kept as low as reasonably achievable (ALARA), taking into account economic and societal factors (ICRP 103, 2007).

- **Dose limits**

The total dose to any individual from regulated sources in planned exposure situations other than medical exposure of patients should not exceed the appropriate limits specified by the ICRP (ICRP 103, 2007).

5.4. Quality Assurance (QA)

Quality assurance is a program used by management to maintain the optimal diagnostic image quality with minimum hazards and sufferings to patients (Osibote and Azevedo, 2008).

5.5. Diagnostic Reference Level (DRL)

A diagnostic reference level (DRL), is defined by the international commission on radiological protection (ICRP), as; a form of investigation level, applied to an easily measured quantity, usually the absorbed dose in air, or tissue equivalent material at the surface of a simple phantom or a representative patient (ICRP, 1996). The Council of the European Union defines DRLs as; dose levels in medical radiodiagnostic practices or, in the case of radiopharmaceuticals, levels of activity, for typical examinations for groups of standard sized patients or standard phantoms for broadly defined types of equipment. These levels are expected not to be exceeded for standard procedures when good

and normal practice regarding diagnostic and technical performance is applied (EC,1997).

Table (5.1)Reference values of entrance surface dose recommended by European Commission for standard five years old patients (EC, 1996).

Radiograph	Entrance surface dose (mGy)
Chest Posterior Anterior (PA)	0.1
Chest Anterior Posterior (AP for non-co-operative patients)	0.1
Chest Lateral (Lat)	0.2
Abdomen (AP/PA with vertical/horizontal beam)	1
Pelvis Anterior Posterior (AP)	0.9

The ARPANSA national DRL is the 75th percentile (third quartile) of the spread of the median doses of common protocols from a national survey of imaging practices. A local practice reference level (PRL) is defined as the median value of the spread of doses for common protocols surveyed at the local radiology practice (Mould, 1995).

5.5.1. Objective of DRLs

The objective of a diagnostic reference level is to help avoid excessive radiation dose to the patient that does not contribute additional clinical information value to the medical imaging task

- Typically, diagnostic reference levels are used as investigation levels (i.e. as a quality assurance tool), they are advisory and not a dose limit therefore should not be applied to individual patients.
- The application of a PRL is for the local imaging practice to establish a reference dose for their common imaging protocols that can be used for internal and external comparison.
- DRLs can also be used for international comparative dosimetry (IAEA, 2002).

5.5.2. Applications of DRLs

DRLs, together with an optimization process, help reduce unnecessary patient doses and the consequent radiation risks. A diagnostic reference level can be used to:

- Improve local, regional, or national distributions of observed doses for a general medical imaging task, by reducing the frequency of unjustified high or low dose values.
- Promote a narrower range of doses that represent good practice for a more specific medical imaging task.
- Promote an optimum range of doses for a specified medical imaging protocol.
- Provide a common dose metric for the comparison of PRLs between practices, protocols and modalities.
- Assess the dose impact of the introduction of new protocols.
- Provide compliance with the relevant state and territory regulatory requirements (ARPANSA, 2008).

Chapter 6

MATERIALS AND METHODS

The main objective of this study is to estimate the dose from diagnostic X-ray machines used in two public hospitals (Benghazi Children Hospital and Alhawari General Hospital). The doses were estimated for adult and paediatric patients using dosecal software package. For paediatric patients, the sample was taken from Benghazi Children Hospital, while for adult patients the sample was taken from Alhawari General Hospital. This chapter describes the equipments used, the experimental setup of these equipments and all necessary procedures and techniques needed to achieve the above objective.

6.1. Materials

6.1.1. X-ray machines

- **Benghazi Children Hospital**

A portable X-ray machine of PhilipsPractix 160 type as shown in Fig.(6.1 A) and Fig.(6.1 D) was used for radiography on paediatric patients at Benghazi Children Hospital with permanent filtration of 0.7Al/75kV.

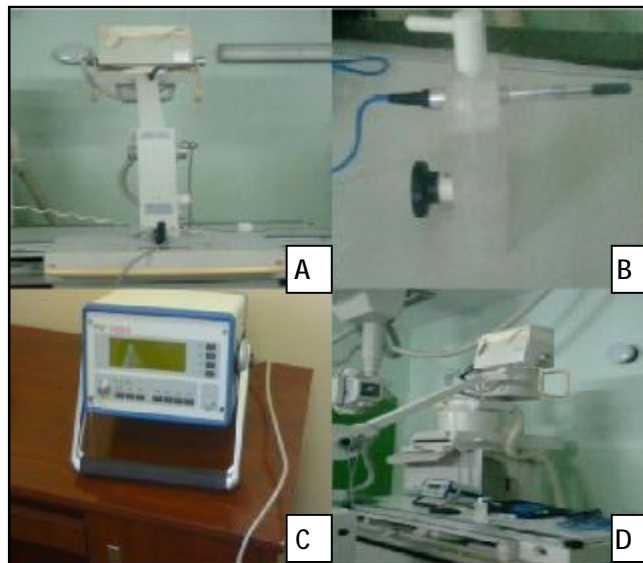


Fig.(6.1): A- X-ray machine, B- Farmer ionization chamber, C- PTW UNIDOS electrometer and D- All of the previous equipments.

- **Alhawari General Hospital**

Philips Bucky Diagnostic X-ray machine as shown in Fig.(6.2) was used for radiography on adult patients at Alhawari General Hospital with permanent filtration of 2.5 Al.



Fig.(6.2): Philips X-ray machine used at Alhawari General Hospital.

6.1.2. Patient data

A total of 247 patients were included in this study. Of those, 146 were paediatric at Benghazi Children Hospital and 101 were adults at Alhawari General Hospital. The exposure parameters employed in radiographic procedures, [peak tube voltage (kVp), exposure current–time product (mAs), and focus to skin distance] and patient information (sex, weight and age) were recorded. For each adult patient, the dose area product (DAP) in $mGym^2$ was recorded.

For Benghazi Children Hospital, the following examinations were used, chest [Antero-Posterior (AP), Postero-Anterior (PA) and Lateral (Lat)], abdomen AP, cervical spine AP and skull lat, while for Alhawari General Hospital, the following examinations were used, abdomen AP, chest PA, cervical spine AP, pelvis AP and lumbar spine AP. In PA projection, the X-ray beam enters the posterior surface of patient's body and exits the anterior surface of the body next to the image, while in AP projection, the X-ray beam enters the anterior surface of patient's body and exits the posterior surface to reach the image receptor. In lateral projection, X-ray beam travels from the left to the right side of the body or vice versa. It is a right lateral projection if the right side of the body is

adjacent to the cassette and a left lateral projection if the left side is adjacent to it as shown in Fig.(6.3).

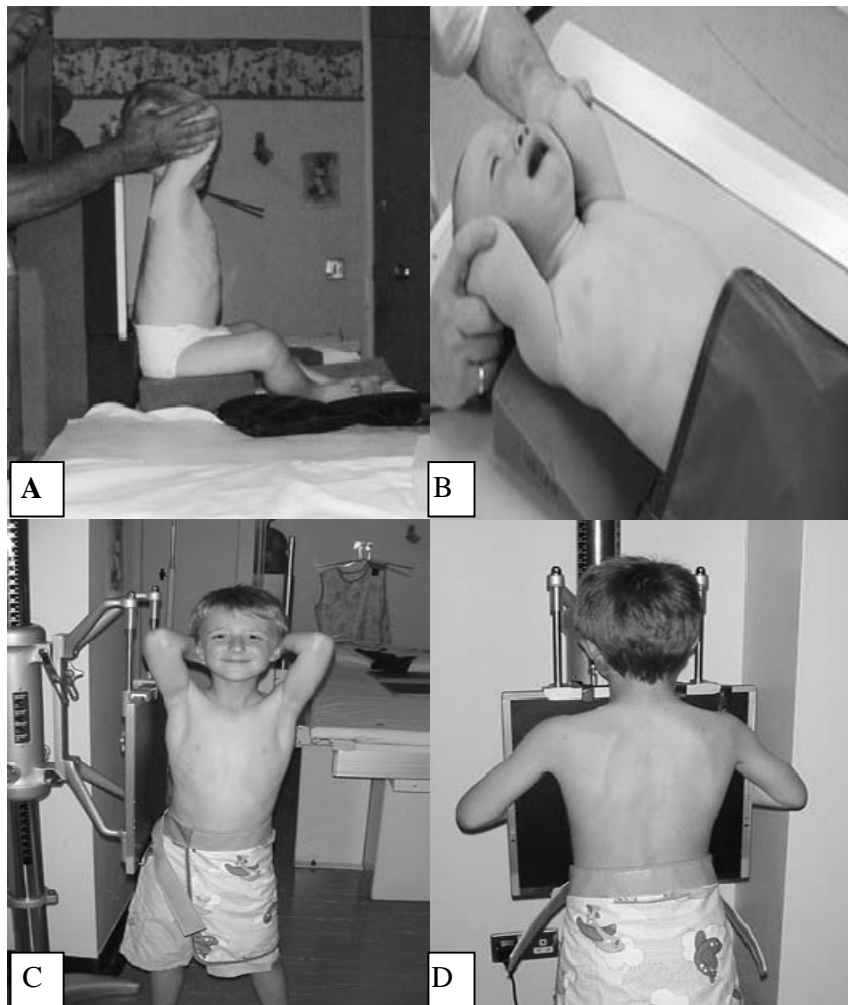


Fig.(6.3): Radiographic procedure on chest. A: Antero-Posterior (erect).B: Antero-Posterior (supine). C: Lateral projection. D: Postero-Anterior projection.

6.2.Method

- **Calibration of X-ray machine used at Benghazi Children Hospital**

The output of the conventional X-ray machine in (mGy/mAs) used for this study was measured by using an ionization chamber and electrometer which had been calibrated at the International Atomic Energy Agency (IAEA) dosimetry laboratory.

Before calculating the dose in mGy, the X-ray machine must be calibrated. The setup for the tube output measurements procedure is depicted in Fig.(6.1) and Fig.(6.4). The calibration procedure was carried out by using a Farmer ionization chamber of type W-30010. The calibrated Farmer ionization chamber was placed at distance (FSD = 100 cm) from the X-ray source and exposed to the X-ray beam at a fixed value of 10 mAs while tube voltage was varied from 40 kV to 110 kV in steps of 10 kV. The ionization chamber was connected to a UNIDOS electrometer for measuring the charge produced in pico Coulomb (pC). The collected charge at the electrometer is then converted to dose in mGy by multiplying by the calibration factor of 54.2 mGy. The results of calibration are grouped in Table (6.1).

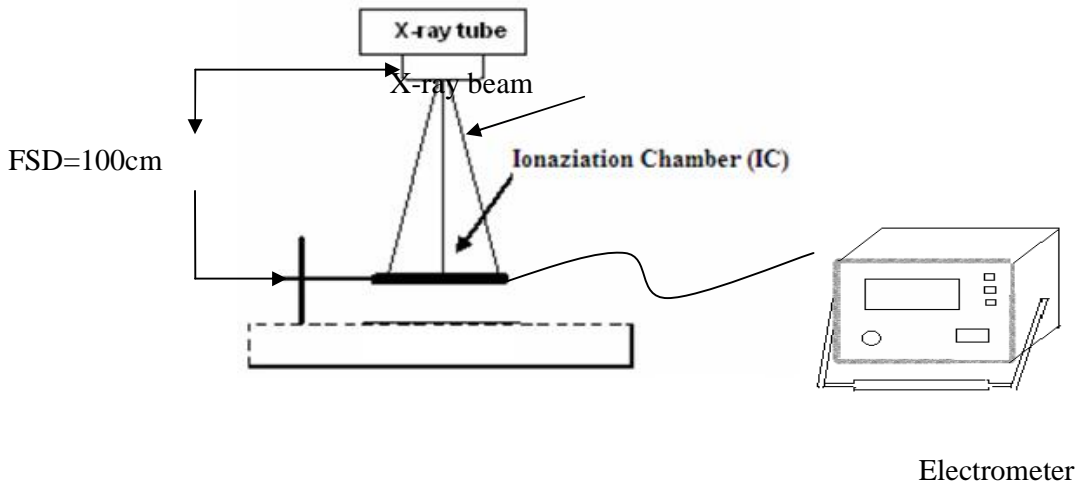


Fig.(6.4): The setup for X-ray tube output measurements.

- **calibration data**

Fig.(6.5) shows the plot of tube output in (mGy/mAs) against tube voltage in (kV). The output data were fitted to second order polynomials in tube voltage. The tube voltage and tube output were strongly positive correlated (correlation coefficient, r is equal to 0.9).

Table (6.1): values of the tube voltage correspond to values of the tube output.

Voltage (kV)	Tube Output (mGy/mAs)
40	0.011
50	0.016
60	0.027
70	0.038
80	0.049
90	0.065
100	0.079
110	0.092

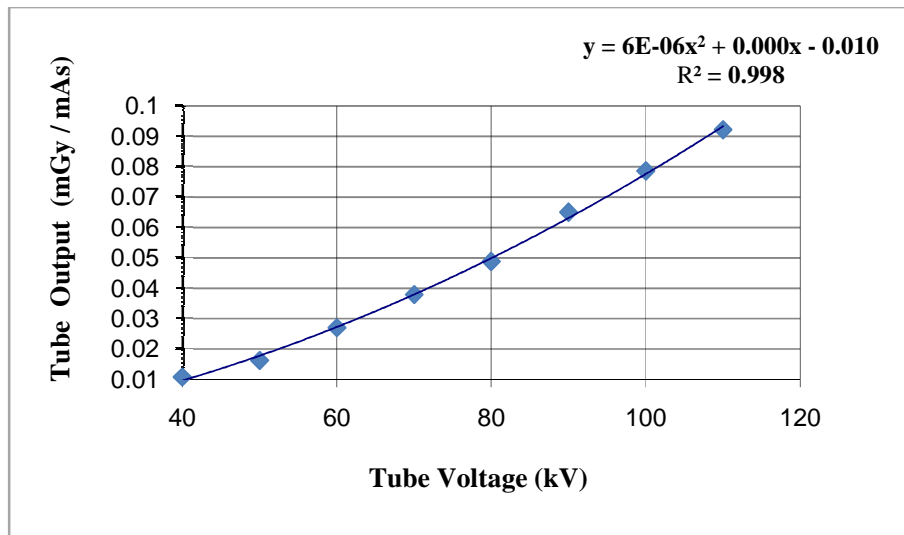


Fig.(6.5): Calibration curve of an X-ray machine for relationship between tube voltage and tube output.

6.3. DoseCal Program

In order to increase the speed and efficiency of the patient dosimetry process, a windows based computer programme, called Dosecal was used in this study. This software has been developed to generate the ESD as well as the ED. The Dosecal software was designed by the Radiological Protection Center of Saint George's Hospital, London. The programme is fast and enables the processing of a large volume of data and serves as a realistic alternative method to Thermoluminescent Dosimeters (TLDs) measurements calculating the ESD and ED from exposure factors recorded at the time of the examination.

In many studies, ESD is directly measured using thermoluminescent dosimeters (TLDs). The value of ESD measured using TLDs had shown a good agreement with that calculated using computational methods as equation (6.1). This was confirmed by the dosimetric survey that was carried out in Rio de Janeiro, Brazil. (Mohamadain, 2004). Once the tube potential, the tube current, the exposure time and the focus to skin distance are known, following formula gives the ESD

$$ESD = OP \times \left(\frac{kV}{80} \right)^2 \times \left(\frac{100}{FSD} \right)^2 \times mAs \times BSF \quad 6.1$$

This formula was used in the Dosecal package. OP is the output in mGy/mAs, of the X-ray tube at 80 kV at a distance of 1m normalized to 10 mAs, kV is the tube potential in kV, mAs is the product of the tube current in mA and the exposure time in seconds, FSD is the focus to skin distance in cm and BSF is the backscatter factor. The dosecal input page is shown in Fig.(6.6).

X-ray tube output



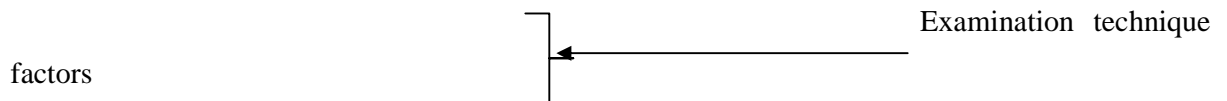


Fig.(6.6): Dosecal input page.

The examinations available in Dosecal software are those listed in NRPB – SR262 (adult) and NRPB-SR279 (paediatric) these software reports,published by the national radiological protection board in the UK contain conversion coefficients, which are applied to the calculated ESDs and measured, DAP values to generate organ and effective doses for a number of common plain film adult and paediatric views. When the input page is complete,the user is required to press the CALC DOSES button to display the ESD and the ED that are derived from the calculated ESDs by applying the kV and examination dependant conversion coefficients selected from the NRPB software reports.The results page of dosecal is shown in Fig.(6.7).



Calculated ESD



Backscatter factor



Calculated effective dose



Fig.(6.7): Dosecalc results page.

The user is then able to generate a list of BOD by pressing the VIEW ORGAN DOSES button. The organ dose page is shown in Fig.(6.8).

	ESD	OWP
Pituitary	2.71E-1	1.00E+0
Spleen	0.000E+0	1.00E+0
Thyroid	2.10E-2	0.00E+0
Eye lenses	0.000E+0	0.00E+0
Salivary glands	2.14E-1	0.00E+0
Stomach	2.17E-1	1.00E+0
Small intestine	7.99E-1	1.00E+0
Upper gastrointestinal	2.17E+0	0.00E+0
Lower gastrointestinal	7.49E-1	0.00E+0
Heart	7.00E-1	1.00E+0
Kidneys	3.88E-1	1.00E+0
Liver	7.13E+0	1.00E+0
Lungs	4.00E-2	0.00E+0

Fig.(6.8): Dosecal organ dosespage.

Chapter 7

RESULTS AND DISCUSSION

- **Benghazi children hospital results**

7.1. Sample distribution according to the type of examination

According to the examination types, the patients were classified into five types of examinations, chest (AP, PA and Lateral projections), abdomen AP projection and skull lateral projection. Of the total sample 146, 124 paediatric patients were undergoing chest AP examination, representing 85% of the total sample. 10 paediatric patients were undergoing chest PA examination, representing 6.8% of the total sample. 4 paediatric patients were undergoing chest lateral examination, representing 2.7% of the total sample. 6 paediatric patients were undergoing abdomen AP examination, representing 4.1% of the total sample. One patient was undergoing skull lateral examination, representing 0.7% of the total sample. One patient was undergoing cervical spine AP, representing 0.7% as shown in Fig.(7.1).

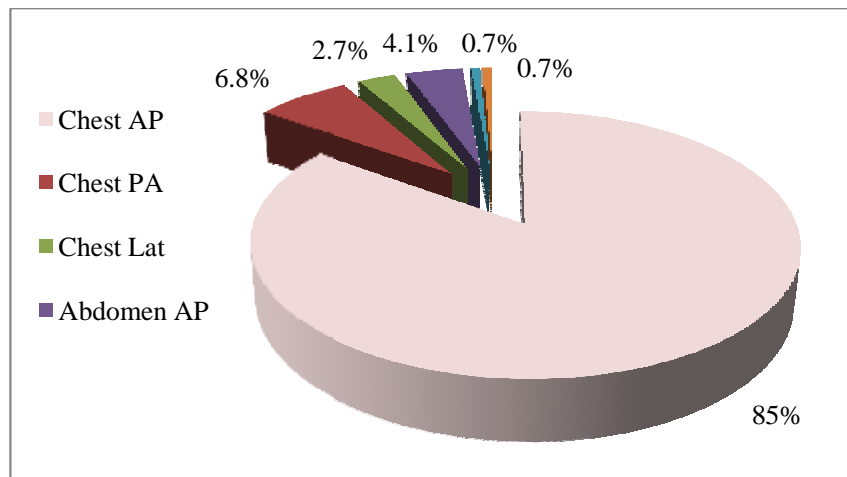


Fig.(7.1): Sample distribution according to examination type at Benghazi Children Hospital.

7.2. Descriptive statistics of exposure parameters and patient data for chest and abdomen X-ray examinations

The technical parameters of exposure, also known as radiographic exposure factors such as tube voltage, tube loading, focus to skin distance in addition to patient data such as weight and patient diameter were recorded. The different statistical terms for exposure parameters and patient data were calculated and grouped in all tables below from Table (7.1) to (7.10). For each age and type of examination, the sample size was also shown.

Table (7.1) Descriptive statistics of exposure parameters and patient parameters for chest AP performed on ages below 1y.

Examination	chest AP				
Age	1y				
Sample Size	86				
	Weight (kg)	Voltage (kV)	Tube Loading (mAs)	FSD (cm)	d (cm)
Mean	6.5	52	5.2	75	11.5
Median	6.8	52	5	74	11.7
Min	2	50	4.5	58	7.1
Max	10.2	56	5.6	101	13.6
3 rd quartile	7.9	53	5.6	79	12.3
STDEV	1.81	1.06	0.34	9.37	1.22
CV%	27.85	2.04	6.54	12.49	10.61

Table (7.2) Descriptive statistics of exposure parameters and patient parameters for chest AP performed on age group (1-5)y.

Examination	chest AP				
Age	(1-5)y				
Sample Size	32				
	Weight (kg)	Voltage (kV)	Tube Loading (mAs)	FSD (cm)	d (cm)
Mean	11.5	53	5.4	77	13.1
Median	10.1	53	5.6	77	13
Min	6.7	52	4.5	63	11.1
Max	19	65	6.3	100	15.9
3 rd quartile	14	53	5.6	79	13.8
STDEV	3.34	2.40	0.40	8.81	1.06
CV%	29.04	4.53	7.41	11.44	8.09

Table (7.3) Descriptive statistics of exposure parameters and patient parameters for chest AP performed on age group (5-10)y.

Examination	chest AP				
Age	(5-10)y				
Sample Size	6				
	Weight (kg)	Voltage (kV)	Tube Loading (mAs)	FSD (cm)	d (cm)
Mean	18.9	56	5.7	72	14.6
Median	19	55	5.6	72	14.7
Min	15	52	5.6	63	13.7
Max	22	65	6.3	84	15.1
3 rd quartile	21.5	55	5.6	74	14.9
STDEV	2.91	4.72	0.29	7.08	0.54
CV%	15.40	8.43	5.09	9.83	3.70

Table (7.4) Descriptive statistics of exposure parameters and patient parameters for chest AP performed on newborn babies

Examination	Chest AP				
Age	Newborn babies				
Sample Size	2				
	Weight (kg)	Voltage (kV)	Tube Loading (mAs)	FSD (cm)	d (cm)
Mean	3.6	52	4.8	73	9.7
Median	3.6	52	4.8	73	9.7
Min	3.5	52	4.5	67	9.6
Max	3.6	52	5	79	9.7
3 rd quartile	3.6	52	4.9	76	9.7
STDEV	0.10	0	0.35	8.49	0.08
CV%	2.78	0	7.29	11.63	0.82

Table (7.5) Descriptive statistics of exposure parameters and patient parameters for chest AP performed on patients with age of 1y

Examination	chest AP				
Age	1y				
Sample Size	20				
	Weight (kg)	Voltage (kV)	Tube Loading (mAs)	FSD (cm)	d (cm)
Mean	9.3	53	5.3	79	12.5
Median	9.3	52	5.6	77	12.6
Min	6.7	52	4.5	66	11.1
Max	11.5	56	5.6	100	13.8
3 rd quartile	10	53	5.6	83	12.9
STDEV	1.25	1.23	0.35	9.63	0.66
CV%	13.44	2.32	6.60	12.19	5.28

Table (7.6) Descriptive statistics of exposure parameters and patient parameters for chest AP performed on patients with age of 5y

Examination	chest AP				
Age	5y				
Sample Size	3				
	Weight (kg)	Voltage (kV)	Tube Loading (mAs)	FSD (cm)	d (cm)
Mean	16.5	53	5.6	69	14.3
Median	16.5	53	5.6	69	14.2
Min	15	52	5.6	63	13.7
Max	18	55	5.6	74	15.1
3 rd quartile	17.3	54	5.6	72	14.7
STDEV	1.50	1.53	0	5.51	0.74
CV%	9.09	2.89	0	7.99	5.17

Table (7.7) Descriptive statistics of exposure parameters and patient parameters for chest PA performed on age group (5-10)y.

Examination	chest PA				
Age	(5 -10)y				
Sample Size	6				
	Weight (kg)	Voltage (kV)	Tube Loading (mAs)	FSD (cm)	d (cm)
Mean	25.7	56	6.6	91	16
Median	25	56	6.7	90	15.5
Min	20	55	5.6	88	14.9
Max	35	57	7.1	93	19
3 rd quartile	26.5	56	7.1	92	16
STDEV	5.20	0.82	0.62	1.76	1.56
CV%	20.23	1.46	9.39	1.93	9.75

Table (7.8) Descriptive statistics of exposure parameters and patient parameters for chest PA performed on age group (10-15)y.

Examination	chest PA				
Age	(10-15)y				
Sample Size	4				
	Weight (kg)	Voltage (kV)	Tube Loading (mAs)	FSD (cm)	d (cm)
Mean	32.1	56	6.7	98	17.5
Median	33	56	6.7	99	17.2
Min	24.5	54	6.3	90	16
Max	38	57	7.1	105	19.7
3 rd quartile	35	56	7.1	101	18
STDEV	5.7	1.26	0.46	6.24	1.56
CV%	17.76	2.25	6.87	6.37	8.91

Table (7.9) Descriptive statistics of exposure parameters and patient parameters for chest LAT performed on age group (0-1)y.

Examination	Chest LAT				
Age	(0 - 1)y				
Sample Size	4				
	Weight (kg)	Voltage (kV)	Tube Loading (mAs)	FSD (cm)	d (cm)
Mean	7.7	56	6.4	91	12.1
Median	7.6	55	5.6	90	12.3
Min	6.8	52	4.5	74	11.2
Max	9	61	10	111	12.6
3 rd quartile	8	58	6.7	107	12.6
STDEV	0.92	4.36	2.44	20.02	0.65
CV%	11.95	7.79	38.13	22	5.37

Table (7.10) Descriptive statistics of exposure parameters and patient parameters for abdomen AP performed on ages under 15y.

Examination	Abdomen AP				
Age	Under 15y				
Sample Size	6				
	Weight (kg)	Voltage (kV)	Tube Loading (mAs)	FSD (cm)	d (cm)
Mean	12.9	52	5.4	97	12.5
Median	6.2	54	5.3	98	11.2
Min	3.3	43	3.6	81	9.7
Max	39.5	56	7.1	112	18.1
3 rd quartile	14.5	55	6.1	104	13.3
STDEV	13.93	4.71	1.21	11.27	3.12
CV%	107.98	9.06	22.41	11.62	24.96

Table (7.11) Exposure parameters and patient parameters for skull Lat

Sample Size	Weight (kg)	Voltage (kV)	Tube loading (mAs)	FSD (cm)	d (cm)
1	33	60	11	85	17.6

Table (7.12) Comparison of exposure parameters used in the present study with the values recommended by European and British guidelines

Examination	Age	Present study (2010)		European Guidelines (1996)	British Guidelines (1998)	
		Tube voltage (kV)	Tube loading (mAs)	Tube voltage (kV)	Tube voltage (kV)	Tube loading (mAs)
Chest AP	Newborn babies	52	5	60-65	*	*
	5y	52-55	5.6	60-80	*	*
Chest PA	(5-10)y	55-57	5.6-7.1	100-150	75	3.5
	(10-15)y	54-57	6.3-7.1		80	3

(*): the value isn't available

7.3. Entrance surface dose (ESD) in mGy and effective dose (ED) in mSv obtained using dosecal software for paediatric patients

The values of ESD and ED were calculated from patient exposure parameters using Dosecal software for chest and abdomen X-ray examinations. For ESD and ED, the minimum, maximum, standard deviation (STDEV), coefficient of variation (CV), mean and median were calculated and tabulated according to kinds of projections AP, PA and LAT as shown in Tables (7.13) and (7.14). The sample size (number of patients) was also shown.

Table (7.13) Descriptive statistics of entrance surface dose (mGy) for paediatric patients undergoing chest and abdomen X-ray examinations

Age	Sample Size	ESD (mGy)							
		Mean	Median	Min	Max	Quartile1 st	3 rd Quartile	STDEV	CV%
ABDOMEN AP									
Under 15y	6	0.147	0.139	0.082	0.205	0.122	0.186	0.05	34.01
CHEST LAT									
(0 -1)y	4	0.225	0.256	0.092	0.296	0.2	0.280	0.09	40
CHEST PA									
(5-10)y	6	0.222	0.227	0.185	0.256	0.209	0.233	0.02	9.01
(10-15)y	4	0.196	0.187	0.162	0.248	0.166	0.217	0.04	20.41
CHEST AP									
< 1y	86	0.228	0.225	0.114	0.365	0.196	0.251	0.05	21.93
(1-5)y	32	0.229	0.222	0.153	0.327	0.206	0.249	0.04	17.47
(5-10)y	6	0.309	0.305	0.240	0.382	0.271	0.349	0.05	16.18
1y	20	0.212	0.211	0.153	0.284	0.197	0.233	0.03	14.15
5y	3	0.304	0.291	0.240	0.382	0.266	0.337	0.07	23.03

Table (7.14) Descriptive statistics of effective dose (mSv) for paediatric patients undergoing chest and abdomen X-ray examinations

Age	Sample Size	ED (mSv)							
		Mean	Median	Min	Max	Quartile1 st	3 rd Quartile	STDEV	CV%
ABDOMEN AP									
Under 15y	6	0.019	0.018	0.011	0.030	0.016	0.021	0.01	52.63
CHEST LAT									
(0 -1)y	4	0.020	0.023	0.008	0.026	0.016	0.026	0.01	50
CHEST PA									
(5-10)y	6	0.016	0.016	0.014	0.020	0.015	0.017	0.002	12.5
(10-15)y	4	0.013	0.012	0.010	0.016	0.011	0.014	0.003	23.08
CHEST AP									
< 1y	86	0.029	0.028	0.015	0.046	0.025	0.032	0.01	34.48
(1-5)y	32	0.028	0.027	0.019	0.045	0.026	0.031	0.01	35.71
(5-10)y	6	0.038	0.037	0.028	0.050	0.032	0.045	0.01	26.32
1y	20	0.027	0.026	0.019	0.035	0.024	0.029	0.004	14.81
5y	3	0.036	0.034	0.028	0.047	0.031	0.041	0.01	27.78

Table (7.15) Mean organ dose (mGy) for paediatric patients undergoing chest and abdomen X-ray examinations

Examination	Age	Lungs	Liver	Kidneys	Heart	Small intestine	Stomach	Gall bladder	Breasts	Brain	Adrenals
Abdomen AP	Under 15 y	0.006	0.041	0.008	0.008	0.033	0.054	0.040	0.001	3.53E-6	0.008
Chest lat	(0-1)y	0.061	0.008	0.004	0.053	7.27E-4	0.020	0.004	0.076	1.63E-4	0.019
Chest PA	(5-10)y	0.064	0.029	0.044	0.018	0.001	0.011	0.007	0.014	6.14E-5	0.069
	(10-15)y	0.051	0.018	0.034	0.012	0.001	0.007	0.005	0.008	5.80E-5	0.052
Chest AP	<1y	0.072	0.027	0.003	0.089	8.04E-4	0.023	0.006	0.158	1.82E-4	0.013
	(1-5)y	0.070	0.034	0.004	0.086	9.44E-4	0.033	0.011	0.159	1.37E-4	0.013
	(5-10)y	0.089	0.062	0.008	0.108	0.002	0.071	0.028	0.215	1.16E-4	0.017

Table (7.15): continued

Examination	Age	Red marrow	Oesophagus	Uterus	Thyroid	Thymus	Spleen	Skin	Pancreas
Abdomen AP	Under 15 y	0.003	0.007	0.032	8.05E-5	5.11E-4	0.014	0.013	0.022
Chest lat	(0-1)y	0.008	0.050	2.39E-4	0.028	0.035	0.034	0.022	0.018
Chest PA	(5-10)y	0.013	0.020	2.42E-4	0.003	0.007	0.059	0.017	0.023
	(10-15)y	0.012	0.016	1.15E-4	0.002	0.005	0.041	0.015	0.015
Chest AP	<1y	0.008	0.035	3.11E-4	0.082	0.132	0.012	0.024	0.015
	(1-5)y	0.008	0.031	2.85E-4	0.048	0.130	0.015	0.021	0.022
	(5-10)y	0.012	0.035	3.73E-4	0.011	0.170	0.026	0.024	0.042

7.4. Comparison of entrance surface dose in the present study with referencedose levels recommended by international bodies and previous studies conducted in other countries.

Table (7.16) Comparison of the mean entrance surface dose in (mGy) calculated using dosecal software with internationaldiagnostic dose levels and other studiescarried out in other countries forpaediatric patients undergoing chest AP examination.

Age (y)	Present study (2010)	Brazil (2009)	Brazil (2004)	Brazil (2006)	Morocco (2010)	Sudan (2004)	Estonia (2002)	UK ^(a) ESAK (1998)	UK ^(b) (1998)	Malaysia ESAK (2006)	Nigeria (2004)	Sweden (1995)
<1	0.228	0.039	0.045	*	*	0.146	0.050	*	0.060	0.27	*	0.10
1-5	0.229	0.058	0.066	0.063	0.162	0.161	0.062	0.030	0.053	0.22	0.52	*
5-10	0.309	0.056	*	*	0.216	*	*	0.040	0.046	0.18	*	*

(*) means the value isn't available - ESAK: Entrance Surface Air Kerma.

(a):Cook, J.V., Shah, K., Pablot, S., et al. *Guidelines on best practice in the X-ray imaging of children; a manual for all X-ray departments.*Queen Mary's Hospital for Children, Carshalton, UK (1998).

(b): Mooney, R. and Thomas, P.S. *Dose reduction in a paediatric X-ray department following optimization of radiographic technique .Br J radiol.*1998; 71(848): 852-860.

Table (7.17) Comparison of the mean entrance surface dose in (mGy) calculated using dosecal software with international diagnostic dose levels and other studies carried out in other countries for paediatric patients' aged 1y and 5y undergoing chest AP examination.

Age (y)	Present study (2010)	Sudan (2008)	Kuwait (2006)	UK ^(c) (2002)	UNSCEAR (2000)	NRPB (2000)	EC (1996)	NRPB (1999)	CEC Trial (1992)	Brazil ESAK (2007)
1	0.212	0.114	0.064	0.08	0.02	0.05	*	*	*	0.055
5	0.304	0.17	*	0.11	0.03	0.07	0.1	0.1	0.089	0.071

examination.

(c): Hart, D., Hillier, M.C. and Wall, B.F. Doses to patients from medical X-ray examinations in the UK-2000 review. NRPB-W14 (Chilton, Didcot: NRPB) (2002).

Table (7.18) Comparison of the mean entrance surface dose in (mGy) calculated using dosecal software with international diagnostic dose levels and other studies carried out in other countries for newborn babies undergoing chest AP examination.

Present Study (2010)	UK ^(d) (2002)	Romania (2011)	Kuwait (2006)	EC (1996)	NRPB (1999)	CEC (1993)	NRPB (2000)	Nigeria (2004)
0.212	0.036	0.092	0.074	0.08	0.08	0.08	0.05	0.35

(d): Armpilia, C.I., Fife, I.A.J. and Croasdale, P.L. Radiation dose quantities and risk in neonates in a special care baby unit. Br J radiol.75:590-595. (2002).

Table (7.19) Comparison of the mean entrance surface dose in (mGy) calculated using dosecal software with other studies carried out in other countries for paediatric patients submitted to chest PA examination.

Age (y)	Present study (2010)	UK ^(a) (1998)ESAK	Estonia (2002)	Malaysia ESAK (2006)	Sudan (2005)	UK ^(b) (1998)
5-10	0.222	0.040	0.097	0.18	0.059	0.046
10-15	0.196	0.050	*	0.17	0.068	0.054

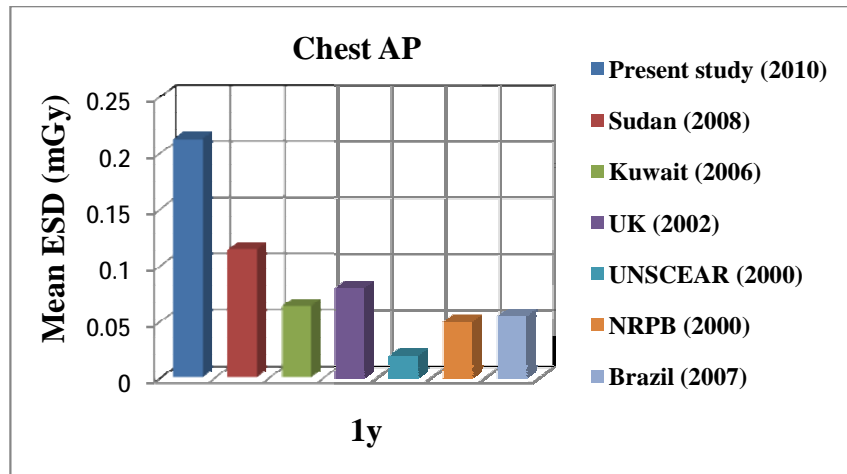


Fig.(7.2) Comparison of the mean entrance surface dose (mGy) in the present study for patients aged 1y undergoing chest AP examination with international diagnostic dose levels and previous studies performed in other countries.

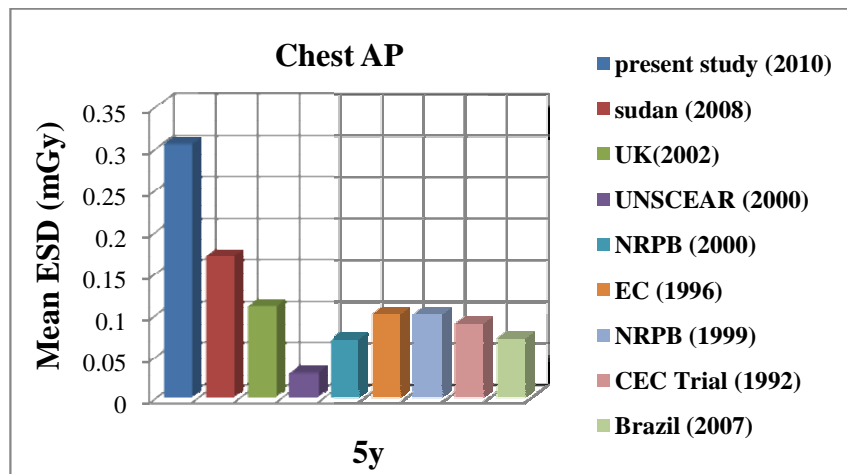


Fig.(7.3) Comparison of the mean entrance surface dose (mGy) in the present study for patients aged 5y undergoing chest AP examination with international reference dose levels and previous studies performed in other countries.

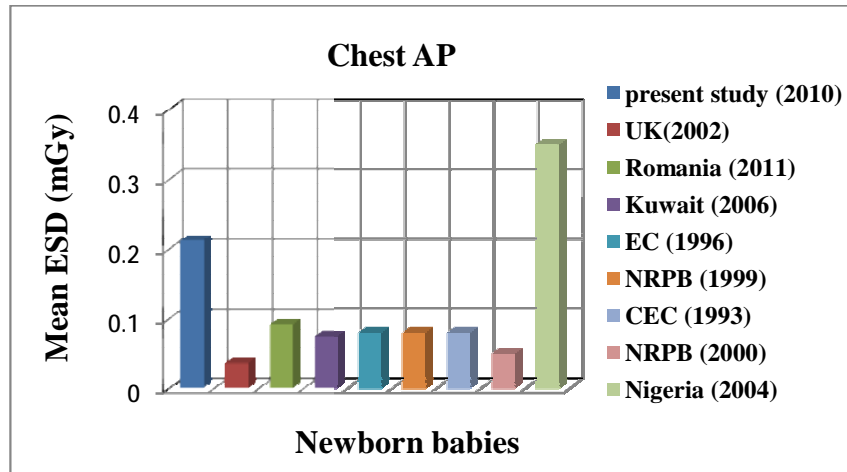


Fig.(7.4): Comparison of the mean entrance surface dose (mGy) in the present study for newborn babies undergoing chest AP examination with international reference dose levels and previous studies performed in other countries.

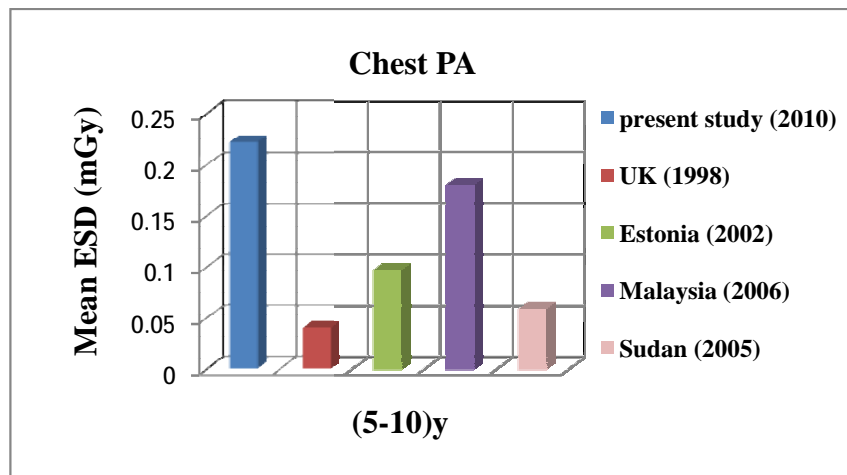


Fig.(7.5): Comparison of the mean entrance surface dose (mGy) in the present study for patients with ages varying from 5 to 10 years undergoing chest PA examination with previous studies performed in other countries

7.5. Patient diameter (d)

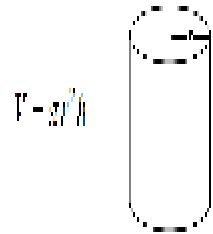
In order to calculate equivalent patient diameter, the patient's body is cylindrical in shape, for cylinder with a known mass m and volume V , we can calculate its density ρ using the following formula:

$$\rho = \frac{m}{V}, \text{hr}^2 V = \pi$$

Since what constitutes the majority of the human body weight is water, the density of the human body is approximately equal to that of the water

$$\rho = \frac{m}{\pi r^2 h}$$

$$r = \sqrt{\frac{m}{\pi h \rho}} \quad (\rho = 1 \frac{\text{gm}}{\text{cm}^3})$$



$$d = 2 \sqrt{\frac{m}{\pi h}}$$

7.1

Where d is the diameter of patient's body in cm, h is the patient's height in cm and m is the patient's mass in grams.

- **Effect of patient diameter (d) on entrance surface dose (ESD)**

For the present study, X-ray tube output was measured at distance equal to 1m and X-ray tube voltage peak in range 40 to 110 kV, in 10 kV steps. The equivalent patient diameter (d) was calculated from the recorded patient's weight and height by using equation (7.1). Film to table top distance (b) was equal to 1cm and backscatter factor (BSF) is equal to 1.35. The value of 1.35 was adopted by Aroua et al, 1998 and Roth, 2008. By applying the equation (4.32) on the patient of this study, there was proportional relationship between equivalent patient diameter and entrance surface dose. As the equivalent patient diameter increased, the entrance surface dose increased. For instance, the patient diameter was 15.01 cm– the calculated ESD value for that patient would be 0.237 mGy. If the diameter of patient was increased by 1cm the value of ESD would increase accordingly as shown in Fig.(7.6).

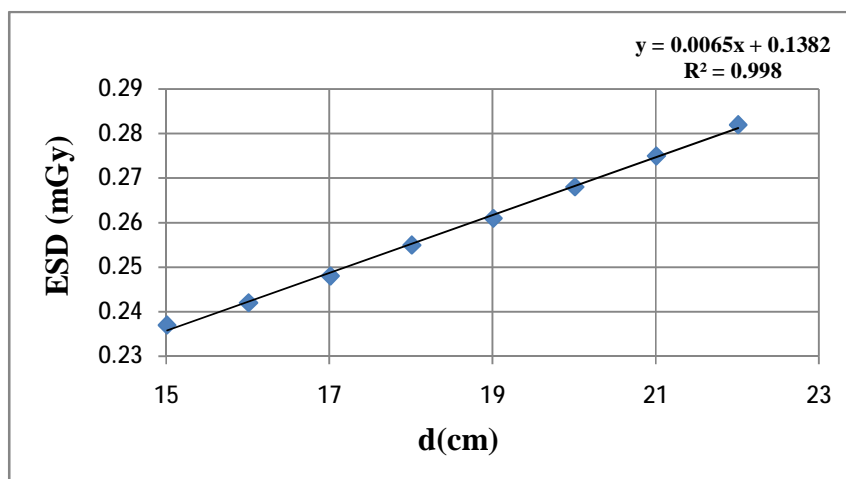


Fig.(7.6): Equivalent patient diameter(cm) against entrance surface dose (mGy)

7.6.Relation between entrance surface dose (ESD)and equivalent patient diameter (d) for chest (AP, PA, Lat projections), abdomen AP, skull Lat and cervical spine APX-ray examinations.

The entrance surface dose values calculated using the equation (4.32) are plotted against equivalent patient diameter (d),patient's age and weight as shown in Figs.(7.7) to (7.60).The equivalent patient diameter in the present study was calculated using the equation (7.1)

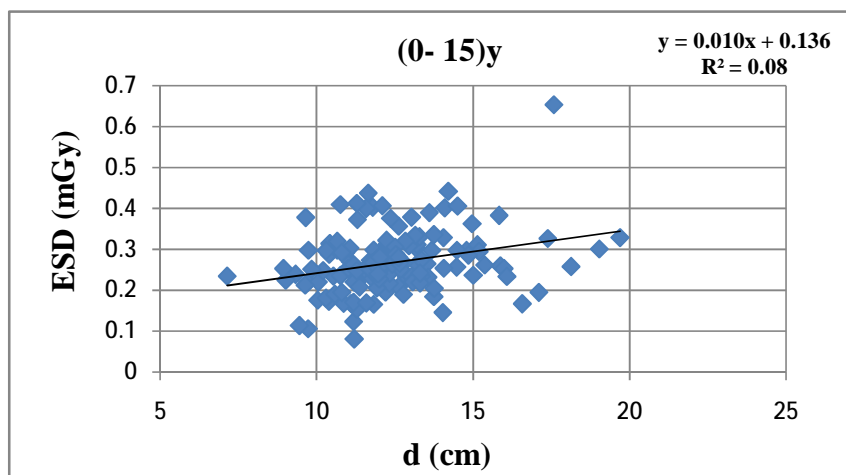


Fig.(7.7) Entrance surface dose (ESD) vs. equivalent patient diameter (d) for age group (0-15)y.

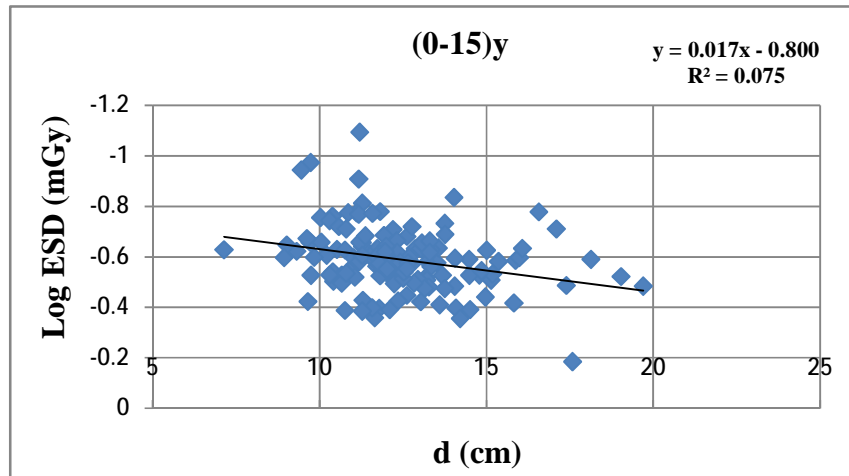


Fig.(7.8) Log entrance surface dose (Log ESD) vs. equivalent patient diameter (d) for age group (0-15)y.

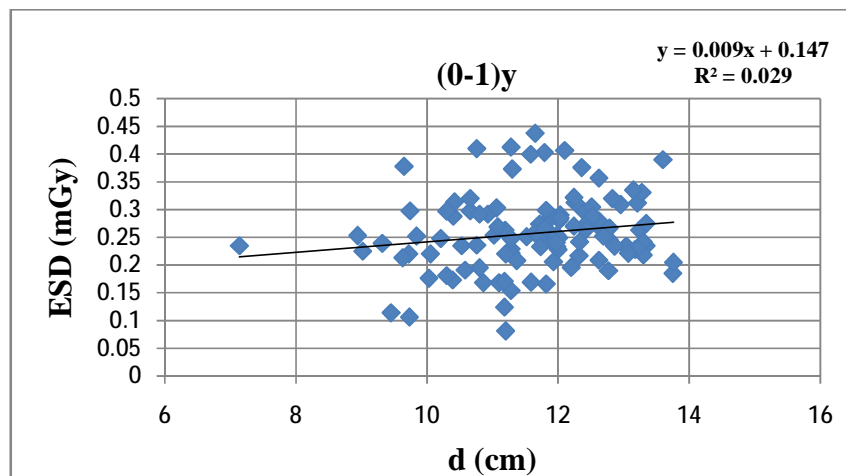


Fig.(7.9) Entrance surface dose (ESD) vs. equivalent patient diameter (d) for age group (0-1)y.

The data for these graphs are found in appendix A {Tables (1A) and (2A)}

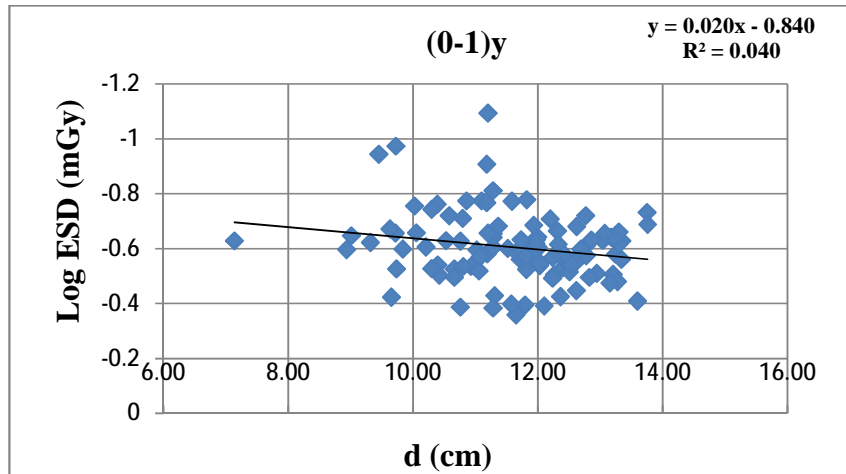


Fig.(7.10) Log entrance surface dose (Log ESD) vs. equivalent patient diameter (d) for age group (0-1)y.

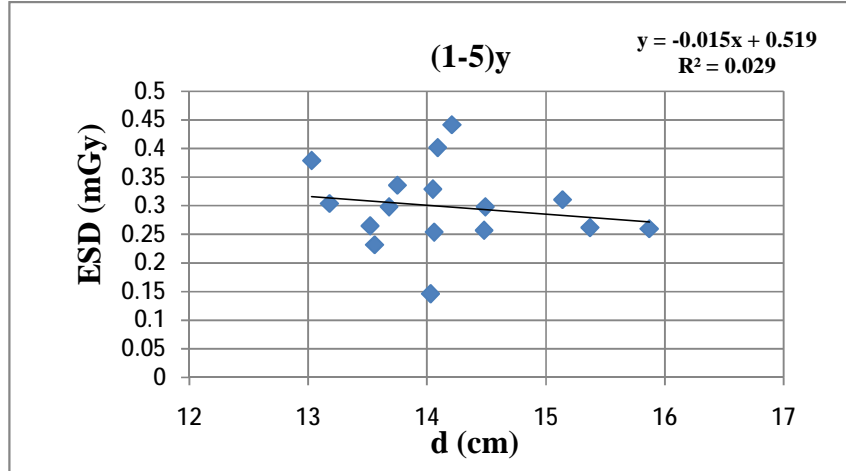


Fig.(7.11) Entrance surface dose (ESD) vs. equivalent patient diameter (d) for age group (1-5)y.

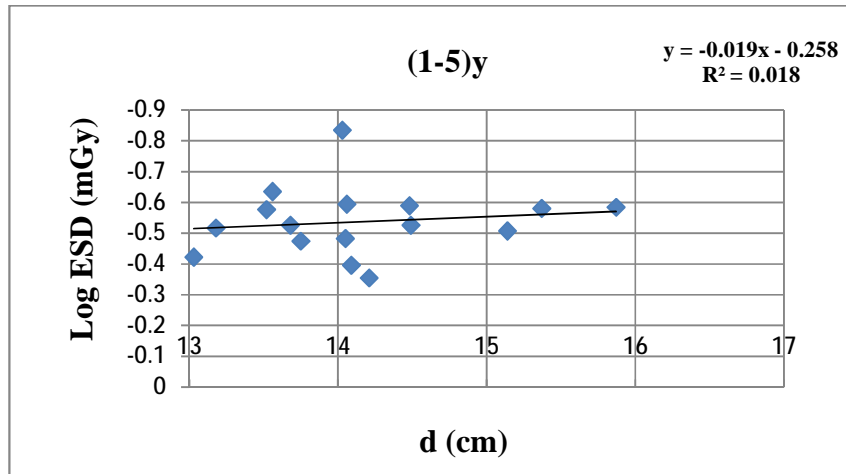


Fig.(7.12) Log entrance surface dose (Log ESD) vs. equivalent patient diameter (d) forage group (1-5)y.

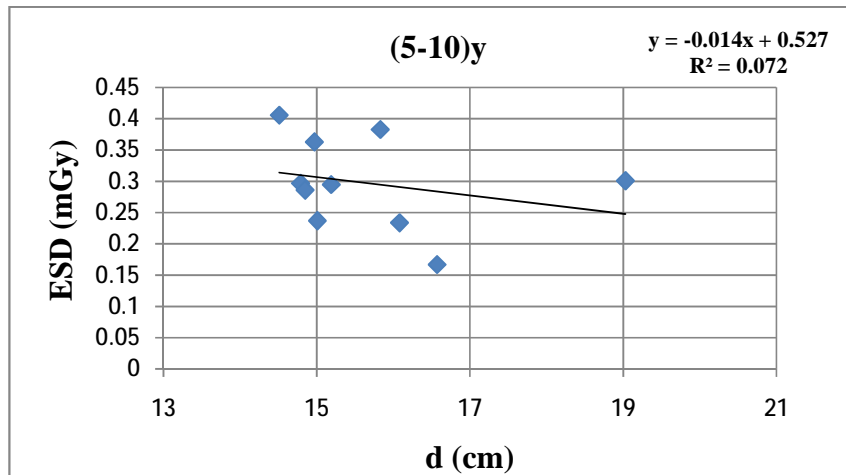


Fig.(7.13) Entrance surface dose (ESD) vs. equivalent patient diameter (d) for agegroup (5-10)y.

The data for these graphs are found in appendix A {Tables (3A) and (4A)}

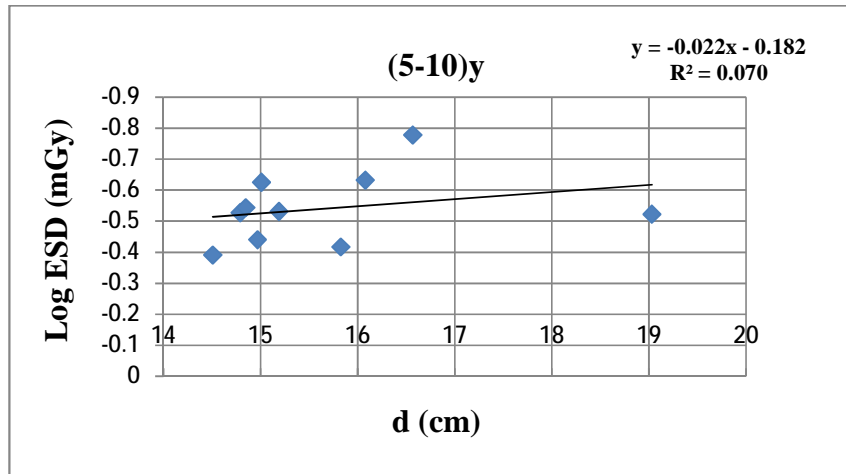


Fig.(7.14) Log entrance surface dose (Log ESD) vs. equivalent patient diameter (d) for age group (5-10)y.

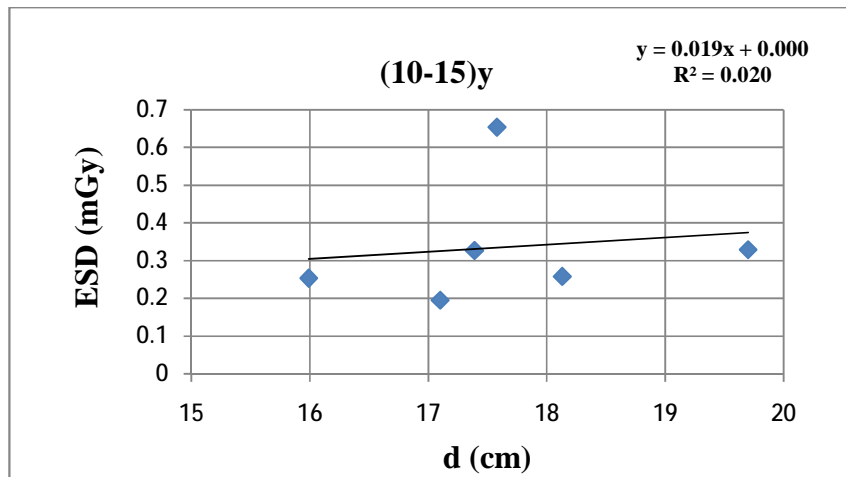


Fig.(7.15) Entrance surface dose (ESD) vs. equivalent patient diameter (d) for age group (10-15)y.

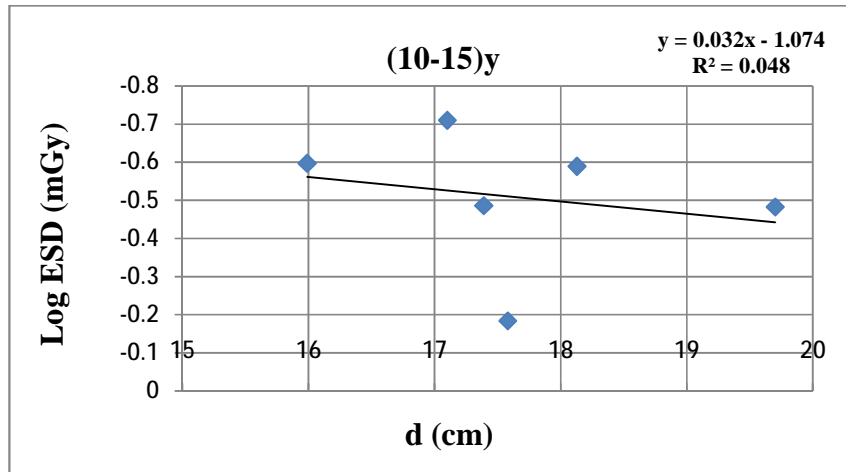


Fig.(7.16) Log entrance surface dose (Log ESD) vs.equivalent patient diameter (d)for agegroup(10-15)y

7.7. Relation between entrance surface dose (ESD) with age and weight for chest (AP, PA, Lat projections), abdomen AP, Skull Lat and cervical spine AP examinations.

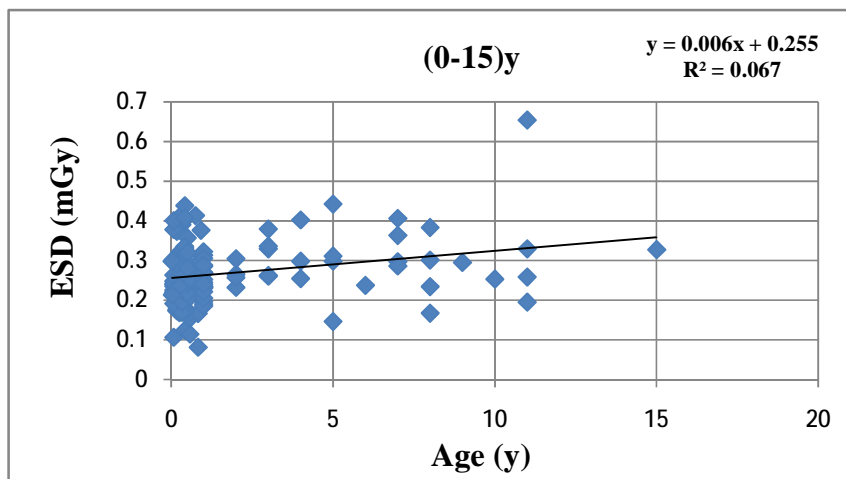


Fig.(7.17) Entrance surface dose (ESD) vs. age from (0-15)y.

The data for these graphs are found in appendix A {Tables (1A) and (5A)}

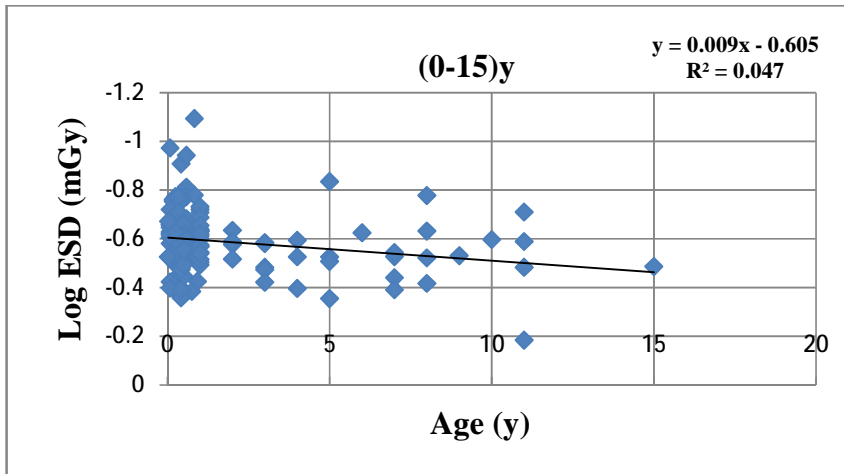


Fig.(7.18) Log entrance surface dose (Log ESD) vs. age from (0-15)y.

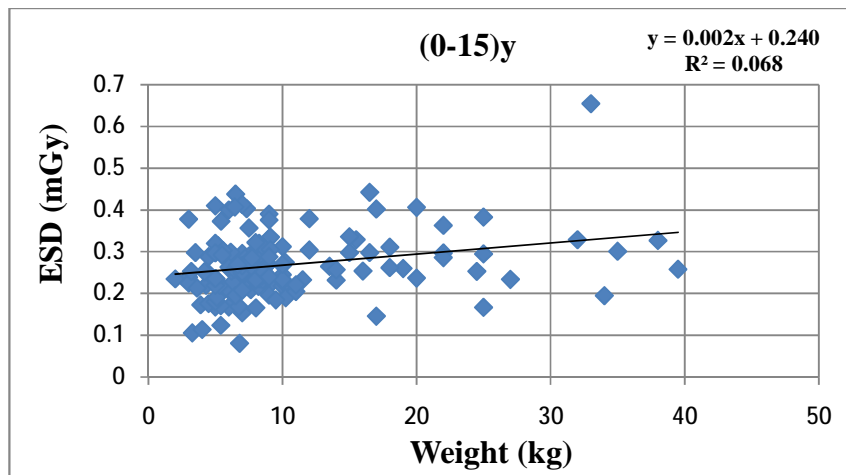


Fig.(7.19) Entrance surface dose (ESD) vs. weight for age group (0-15)y.

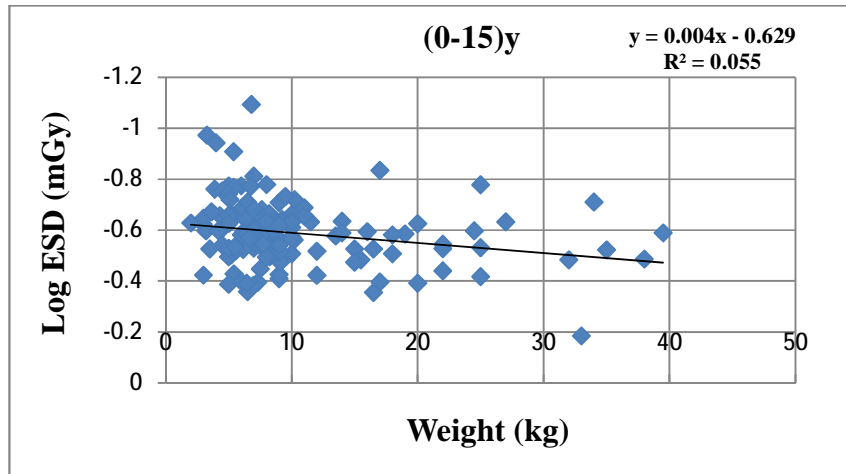


Fig.(7.20) Log entrance surface dose (Log ESD) vs. weight for age group (0-15)y.

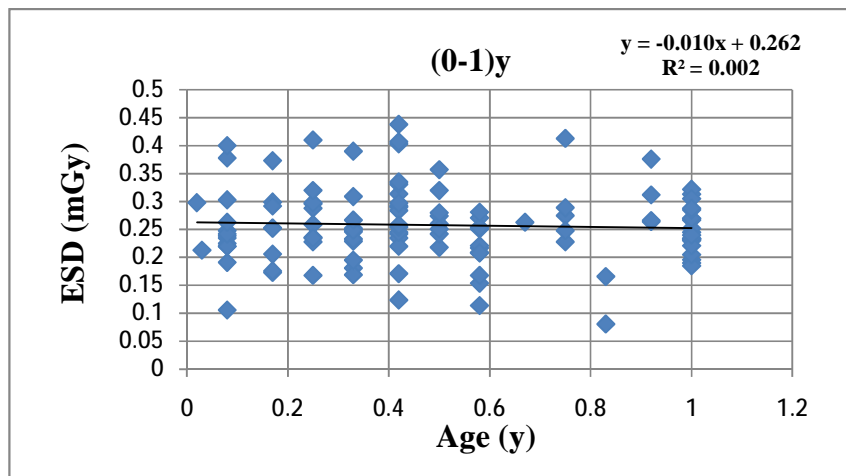


Fig.Entrance surface dose (ESD) vs. age from (0-1)y. (7.21)

The data for these graphs are found in appendix A {Tables(1A) and (2A)}

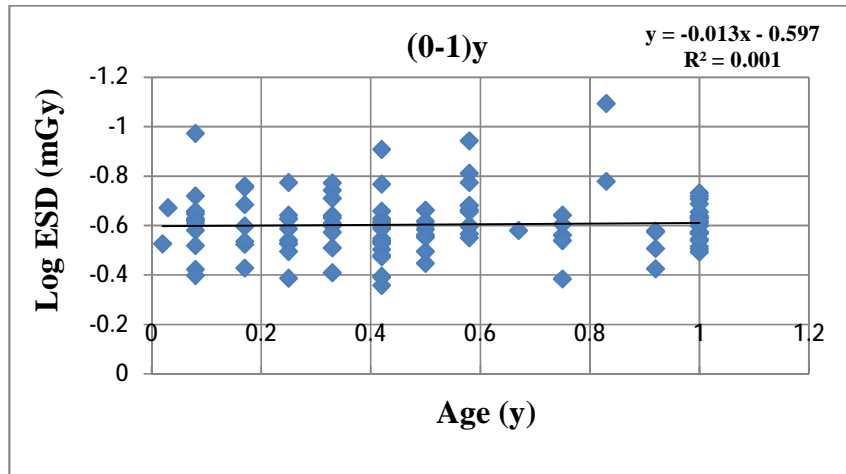


Fig. Log entrance surface dose (Log ESD) vs. age from (0-1)y. (7.22)

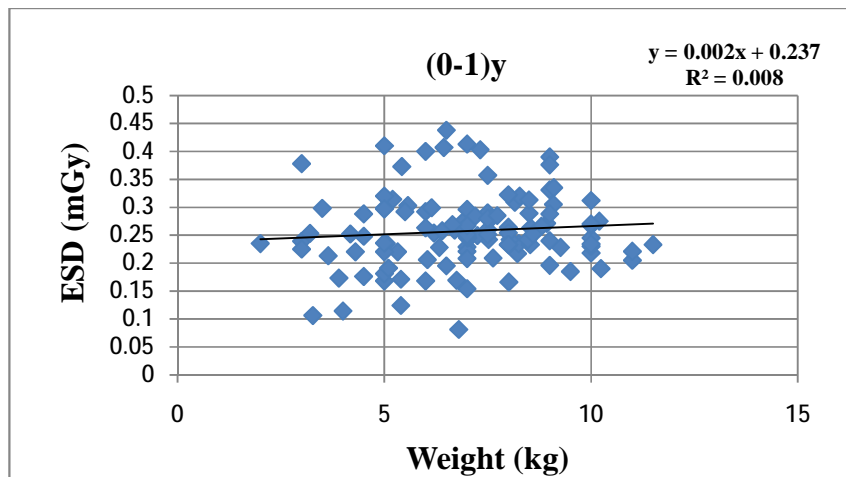


Fig.(7.23) Entrance surface dose (ESD) vs. weight for age group (0-1)y.

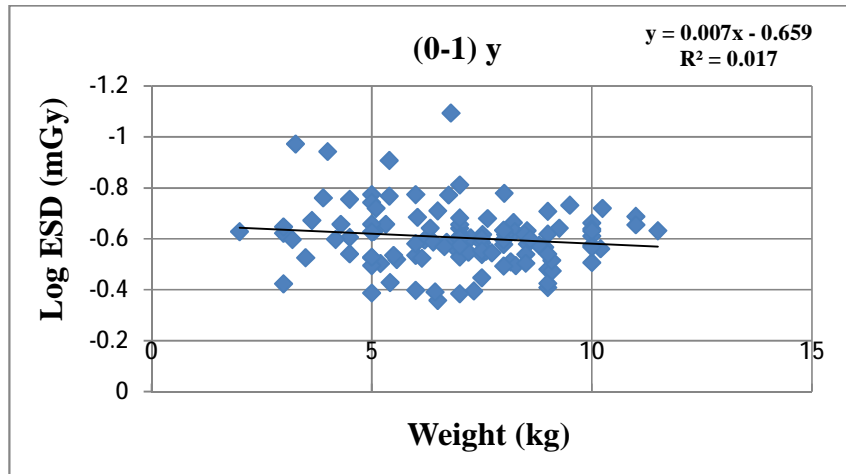


Fig.(7.24) Log entrance surface dose (Log ESD) vs. weight for age group (0-1)y.

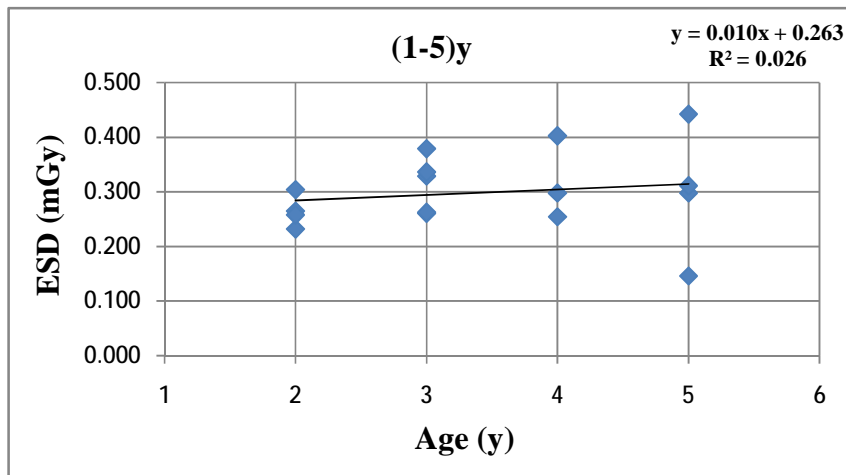


Fig.(7.25) Entrance surface dose (ESD) vs. age from (1-5)y.

The data for these graphs are found in appendix A {Tables (2A) and (3A)}

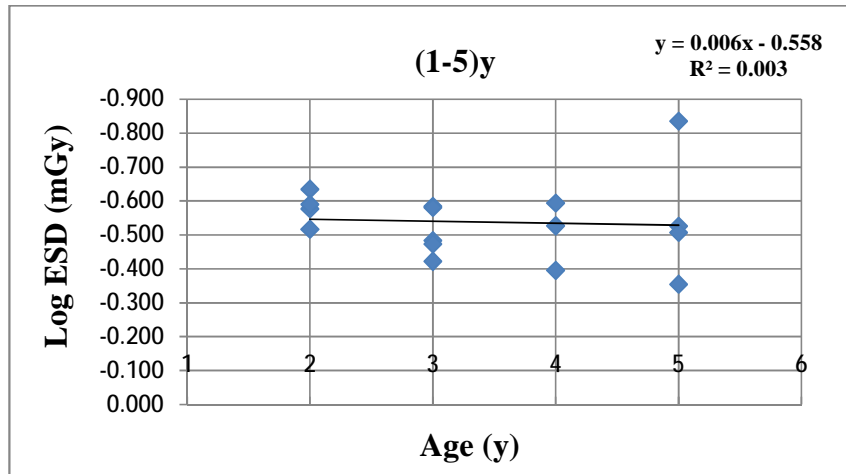


Fig.(7.26) Log Entrance surface dose (Log ESD) vs. age from (1-5)y.

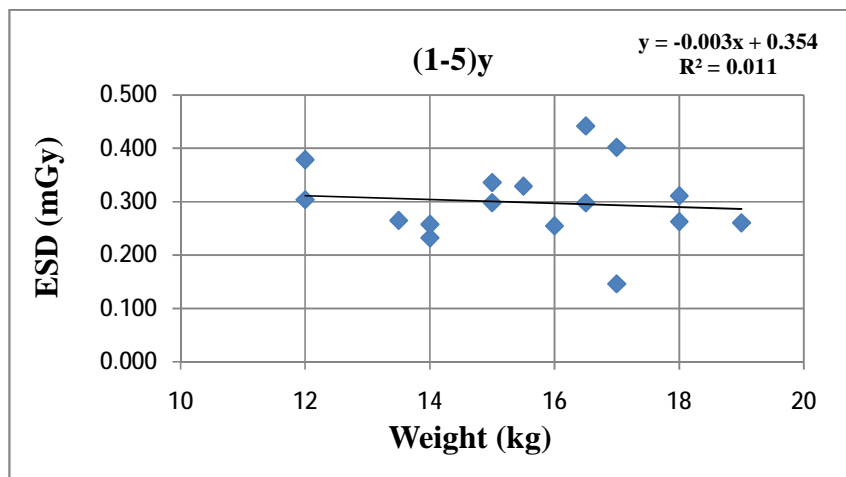


Fig.(7.27) Entrance surface dose (ESD) vs. weight for age group (1-5)y.

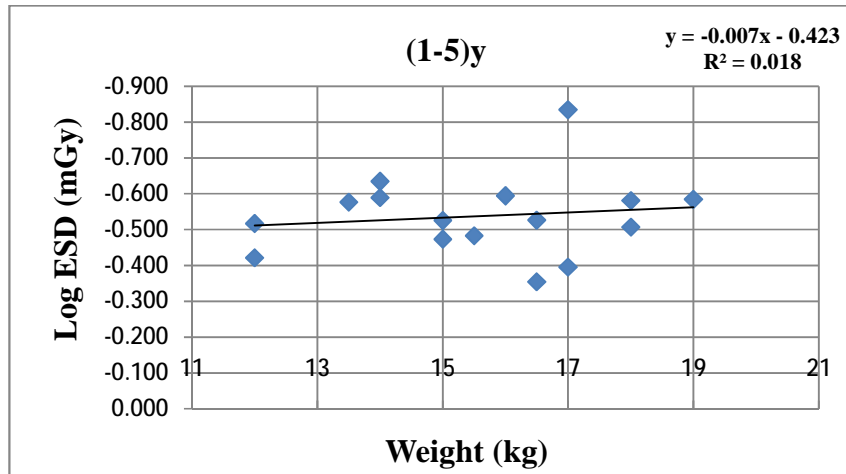


Fig.(7.28) Log entrance surface dose (Log ESD) vs. weight for age group (1-5)y.

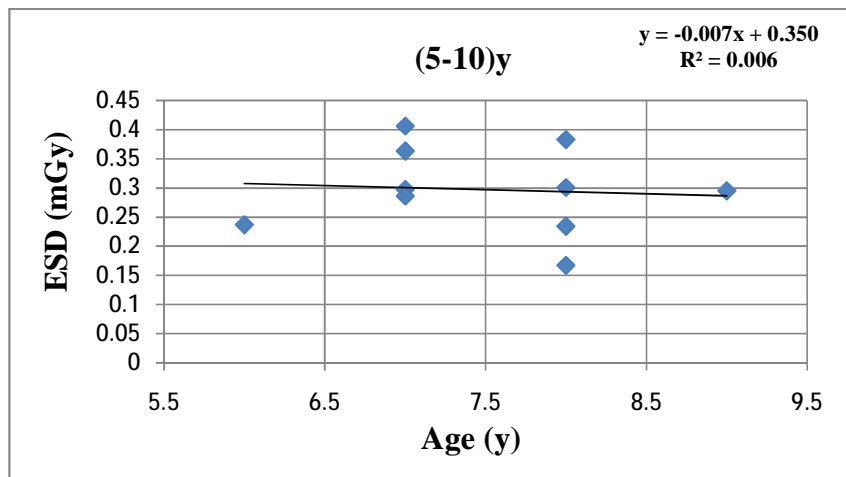


Fig.(7.29) Entrance surface dose (ESD) vs. age from (5-10)y.

The data for these graphs are found in appendix A (Tables (3A) and (4A))

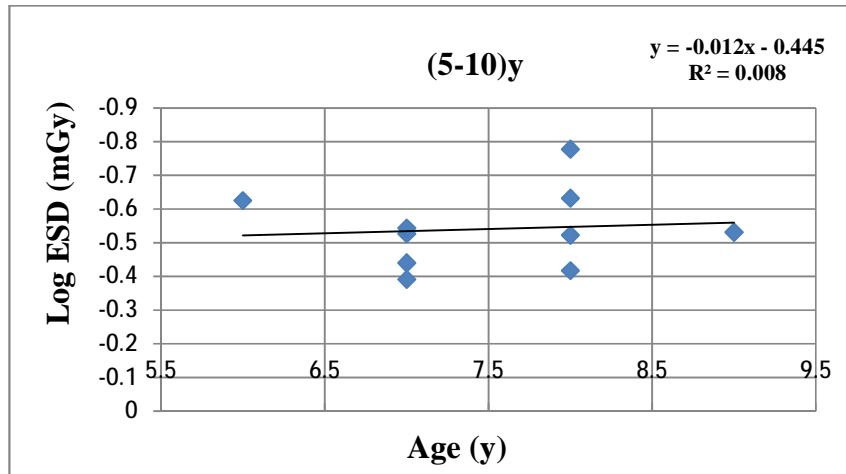


Fig.(7.30) Log entrance surface dose (Log ESD) vs. age from (5-10)y.

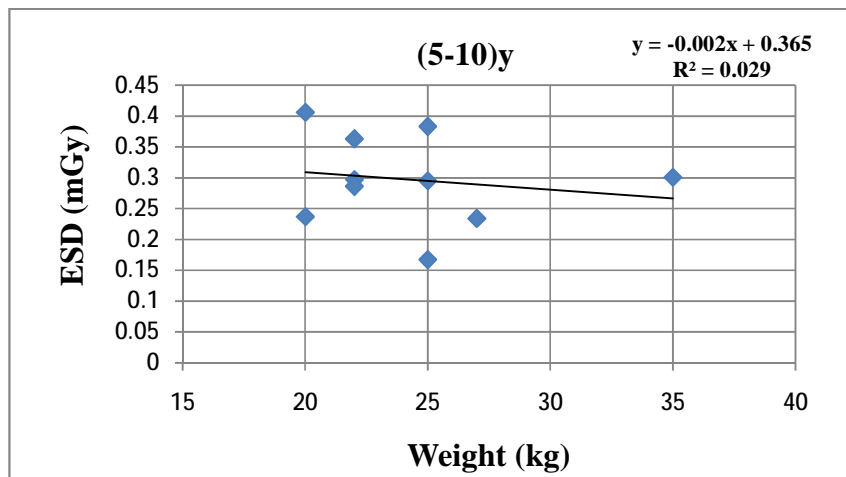


Fig.(7.31) Entrance surface dose (ESD) vs. weight for age group (5-10)y.

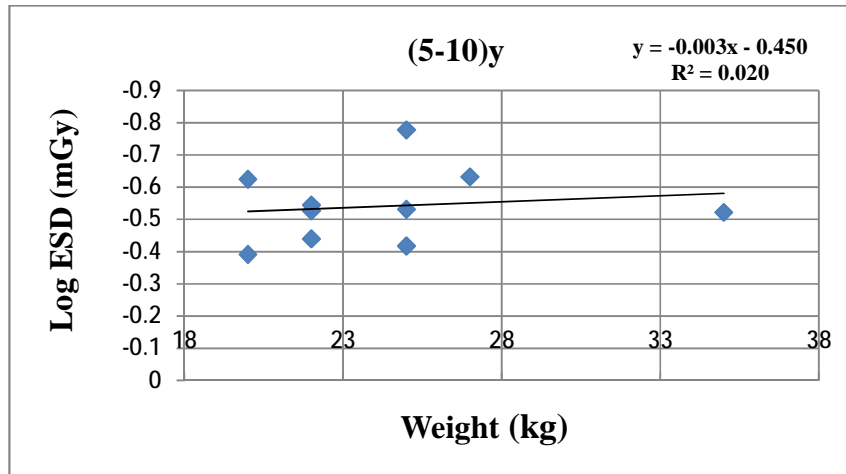


Fig.(7.32) Log entrance surface dose (Log ESD) vs. weight for age group (5-10)y.

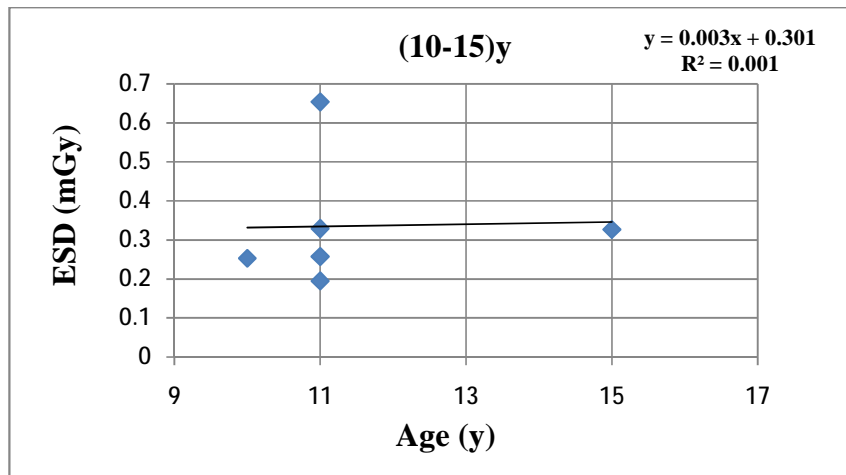


Fig.(7.33) Entrance surface dose (ESD) vs. age from (10-15)y.

The data for these graphs are found in appendix A {Tables (4A) and (5A)}

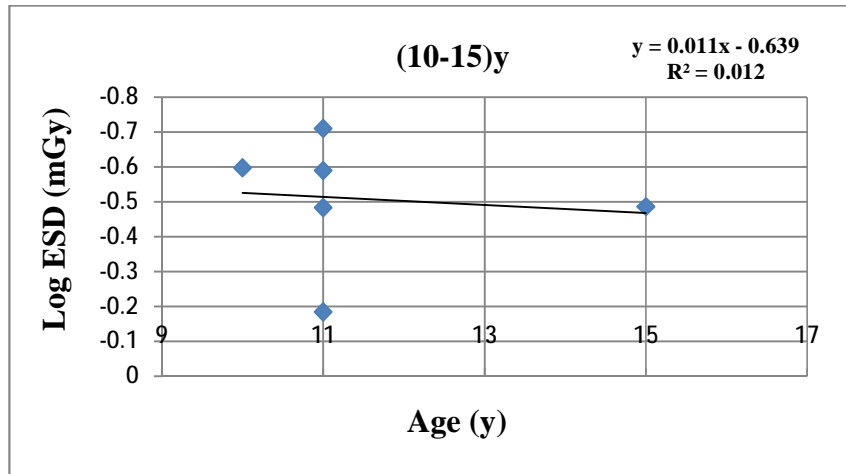


Fig.(7.34) Log entrance surface dose (Log ESD) vs. age from (10-15)y.

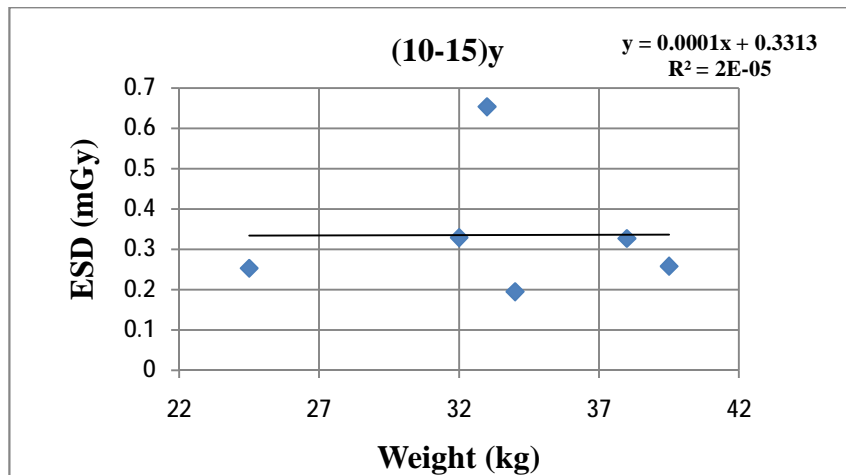


Fig.(7.35) Entrance surface dose (ESD) vs. weight for age group (10-15)y.

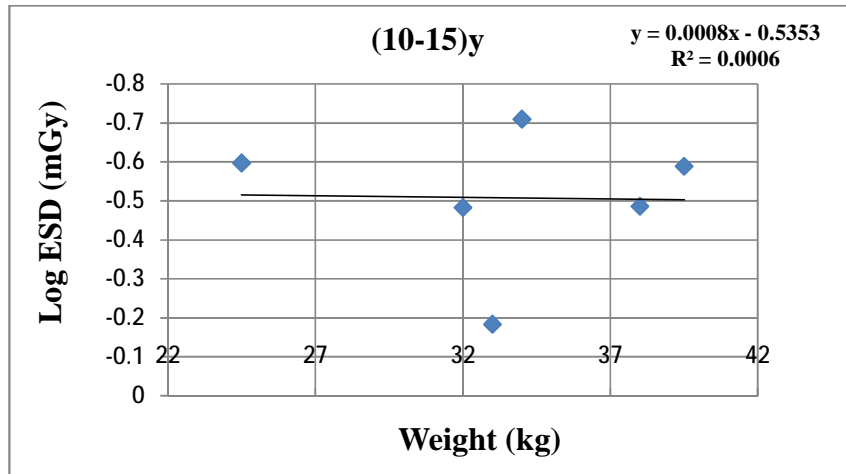


Fig.(7.36) Log entrance surface dose (Log ESD) vs. weight for age group (10-15)y.

7.8. Relation between entrance surface dose (ESD) with age and weight for chest AP

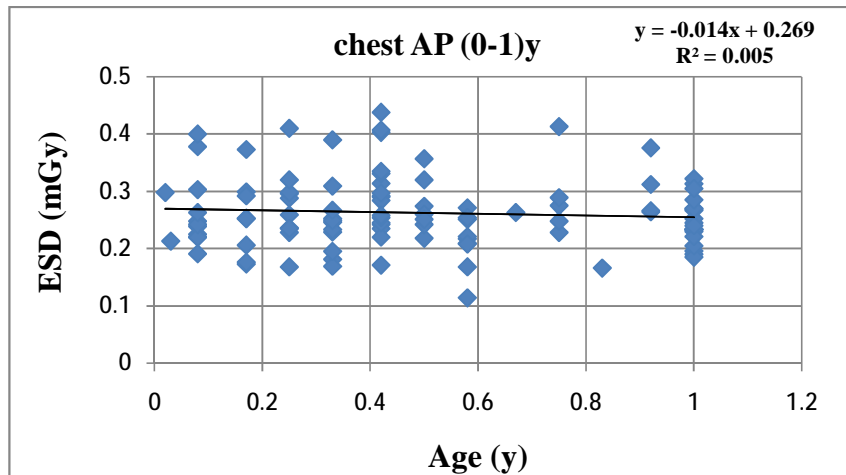


Fig.(7.37) Entrance surface dose (ESD) vs. age from (0-1)y.

The data for these graphs are found in appendix A {Tables (5A) and (6A)}

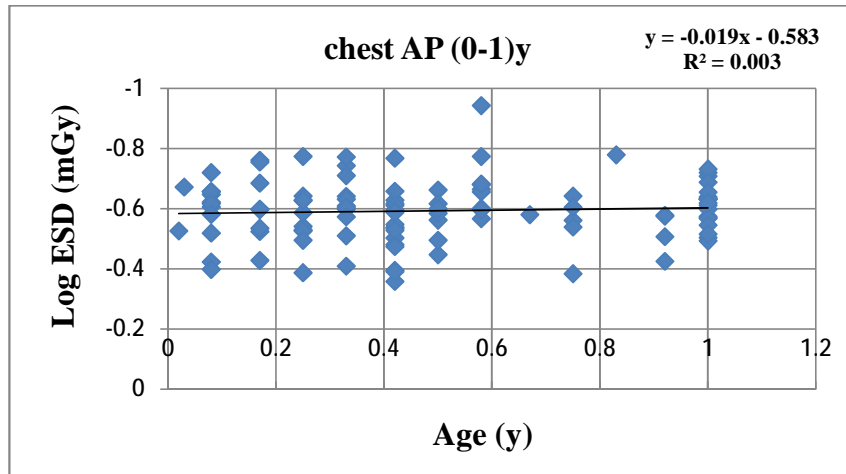


Fig.(7.38) Log entrance surface dose (Log ESD) vs. age from (0-1)y

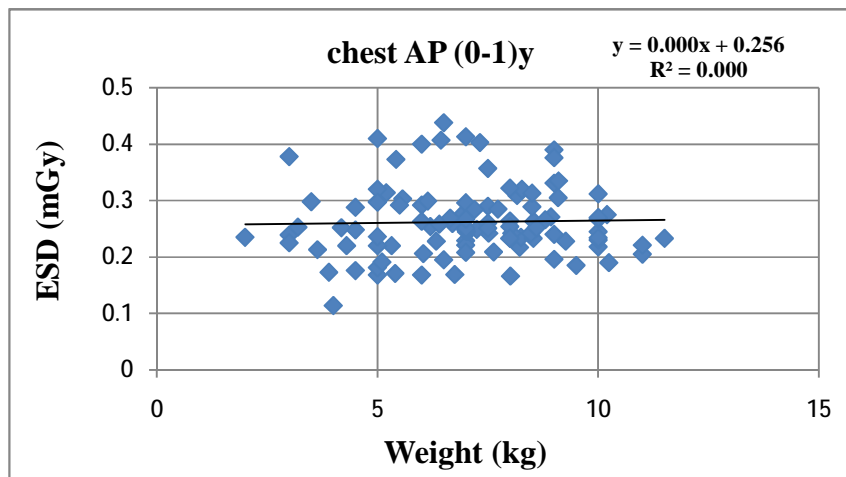


Fig.(7.39) Entrance surface dose (ESD) vs. weight for age group (0-1)y.

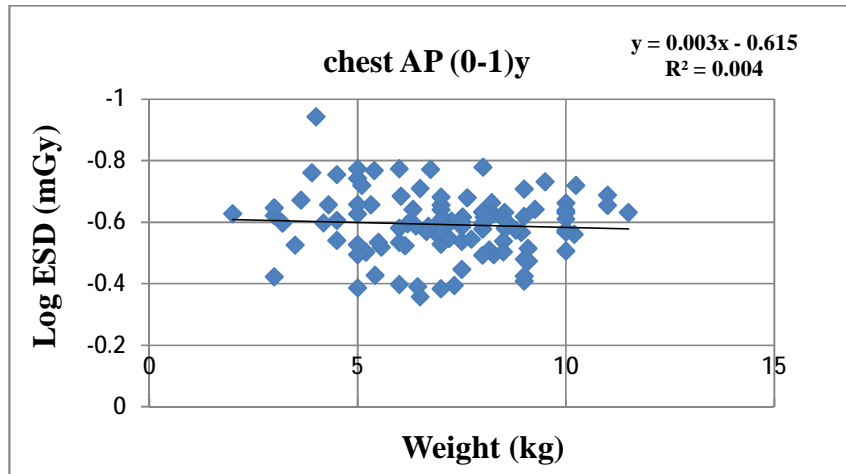


Fig.(7.40) Log entrance surface dose (Log ESD) vs. weight for age group (0-1)y.

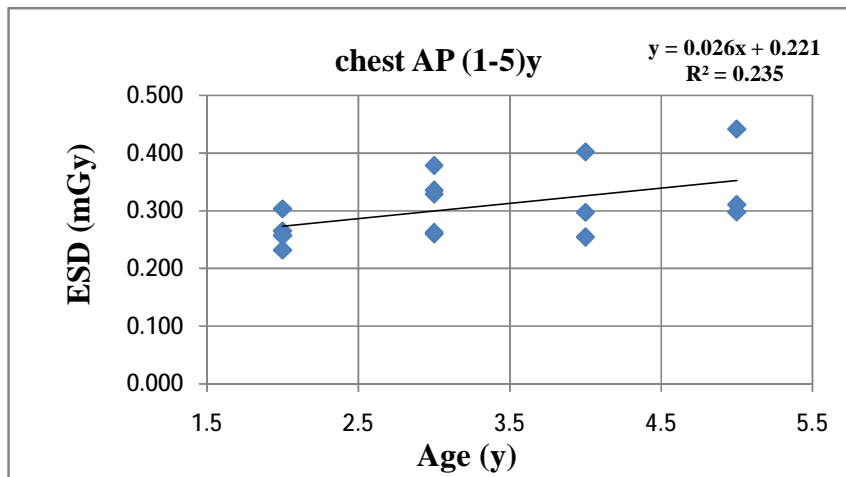


Fig.(7.41) Entrance surface dose (ESD) vs. age from (1-5)y.

The data for these graphs are found in appendix A {Tables (6A) and (7A)}

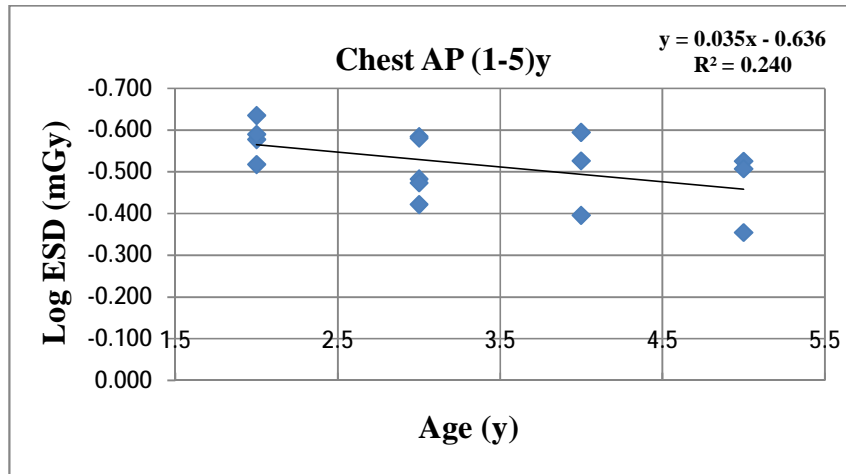


Fig.(7.42) Log entrance surface dose (Log ESD) vs. age from (1-5)y.

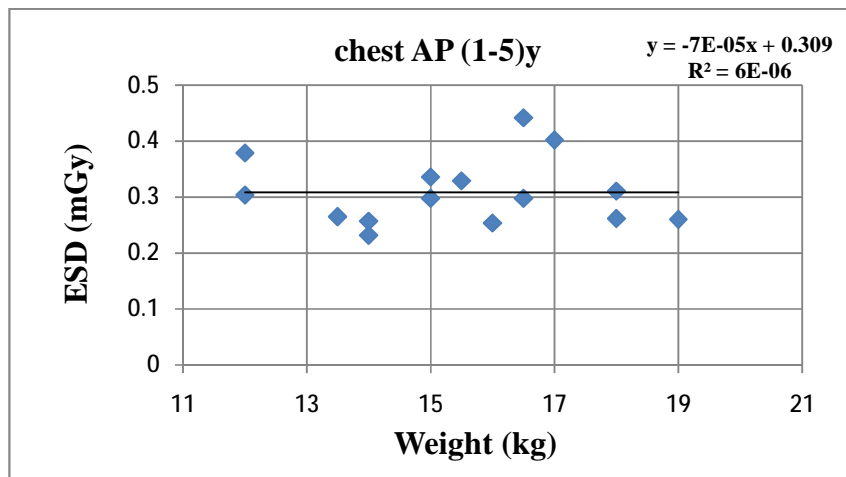


Fig.(7.43) Entrance surface dose (ESD) vs. weight for age group (1-5)y.

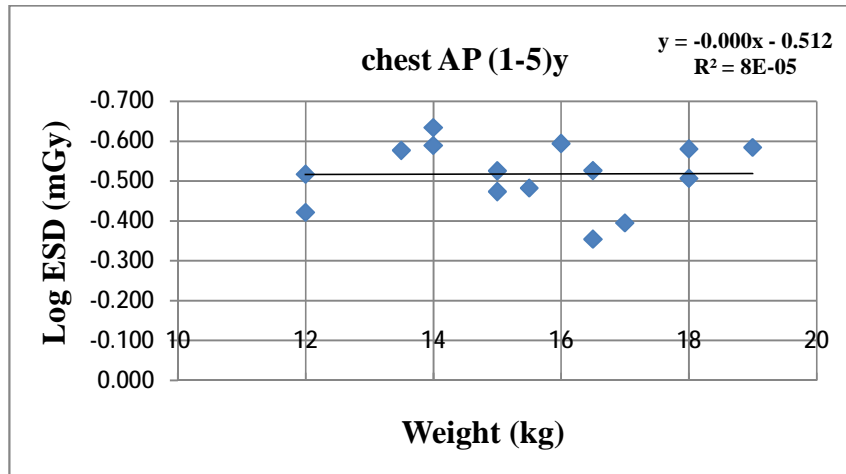


Fig.(7.44) Log entrance surface dose (Log ESD) vs. weight for age group (1-5)y.

7.9. Relation between entrance surface dose (ESD) with age and weight for chest PA

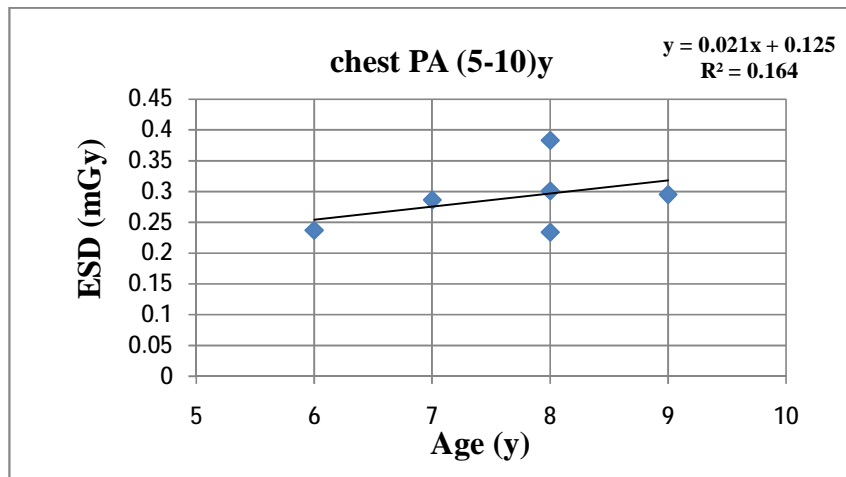


Fig.(7.45) Entrance surface dose (ESD) vs. age from (5-10)y.

The data for these graphs are found in appendix A {Tables (7A) and (8A)}

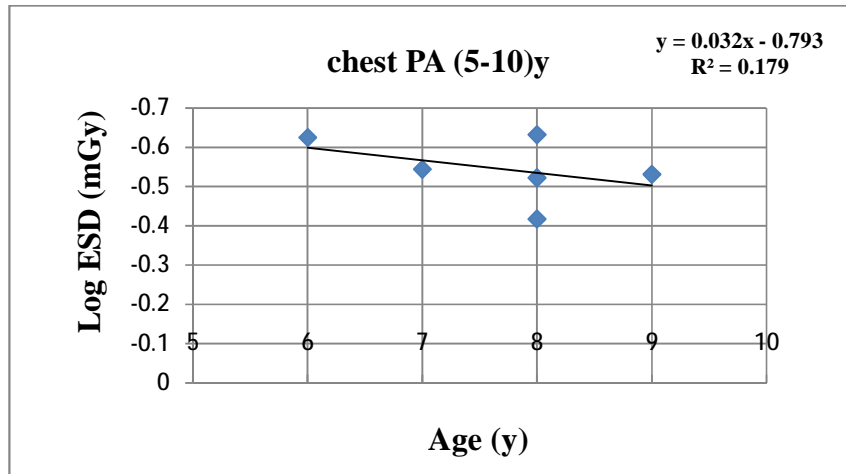


Fig.(7.46) Log entrance surface dose (Log ESD) vs. age from (5-10)y.

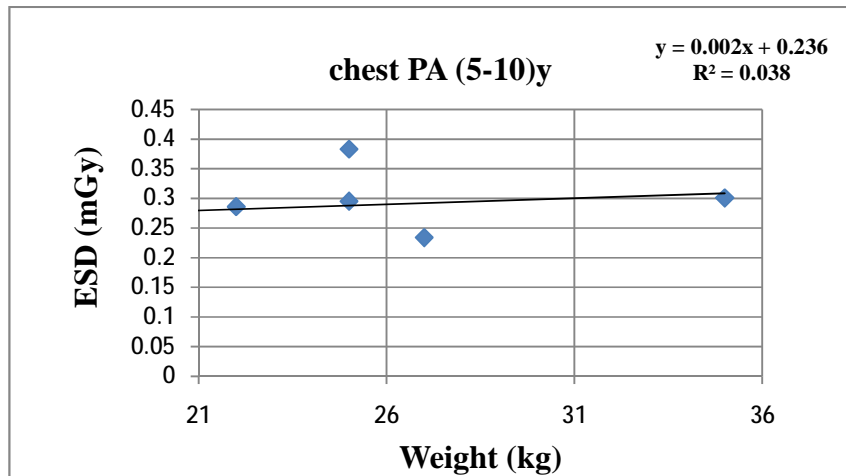


Fig.(7.47) Entrance surface dose (ESD) vs. weight for age group (5-10)y.

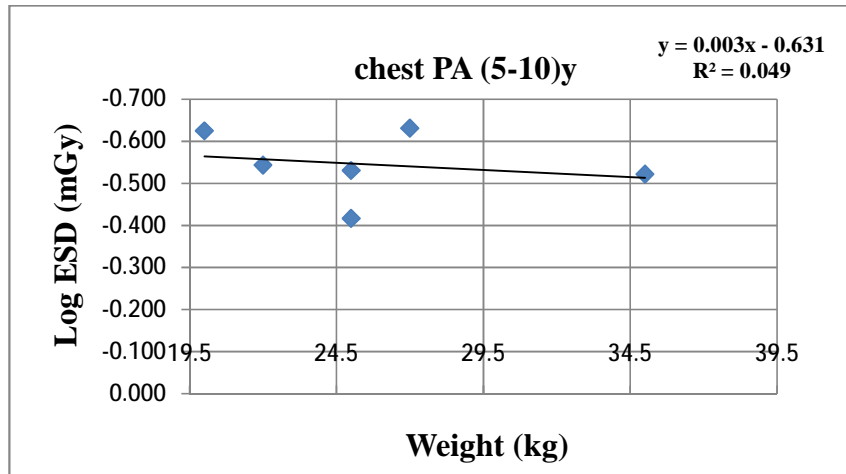


Fig.(7.48) Log entrance surface dose (Log ESD) vs. weight for age group (5-10)y.

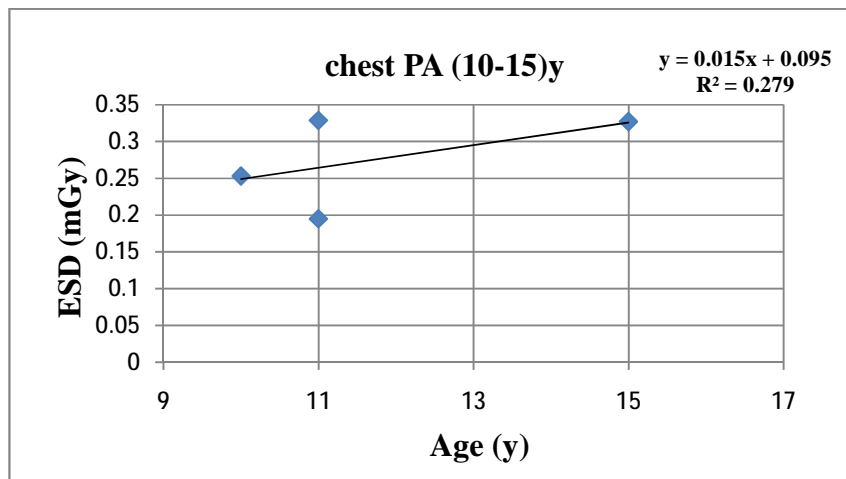


Fig.(7.49) Entrance surface dose (ESD) vs. age from (10-15)y.

The data for these graphs are found in appendix A {Tables (8A) and (9A)}

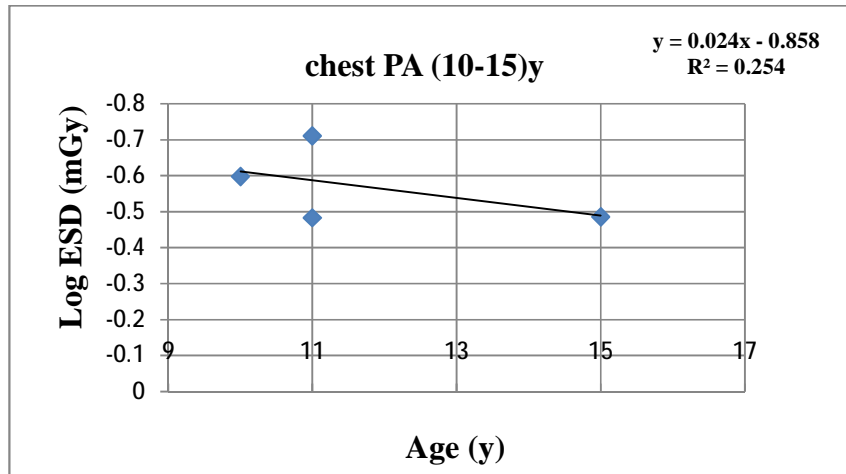


Fig.(7.50) Log entrance surface dose (Log ESD) vs. age from (10-15)y.

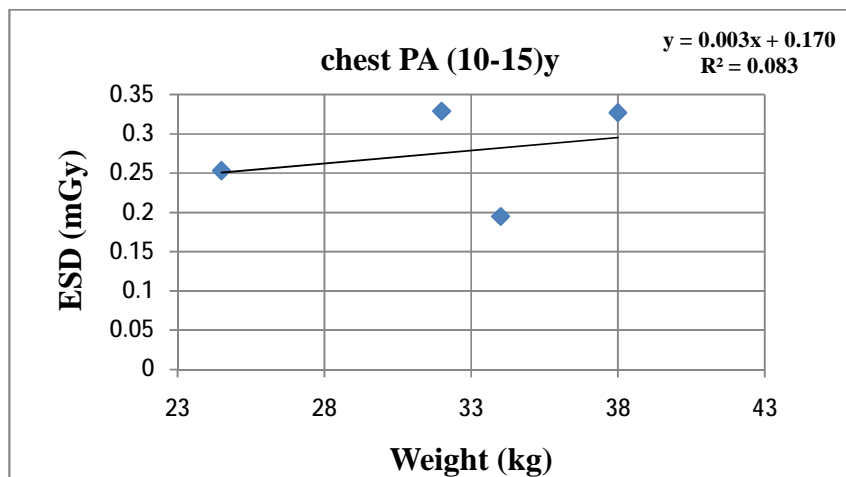


Fig.(7.51) Entrance surface dose (ESD) vs. weight for age group (10-15)y.

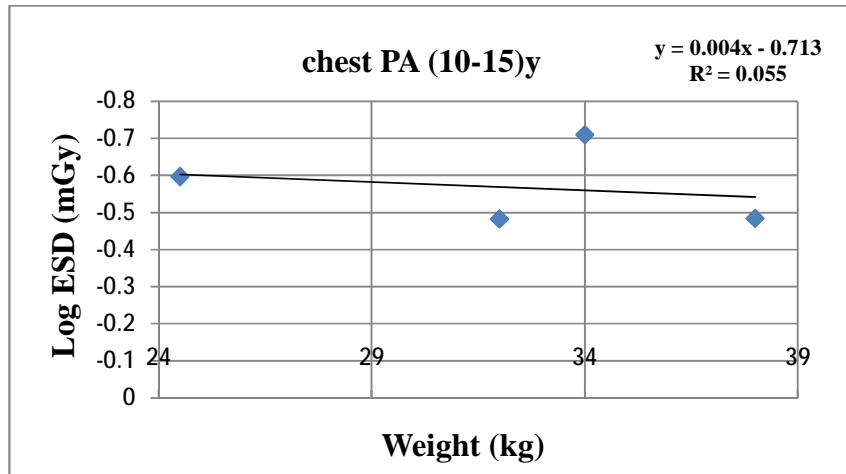


Fig.(7.52) Log entrance surface dose (Log ESD) vs. weight for age group (10-15)y.

7.10.Relation between entrance surface dose (ESD) with age and weight for chest lat

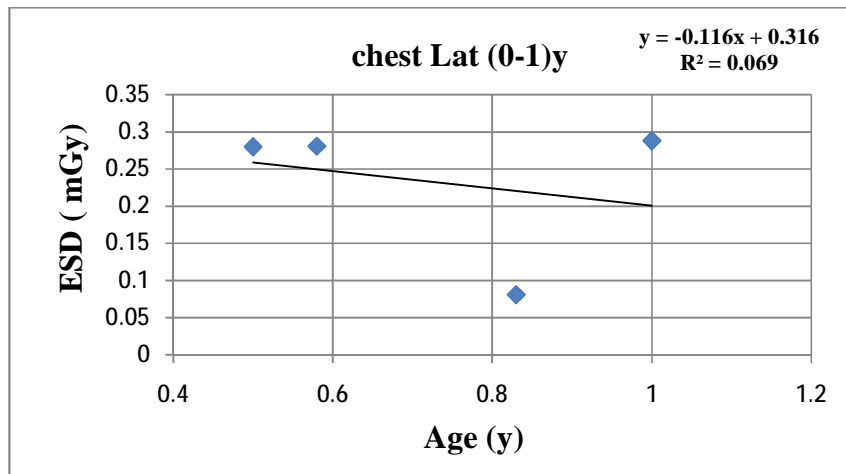


Fig.Entrance surface dose (ESD) vs. age from (0-1)y. (7.53)

The data for these graphs are found in appendix A {Tables (9A) and (10A)}

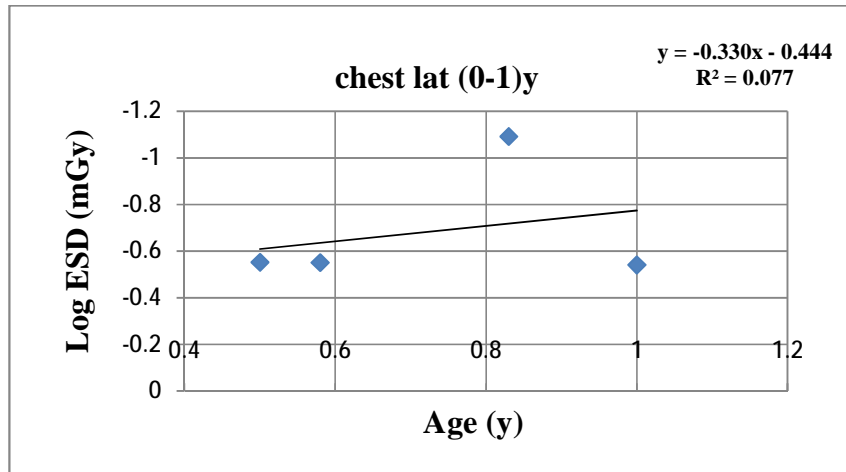


Fig.(7.54) Log entrance surface dose (Log ESD) vs. age from (0-1)y.

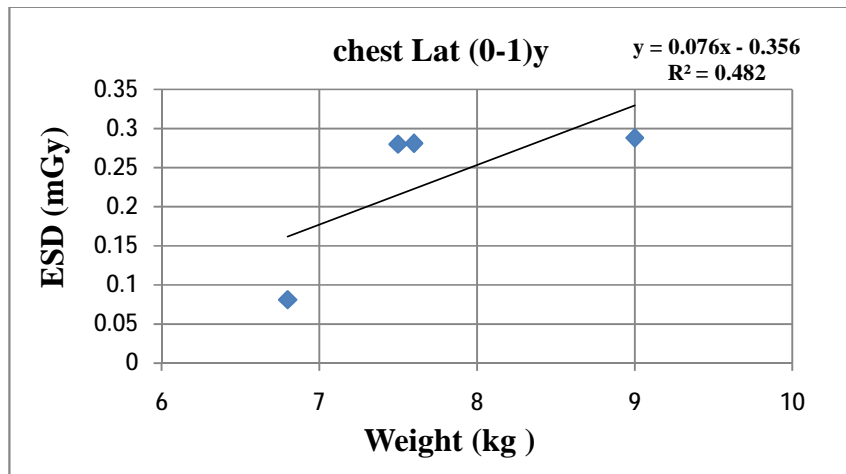


Fig.(7.55) Entrance surface dose (ESD) vs. weight for age group (0-1)y.

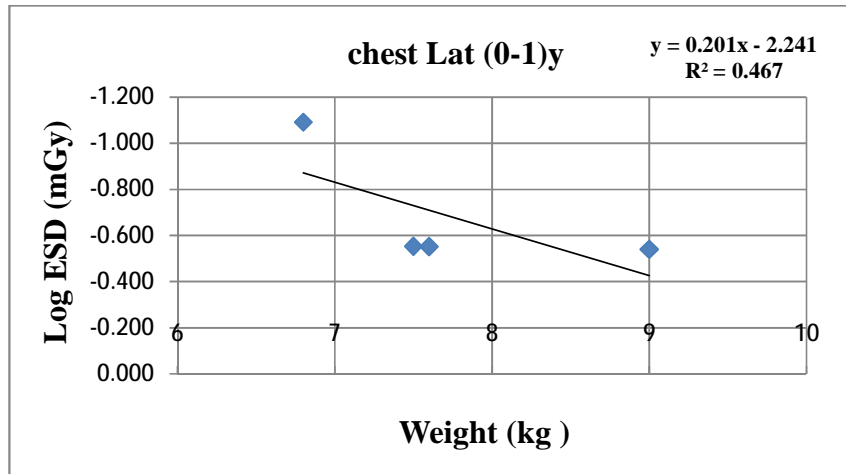


Fig.(7.56) Log entrance surface dose (Log ESD) vs. weight for age group (0-1)y.

7.11.Relation between entrance surface dose (ESD) with age and weight for abdomenAP

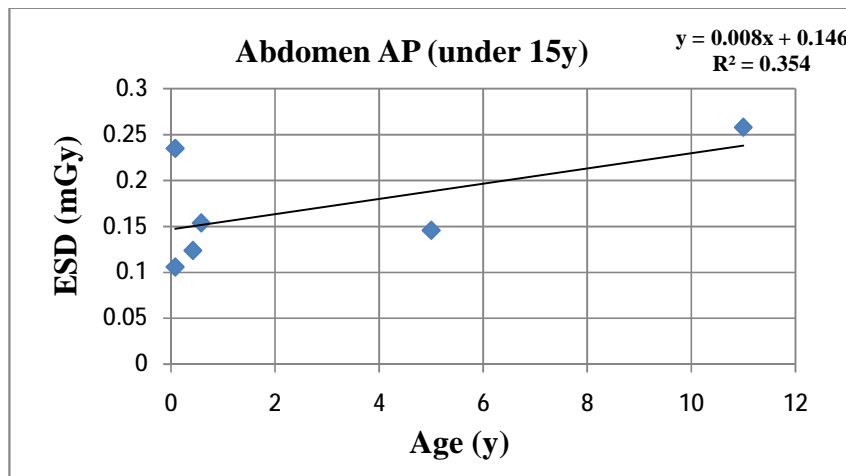


Fig.(Entrance surface dose (ESD) vs. age (under 15y). 7.57)

The data for these graphs are found in appendix A {Tables (10A) and (11A)}

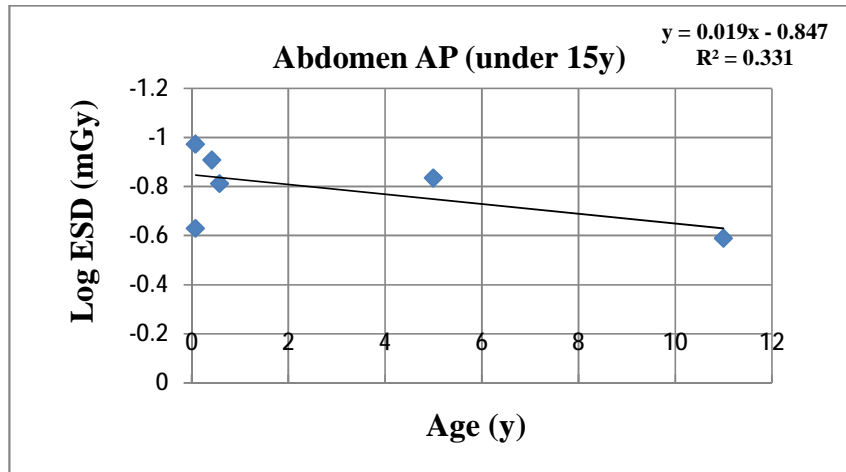


Fig.(7.58) Log entrance surface dose (Log ESD) vs. age (under 15y).

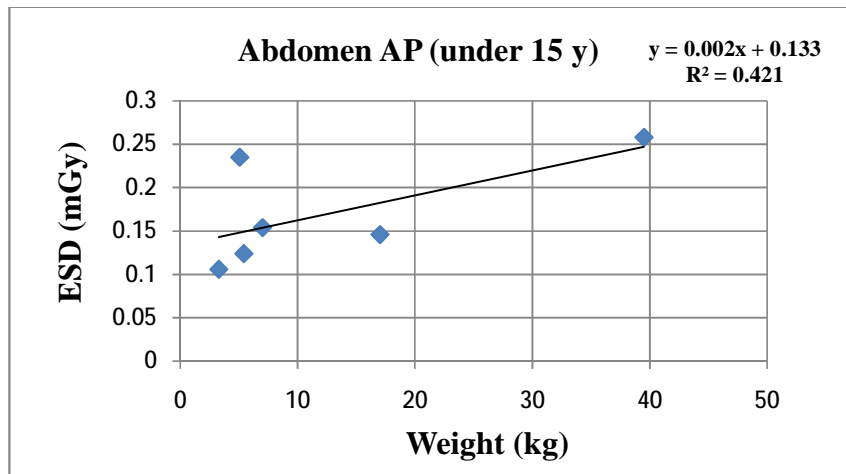


Fig.(7.59) Entrance surface dose (ESD) vs. weight for age group under 15y.

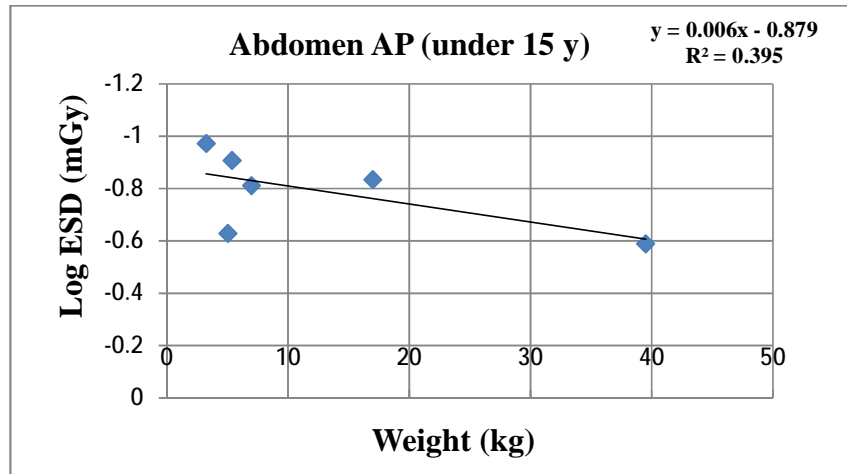


Fig.(7.60) Log entrance surface dose (Log ESD) vs. weight for age group under 15y.

7.12. Discussion of Benghazi children hospital results

The patient information such as weight, age and exposure parameters (tube voltage, tube current-exposure time product, focus to skin distance) for X-ray examinations (chest, abdomen, skull and cervical spine) performed on paediatric patients were recorded. The Descriptive statistics of patients' data and exposure parameters are shown in Tables (7.1) to (7.10). The tube voltage used in the present study was shown to change according to the type of examination. The highest voltage was 65 kV (for the two age groups (1-5)y, (5-10)y submitted to chest AP) as shown in Tables (7.2) and (7.3). The lowest tube voltage was 43 kV (for patients with ages under 15y undergoing abdomen AP) as shown in Table (7.10).

A comparison of exposure factors used in the present study with values proposed by the European and British guidelines is given in Table (7.12). For patients aged from 5 to 10 years undergoing chest PA, the range of tube voltage used in this study is lower than the range established by European guidelines. For patients with ages from 10 to 15 years undergoing chest PA, the range of tube voltage used is lower than the values recommended by European and British guidelines. In chest AP carried out on newborn babies, the tube voltage in the present study is outside the range recommended by European commission in (1996).

It was observed that, the range of tube loading (mAs) varied according to the type of examination. The highest tube loading was 11 mAs (for skull lat), while the lowest value was 3.6 mAs (for patients aged below 15y undergoing abdomen AP). The range of tube current – exposure time product in our study for chest PA performed on the two age groups (5-10)y and (10-15)y were higher than the values recommended by British guidelines as shown in Table (7.12).

The range of focus to skin distance (FSD) was changed according to the type of examination. The maximum focus skin distance was 112 cm (for paediatric patients aged under 15y submitted to abdomen AP), whereas the minimum value was 58 cm (for paediatric patients with ages below 1y undergoing chest AP). The variation coefficient of weight for abdomen AP performed on ages under 15y is larger than the variation

coefficients of weights for chest (AP, PA and Lat projections). The large value indicates that the data is more variable and it is less stable or less uniform.

There is no variation in tube loading value for paediatric patients aged 5 years submitted to chest AP examination as shown in Table (7.6).

The entrance surface dose and effective dose values were calculated for paediatric patients using Dosecal software. The descriptive statistics of entrance surface dose (ESD) and effective dose (ED) for chest and abdomen X-ray examinations are grouped in Tables (7.13) and (7.14). From Table (7.13), the ESD value was found to range from 0.185 to 0.256 mGy for the age group from (5-10) years for those undergoing chest PA examination and from 0.240 to 0.382 mGy for chest AP examination. For chest PA examination performed on the age group from (10-15) years, it varied from 0.162 to 0.248 mGy. For chest lat examination performed on the age group from (0-1) years, the ESD value varied from 0.092 to 0.296 mGy, while for abdomen AP examination performed on ages under 15 years, it varied from 0.082 to 0.205 mGy.

From Table (7.14), the effective dose value (ED) varied from 0.014 to 0.020 mSv for the age group from (5-10) years for those undergoing chest PA examination and from 0.028 to 0.05 mSv for chest AP. For chest PA examination performed on the age group from (10-15) years, it varied from 0.010 to 0.016 mSv. For chest lat examination performed on the age group from (0-1) years, the ED value ranged from 0.008 to 0.026 mSv, while for abdomen AP examination performed on ages under 15 years, it ranged from 0.011 to 0.030 mSv.

The body organ dose (BOD) in mGy in our study was calculated using dosecal software for chest and abdomen X-ray examinations and grouped in Table (7.15). It was observed that, the highest body organ dose for abdomen AP was to the stomach (0.054 mGy), while the least organ dose was to the brain (3.53×10^{-6} mGy). For chest lat performed on the age group (0-1)y, the highest organ dose was to the breasts (0.076 mGy), whereas the least organ dose was to the brain (1.63×10^{-4} mGy). For chest PA carried out on the age group (5-10)y, the highest organ dose was to the adrenals (0.069 mGy), while the least organ dose was to the brain (6.14×10^{-5} mGy).

It was observed from Table (7.15) that, the breasts receive the highest dose (0.159 mGy) from chest AP scans performed on the age group (1-5)y, while the brain receives the lowest dose (1.37×10^{-4} mGy).

For the age group (5-10)y undergoing chest AP, the highest organ dose was to the breasts (0.215 mGy), while the least organ dose was to the brain (1.16×10^{-4} mGy).

It could be observed that, the chest and abdomen X-ray examinations give lowest doses to the brain. The mean absorbed dose in a specified tissue or organ depends on the ambient radiation field, on the beam size and orientation of the body in this field and on the organ. That is why brain has the lowest values because it is located far away from the X-ray beam.

The values of calculated entrance surface dose in our study were compared with entrance surface dose values recommended by the European Commission, National Radiological Protection Board of the UK in addition to previous studies performed in other countries as shown in Tables (7.16) to (7.19). The mean entrance surface dose found in this study for paediatric patients aged below 1y undergoing chest AP was higher than the values obtained from other studies carried out in other countries as Brazil, Sudan, United Kingdom, Sweden and Estonia as shown in Table (7.16). For patients aged from 1 to 5 years subjected to chest AP, the mean entrance surface dose value in our study was higher than those values of other studies except for Nigerian study. The mean entrance surface dose value in our study was a little bit higher than that value for Malaysia.

Table (7.17) shows that, the mean entrance surface dose values found in this study for paediatric patients with ages 1y and 5y undergoing chest AP were higher than the values suggested by National Radiological Protection Board (NRPB), United Nations Scientific Committee on the Effects of Atomic Radiation (UNSCEAR) and those values obtained from previous studies performed in other countries as Brazil, United Kingdom and Sudan. For chest AP performed on newborn babies, the mean entrance surface dose in the present study was found to be higher than the European Commission reference dose of 0.080 mGy, National Radiological Protection Board (2000) of 0.050 mGy and values mentioned in studies for the UK, Romania and Kuwait.

The reasons for these high entrance surface doses (ESDs) in chest X-ray examination could be accounted from the radiographic technical parameters (kV, mAs) used in Benghazi Children Hospital. A dose survey of paediatric patients in countries of the European Union showed that approximately 80% of chest examinations (AP and PA projections) in children with a mean age of 5 years used tube potentials more than 60 kV, whereas tube voltages used in this study were lower than 60 kV as shown in Table (7.12). The use of a low tube potential and high mAs values was common in Benghazi Children Hospital and has been observed as a cause of high doses. The radiographers when ask could not give any reasons for this other than it gives good resolution.

It is known that entrance surface dose (ESD) is proportional to the tube current, the length of exposure, the square of the peak voltage and the distance between X-ray source and patient. The use of higher peak kilovoltages increases beam penetration and this may allow the use of a lower tube current, thus reducing the dose, also increasing the FSD reduces the dose greatly, for example, if the FSD is doubled, the dose will be reduced by a factor of four. It has been reported that comparison of doses with two typical exposures at 120 kVp and 70 kVp shows that high kVp technique delivers a higher ESD (Fung, 2004) and higher potential values allows considerable dose reduction without losing image quality.

Table (7.12) shows that, Benghazi Children Hospital does not utilize exposure parameters optimized accordingly the European and British guidelines. Choosing the optimum potential of the X-ray tube is very important since this depends on the part of the body that needs to be visualized, on the size of the patient, the type of requested clinical information and the response of the image receptor (the radiological film).

There many other factors, in addition to radiographic techniques employed in chest X-ray examination can be a cause of such high doses such as lack of quality assurance programme (QAP), the absence of regulatory institutions, performance of equipment, clinical condition, radiologist skill and total filtration.

The formation of X-ray image involves the interaction of several factors. In order to get a correct balance between the patient's dose and the image quality, it is necessary to understand the way of formation of the radiological image and to know the factors that

are influencing the quality of the image, as well as the radiation doses received by the patient, so that the most adequate options shall be selected (Sorop and Dadulescu, 2011). Relationships between entrance surface dose (ESD) and equivalent patient diameter (d), patient's weight and patient's age were studied to assess which parameters might be most suitable for making dose comparisons for children of different size.

The entrance surface dose values calculated using the equation (4.32) plotted as a function of equivalent patient diameter (d), patient's age and weight as shown in Figs.(7.7) to (7.60). It was observed that, there is a weak positive relationship (correlation coefficient, $r = 0.17$) between patient diameter (d) in cm and entrance surface dose in mGy for the age group (0-1)y as shown in Fig.(7.9). For the age group (1-5)y, the relationship between equivalent patient diameter and entrance surface dose is weak negative ($r = -0.17$) as shown in Fig.(7.11). Similarly, for the age group (5-10)y, the relationship between patient diameter and entrance surface dose is weak negative ($r = -0.3$) as shown in Fig.(7.13). For the age group (10-15)y, there is weak positive correlation between patient diameter and entrance surface dose ($r = 0.14$) as shown in Fig.(7.15).

For chest AP examination, the relation between entrance surface dose and age from (0-1)y is weak negative (correlation coefficient, $r = -0.1$), while there is no correlation between weight and entrance surface dose ($r = 0$) as shown in Figs.(7.37) and (7.39).

For the age group (1-5)y undergoing chest AP, the relation between age with entrance surface dose is positive ($r = 0.5$), while there is no relation between weight and entrance surface dose as shown in Figs.(7.41) and (7.43).

For chest PA performed on the age group (5-10)y, the relationship between age and entrance surface dose is weak positive ($r = 0.4$) and the relation between weight and entrance surface dose is also weak positive ($r = 0.20$) as shown in Figs (7.45) and (7.47). For chest lat performed on the age group (0-1)y, there is weak negative correlation between age and entrance surface dose ($r = -0.3$), while the correlation between weight with entrance surface dose is strong positive ($r = 0.7$) as shown in Figs.(7.53) and (7.55). For abdomen AP examination performed on ages under 15y, the relation between entrance surface dose with age and weight are positive as shown in Figs.(7.57) and (7.59).

- **Alhawari general hospital results**

7.13. Sample distribution according to the type of examination

According to examination types, the patients were classified into five types of examinations, chest PA, abdomen AP, cervical spine AP, pelvis AP and lumbar spine AP. Of the total sample 101, 77 adult patients were undergoing chest PA examination, representing 76% of the total sample. 5 adult patients were undergoing abdomen AP examination, representing 5% of the total sample. 5 adult patients were undergoing cervical spine AP examination, representing 5% of the total sample. 5 adult patients were undergoing pelvis AP examination, representing 5% of the total sample. 9 adult patients were undergoing lumbar spine AP examination, representing 9% of the total sample as shown in Fig.(7.61).

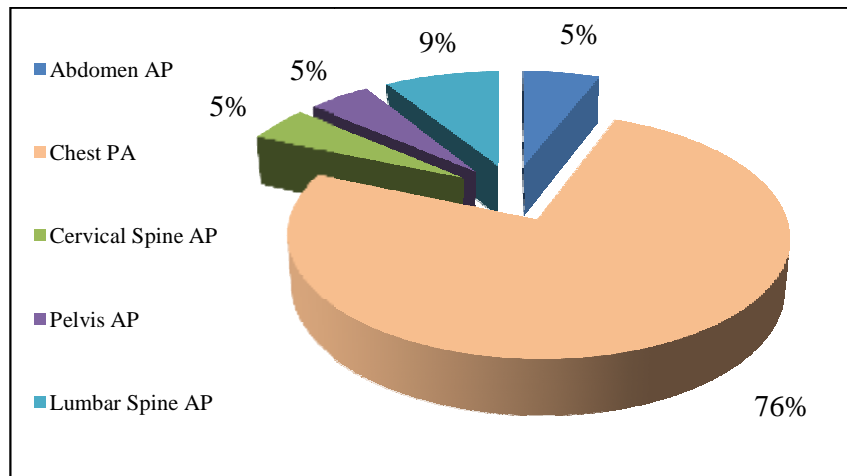


Fig.(7.61): Sample distribution according to examination type at Alhawari General Hospital.

7.14. Descriptive statistics of exposure parameters and weights for adult patients undergoing different X-ray examinations.

The parameters of exposure in addition to patient's weight were recorded. The different statistical terms of exposure parameters and weights for adult patients were calculated and grouped in all tables below from Table (7.20) to (7.24). For each type of examination, the sample size was also shown.

Table (7.20): Descriptive statistics of exposure parameters and weights for adult patients undergoing abdomen AP

Examination	Abdomen AP			
Sample Size	5			
	Weight (kg)	Voltage (kV)	Tube Loading (mAs)	FSD (cm)
Mean	72.2	77	10.9	116.2
Median	77	77	8.9	127
Min	57	77	7	81
Max	85	77	16.2	146
3 rd quartile	80	77	14.9	132
STDEV	12.07	0	4.35	27.12
CV%	16.72	0	39.91	23.34

Table (7.21): Descriptive statistics of exposure parameters and weights for adult patients undergoing chest PA

Examination	Chest PA			
Sample Size	77			
	Weight (kg)	Voltage (kV)	Tube Loading (mAs)	FSD (cm)
Mean	81.8	124	1.3	129
Median	82	125	1.1	126
Min	52	77	0.6	116
Max	118	125	13.1	161
3 rd quartile	95	125	1.4	129
STDEV	17.84	5.47	1.42	10.08
CV%	21.81	4.41	109.23	7.81

Table (7.22):Descriptive statistics of exposure parameters and weights for adult patientsundergoingcervical spine AP

Examination	Cervical spine AP			
Sample Size	5			
	Weight (kg)	Voltage (kV)	Tube Loading (mAs)	FSD (cm)
Mean	79.6	70	7.5	129
Median	78	70	5.8	134
Min	55	70	1.4	67
Max	100	70	13.1	165
3 rd quartile	99	70	11.7	157
STDEV	19.91	0	4.82	38.68
CV%	25.01	0	64.27	29.98

Table (7.23):Descriptive statistics of exposure parameters and weights for adult patientsundergoingpelvis AP

Examination	Pelvis AP			
Sample Size	5			
	Weight (kg)	Voltage (kV)	Tube Loading (mAs)	FSD (cm)
Mean	79.4	80	18.2	85
Median	72	80	13.6	84
Min	67	80	4.5	79
Max	97	80	31.5	93
3 rd quartile	91	80	29.7	86
STDEV	13.61	0	11.81	5.41
CV%	17.14	0	64.89	6.36

Table (7.24): Descriptive statistics of exposure parameters and weights for adult patients undergoing lumbar spine AP

Examination	Lumbar spine AP			
Sample Size	9			
	Weight (kg)	Voltage (kV)	Tube Loading (mAs)	FSD (cm)
Mean	84.8	80	26.4	103
Median	86	77	24.9	93
Min	52	77	5.2	68
Max	115	90	61.9	158
3 rd quartile	95	77	26.3	96
STDEV	17.62	5.73	16.70	32.26
CV%	20.78	7.16	63.26	31.32

Table (7.25): Comparison of tube voltage values in the present study with the values obtained by UK (2002).

Examination	Tube voltage (kV)	
	Present study (2011)	UK (2002)
Abdomen AP	77	49-156
Chest PA	77-125	50-150
Pelvis AP	80	54-96
Lumbar spine AP	77-90	55-100

Table (7.26) Descriptive statistics of effective dose (ED) and dose area product (DAP) for adult patients undergoing chest PA, abdomen AP and pelvis AP examinations.

Examination	Present study (2011)		UK (1997)	Nordic Countries (1996)		USA (2008)	AAPM (2008)
	Chest PA	Abdomen AP	Pelvis AP	Chest PA	Abdomen AP	Pelvis AP	
Mean	0.025	0.186	0.540	0.14	1	2.41	
Median	0.020	0.155	0.499	0.11	0.83	2.23	
Min	0.004	0.106	0.124	0.02	0.57	0.56	
Max	0.141	0.394	0.853	0.82	2.12	3.81	
1 st quartile	0.013	0.119	0.402	0.07	0.64	1.80	
3 rd quartile	0.029	0.155	0.820	0.15	0.84	3.66	
STDEV	0.020	0.119	0.304	0.12	0.64	1.36	
CV%	80	63.98	56.30	85.71	64	56.43	

Table (7.27) Descriptive statistics of effective dose (ED) and dose area product (DAP) for adult patients undergoing cervical spine AP and lumbar spine AP examinations.

	ED (mSv)		DAP (Gy cm ²)	
	Cervical spine AP	Lumbar spine AP	Cervical spine AP	Lumbar spine AP
Mean	0.040	0.501	0.19	2.30
Median	0.041	0.615	0.20	2.49
Min	0.008	0.076	0.04	0.36
Max	0.087	0.832	0.41	3.99
1 st quartile	0.014	0.179	0.07	0.86
3 rd quartile	0.049	0.790	0.23	3.79
STDEV	0.032	0.313	0.15	1.46
CV%	80	62.48	78.95	63.48

Chest PA	0.025	0.02	0.2	0.05	0.1-0.2
Abdomen AP	0.186	0.7	*	0.4	*
Pelvis AP	0.540	0.7	1.2	*	*
Lumbar spine AP	0.501	0.7	2.1	*	0.5-1.5

Table (7.28): Comparison the mean value of effective dose in mSv calculated using dosecal software with other studies carried out in other countries.

(*): the value isn't available

Nordic countries: the northwestern European countries of Scandinavia (Denmark, Norway, Sweden), as well as Iceland and Finland

Table (7.29): Comparison the third quartile values of dose area product in Gy cm^2 for adult patients undergoing different X-ray examinations with values obtained by United Kingdom.

Examination	Present study (2011)	UK (2002)	UK (mid 1980)
Chest PA	0.15	0.12	*
Abdomen AP	1.80	3	8
Pelvis AP	3.66	3	5
Lumbar spine AP	3.79	1.6	15

(*): the value isn't available

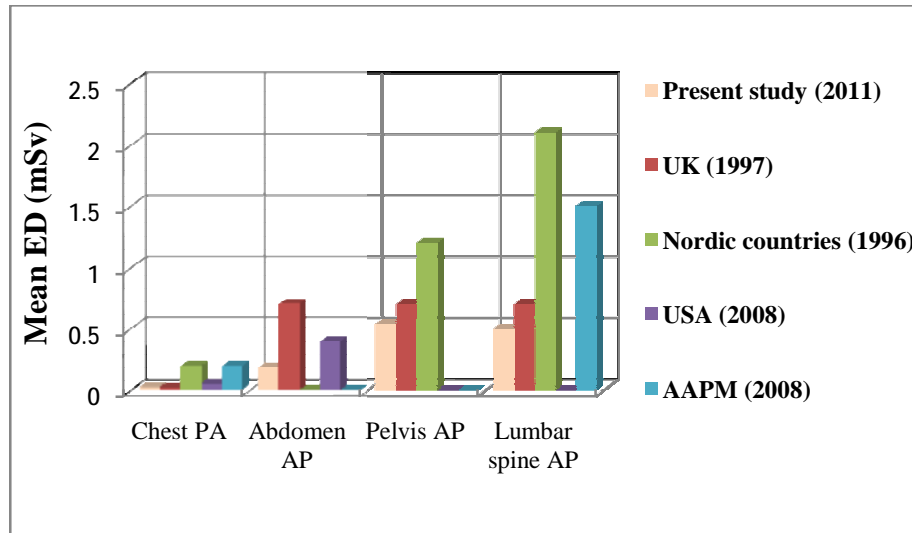


Fig.(7.62):Comparison of mean effective dose in this study with previous studies carried out in other countries.

7.15. The effective dose in (mSv) against age and weight for adult patients subjected to some common X-ray examinations

The effective dose values in (mSv) calculated using the dosecal software were plotted against age and weight for different X-ray examinations performed on adult patients as shown in figs (7.63) to (7.72).

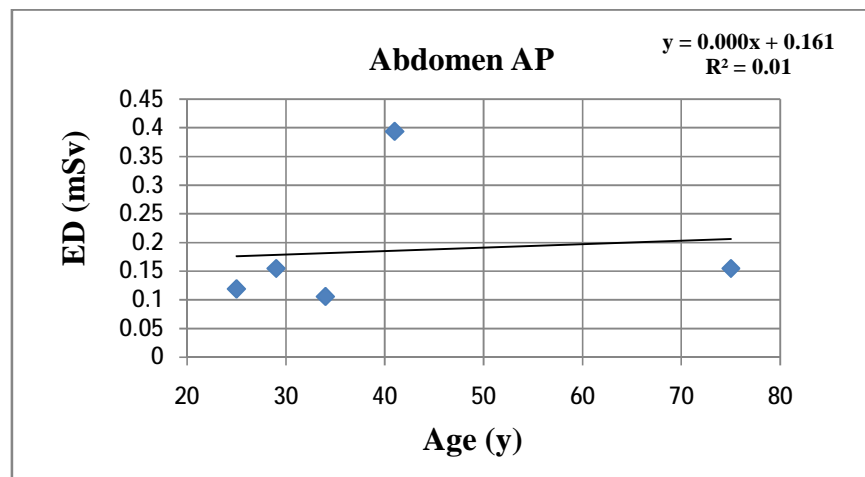


Fig.(7.63) Age vs. effective dose for adult patients undergoing abdomen A

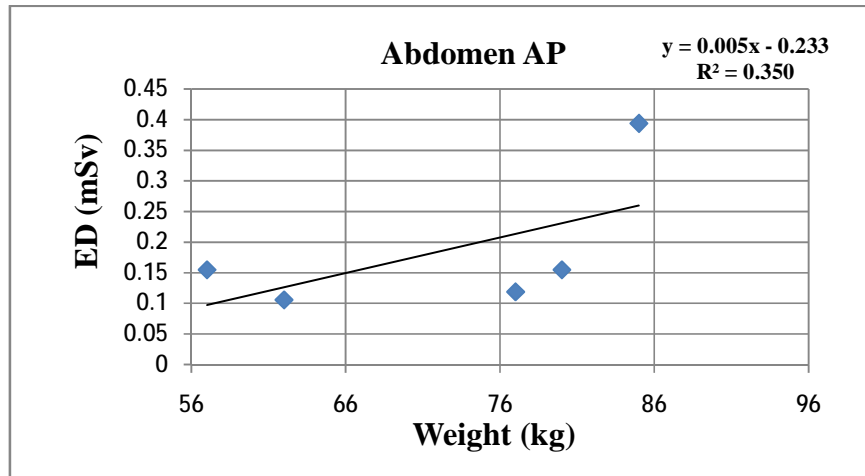


Fig.(7.64) Weight vs. effective dose for adult patients undergoing abdomen AP

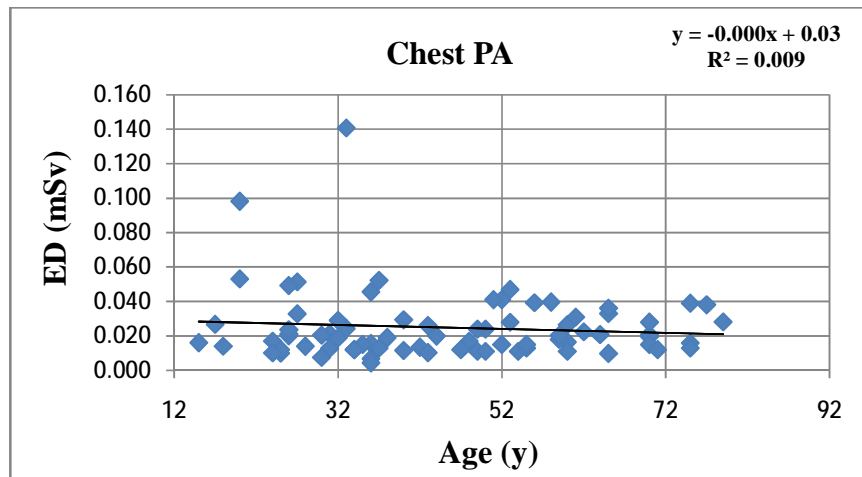


Fig.(7.65) Age vs. effective dose for adult patients undergoing chest PA

The data for these graphs are found in appendix B {Tables(1B) and (2B)}

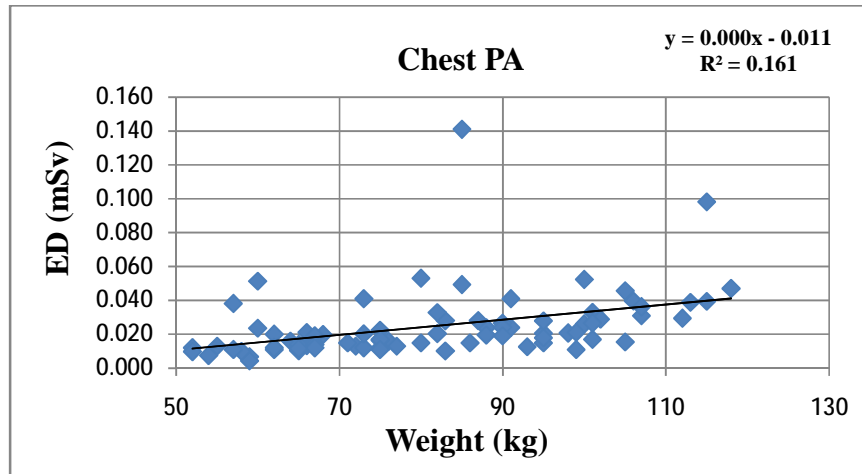


Fig.(7.66) Weight vs. effective dose for adult patients undergoing chest PA

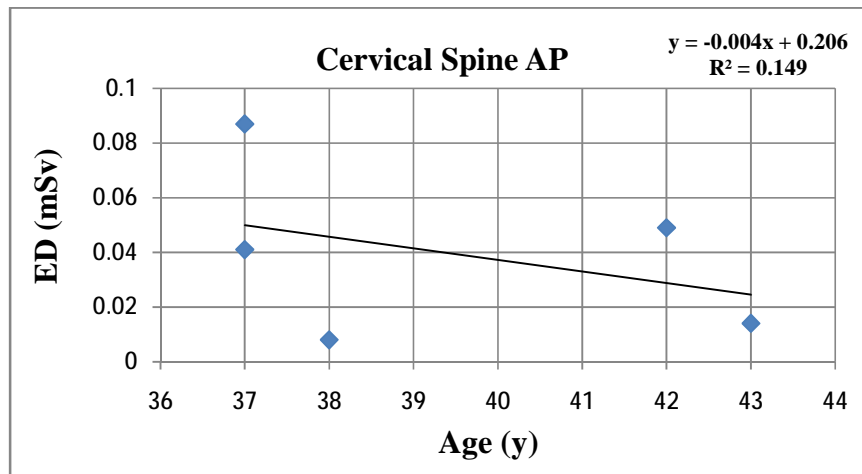


Fig.(7.67) Age vs. effective dose for adult patients undergoing cervical spine AP

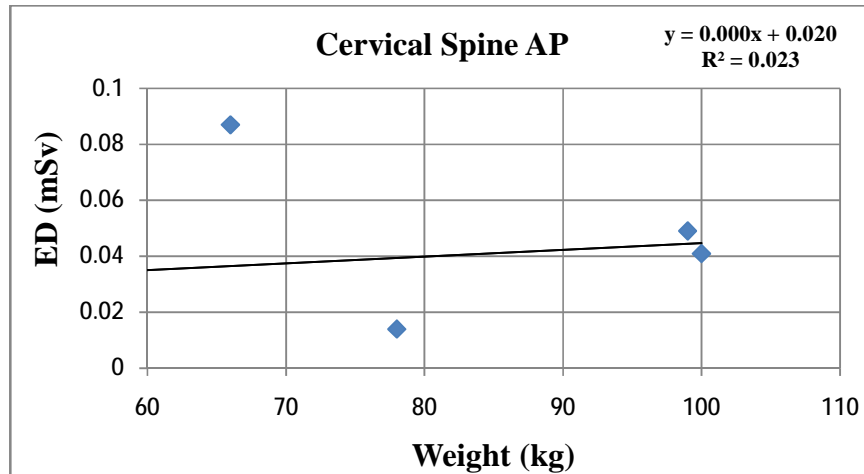


Fig.(7.68) Weight vs. effective dose for adult patients undergoing cervical spine AP

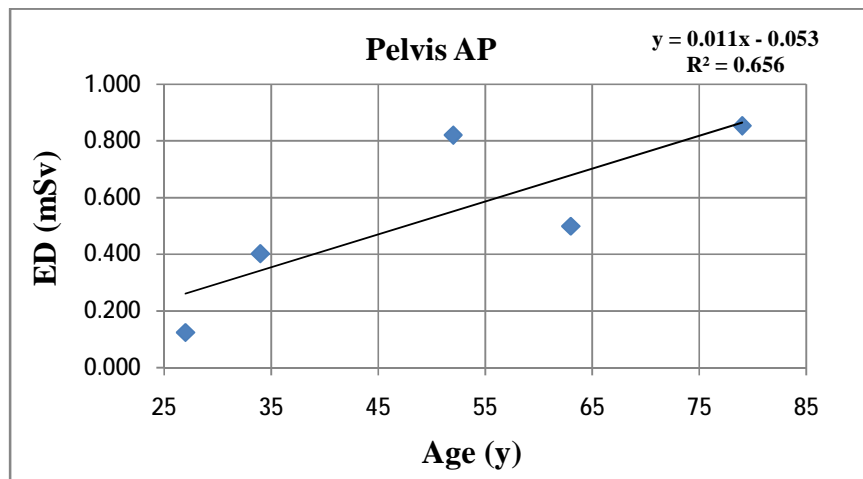


Fig.(7.69) Age vs. effective dose for adult patients undergoing pelvis AP

The data for these graphs are found in appendix B {Tables (3B) and (4B)}

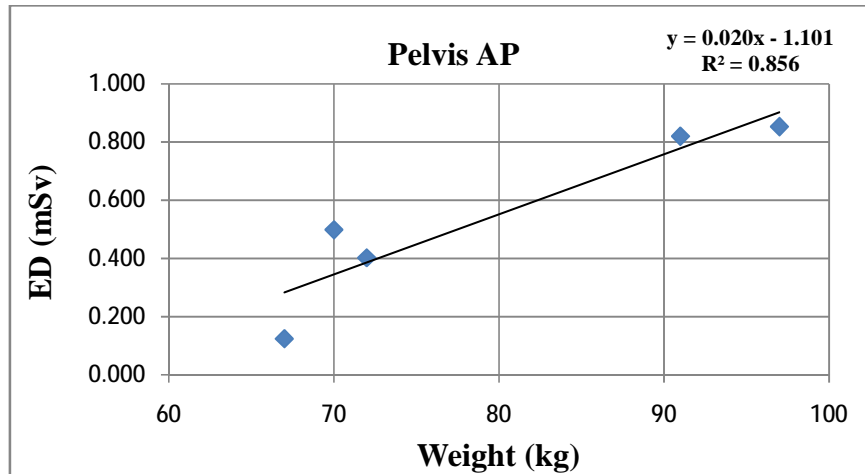


Fig.(7.70) Weight vs. effective dose for adult patients undergoing pelvis AP

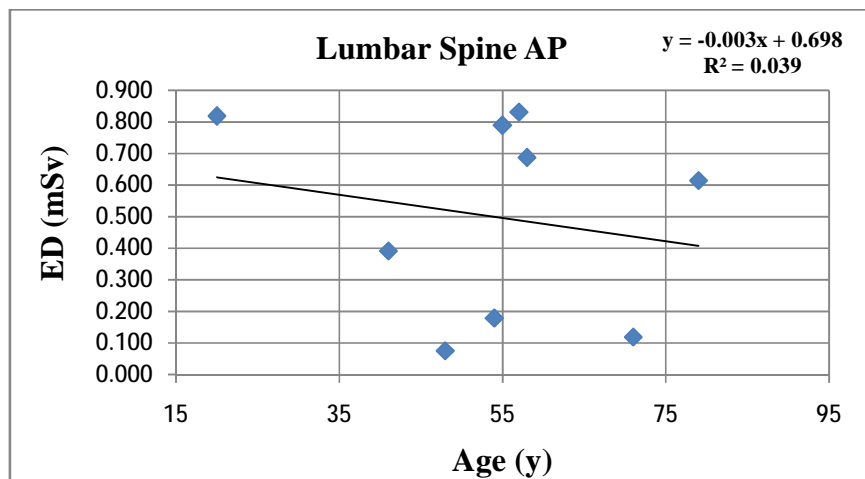


Fig.(7.71) Age vs. effective dose for adult patients undergoing lumbar spine AP

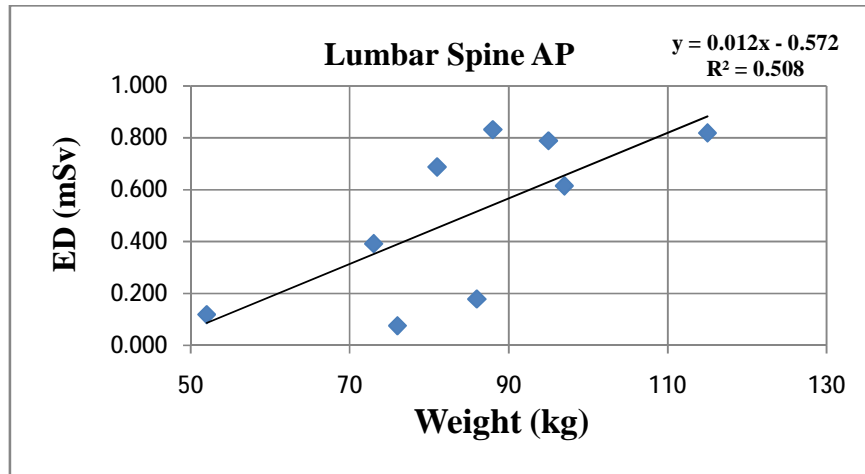


Fig.(7.72) Weight vs. effective dose for adult patients undergoing lumbar spine AP

The data for this graph are found in appendix B {Table (5B)}

7.16. Discussion of alhawari general hospital results

The radiographic exposure factors for adult patients undergoing different X-ray examinations were recorded. The descriptive statistics (mean, median, standard deviation...etc) of exposure factors and weight for adult patients are given in Tables (7.20) to (7.24).

The voltage value in the present study varied according to the type of examination. It was observed that, the maximum voltage was 125 kV (for adult patients undergoing chest PA examination). The minimum value was 70 kV (for adult patients undergoing cervical spine AP examination) as shown in Table (7.22).

Table (7.25) shows the values of tube voltage in the present study for different X-ray examinations and their comparison with the UK recommendations. The voltage values in our study for pelvis and abdomen X-ray examinations are within the range proposed by the UK in (2002).

The tube current- exposure time product (mAs) in the present study varied according to the type of examination. The maximum value was 61.9 mAs (for patients undergoing lumbar spine AP examination), whereas the minimum value was 0.6 mAs (for adult patients undergoing chest PA examination).

The focus skin distance varied according to the type of examination. The maximum value was 165 cm (for cervical spine AP), whereas the minimum value was 67 cm also (for cervical spine AP examination).

The descriptive statistics of effective dose (ED) and dose area product (DAP) for some common X-ray examinations carried out on adult patients are summarized in Tables (7.26) and (7.27). In chest PA examination, the effective dose varied from 0.004 to 0.141 mSv and the dose area product (DAP) varied from 0.02 to 0.82 Gy cm^2 . In abdomen AP examination, the effective dose varied from 0.106 to 0.394 mSv and the dose area product (DAP) varied from 0.57 to 2.12 Gy cm^2 .

Some studies have indicated that, effective dose values obtained from DAP measurements represent a more accurate estimation of effective dose compared with effective dose values obtained from entrance surface dose measurements. This is mainly because the dose area product (DAP) takes into account the area of the patient's body which is irradiated and hence affects the number of organs irradiated. The entrance

surface dose is measured at the center of X-ray field and does not include any information about the area irradiated.

The comparison of the mean effective dose in (mSv) calculated in this study with values established by American Association of Physicists in Medicine(AAPM), UK, USA and Nordic countries is demonstrated in Table (7.28). The mean effective dose for chest PA examination carried out on adult patients (0.025 mSv) is a little bit higher than UK value. At the same time, it is lower than the values for Nordic countries, USA and American Association of Physicists in Medicine (AAPM). For abdomen AP, the mean effective dose in the present study is 0.186 mSv. This value is lower compared to those for UK and USA. For pelvis AP, the mean effective dose calculated in our study (0.540 mSv) is lower than the values previously reported in UK and Nordic countries. This means that, the radiation risk to adult patients in Alhawari General Hospital included in this study is low.

The third quartile values of dose area product in Gycm^2 in this study were compared with those reported in UK surveys as shown in Table (7.29).

It was noted that, the third quartile of dose area product for pelvis AP (3.66 Gy cm^2) was found to be higher than value of UK (2002), whereas it was less than that for UK (mid 1980). For lumbar spine AP, the third quartile of dose area product in this study (3.79 Gy cm^2) was higher than that value for UK (2002), while it was much less than value for UK (mid 1980).

The effective dose values were plotted as function of patient's weight and age for some X-ray examinations. For abdomen AP examination, there is weak positive correlation (correlation coefficient, $r = 0.1$) between age and effective dose (ED) as shown in Fig.(7.63). For the same type of examination, the correlation between weight and effective dose is positive ($r = 0.6$) as shown in Fig.(7.64).

For chest PA examination, there is weak negative correlation between age and effective dose ($r = -0.1$), while the correlation between weight and effective dose is weak positive ($r = 0.40$) as shown in Figs.(7.65) and (7.66). For cervical spine AP examination, there is weak negative correlation between age and effective dose ($r = -0.4$), whereas, there is weak positive correlation between weight and effective dose (correlation coefficient, $r = 0.2$) as shown in Figs.(7.67) and (7.68). For pelvis AP, there is strong positive

correlation between age and effective dose (correlation coefficient, $r = 0.8$), also the relationship between weight and effective dose is strong positive ($r = 0.9$), Figs. (7.69) and (7.70) show that. However the relation between weight and effective dose for pelvis AP is significant ($p=0.024$). For lumbar spine AP examination, there is weak negative correlation between age and effective dose (correlation coefficient, $r = -0.2$), while there is strong positive correlation between weight and effective dose ($r = 0.7$) as shown in Figs. (7.71) and (7.72). However the relation between weight and effective dose for lumbar spine AP is significant ($p = 0.031$).

CONCLUSION

It is very important in the diagnostic radiology departments to monitor and control doses to patients during imaging procedures. The doses delivered to patients in any medical imaging procedure should always be optimized for the given purpose. Evaluation of patient doses is an important part of quality assurance programme in diagnostic radiology.

The results show the need for changes in the working procedures and equipments used. It is necessary to investigate the reasons for higher dose levels in Benghazi Children Hospital so as to review and reduce it. Training facilities for the medical and technical staff are also necessary. These facts could be achieved if the radiology departments implement quality assurance programme (QAP) and establish national and/or regional diagnostic reference levels. This would promote a reduction on the variability of entrance surface dose as well as aid in the optimization of radiation protection so as to keep the patient doses low as reasonably achievable.

We conclude that standardisation of radiological practices is necessary to optimise radiological procedures and consequently the absorbed dose of patients.

Recommendations

1. Need for Quality Assurance (QA) programs to be undertaken to avert considerable cost and high patient doses.
2. Establishment national and/or regional diagnostic reference levels in Libya.
3. Estimation dose for different X-ray procedures such as CT (computed tomography), fluoroscopy and Mammogram.
4. Train the technicians how to use the technical factors and other measures of radioprotection (use of protective lead clothes- equipments to protect patients and accompanying person).
5. Optimization of the technical and clinical factors may lead to a substantial patient dose reduction.
6. Balance between radiation dose and image quality
7. Implemented system of radioprotection applying the basic principle of justifications, optimization and dose limitations.
8. Benghazi children hospital will have to undergo an investigation into its high departmental doses and either justify high doses or else revise techniques or equipment to bring its radiation doses in line with dose reference levels recommended by international bodies
9. Implemented a preventive maintenance system with regular checking the X-ray equipments by scientific engineering.
10. The formation of medical physical team within largest hospitals and radiation safety officer.

References

- Akhdar, H.F. *Assessment of entrance skin dose and effective dose of some routine X-ray examinations using calculation technique*. 2007.
<http://repository.ksu.edu.sa>
- Allisy - Roberts, P.J and Williams, J. *Farr's physics for medical imaging*. 2007. 2nd ed. Saunders Ltd. ISBN: 9780702028441.
- Almen, A., Mattson,S. *Dose distribution at chest radiography of children*.1995. Rad Prot Dosim 57: 463-467.
- Alshehri, S.A.A. *Assessment of beam characteristics of some X-ray units at security forces hospital and their applications in paediatric dose calculation*. 2006.
<http://repository.ksu.edu.sa/jspui/bitstream/123456789/8774/1>
- American Association of Physicists in Medicine Report 96: *The Measurement, Reporting and Management of Radiation Dose in CT*. 2008. <http://aapm.org>.
- Andreassi, M.G. *The Biological Effects of Diagnostic Cardiac Imaging on Chronically Exposed Physicians: The Importance of being Non-ionized*, Cardiovascular ultrasound 2004, 2:25.
- Armpilia, C.I., Fife, I.A. and Croasdale, P.L. *Radiation dose quantities and risk in neonates in a special care baby unit* .2002. Br J radiol.75:590-595.
<http://bjr.birjournals.org/content/75/895/590.full.pdf>
- ARPANSA RPS 14. *Code of Practice for Radiation Protection in the Medical Applications of Ionizing Radiation*; Australian Radiation Protection & Nuclear Safety Agency: Yallambie, 2008.
- Attix, F.H. *Introduction to radiological physics and radiation dosimetry*. 1986. 1st ed. Wiley-VCH. ISBN: 0471011460.
- Azevedo, A.C.P., Osibote, O.A. and Boechat, M.C.B. *Paediatric X-ray examinations in Rio de Janeiro*. 2006. Phys. Med. Biol. 51(15): 3723–3732.
<http://iopscience.iop.org/0031-9155/51/15/008>
- Baltas, D., Sakelliou, L. and Nikolaos. *The physics of modern brachytherapy for oncology (Series in medical physics and biomedical engineering)*. 2006. 1st ed. Taylor & Francis. ISBN: 0750307080.

Brenner, D. and Huda, W. *Effective dose: a useful concept in diagnostic radiology*.2008.Radiat prot dosimetry 128(4): 503-508.

Brindhaban, A.and Eze, C.U.*Estimation of radiation dose during diagnostic X-ray examinations of newborn babies and 1year old infants*.2006. Med PrincPract.15 (4):260-265.

<http://content.karger.com/produktedb/produkte.asp?typ=pdf&file=MPP2006015004260A>.

Bushberg, J.T., Seibert, J.A., Leidholdt, E.M. and Boone, J.M. *The essential physics of medical imaging*. 2001. 2nd ed. Lippincott Williams and Wilkins. ISBN:0-683301187.

Bushong, S.C. *Radiologic Science for Technologists Physics, Biology andProtection*. 1997. 6th ed. Mosby-year book. ISBN: 0-8151-1579-2.

Bushra, E., Sulieman, A. and Osman, H. *Radiation Measurement and Risk Estimation for Pediatric Patients during Routine Diagnostic Examination*.Tenth Radiation Physics & Protection Conference, 27-30 November 2010, Nasr City - Cairo, Egypt.

Capps III, C.J. *Medical, Scientific and Commercial Uses of Roentgens X-rays Today*. 2006. Journal of Business and Economics Research. 4(1).

Carroll,Q.B.andFuchs,A.W.*Funchs's radiographic Exposure and QualityControl*. 2003. 7th ed. Charles C. Thomas Pub Ltd.ISBN: 0398073732.

Cattin, P.*Basics of X-ray Principles of Medical Imaging*. MIAC, University of Basel. Nov 7th, 2011.

<http://miac.unibas.ch/PMI/01-BasicsOfXray.html>

Cember, H. and Johnson, T. *Introduction to Health Physics*. 2009. McGraw-Hill Medical. ISBN: 978-0-07-164323-8.

Cherry, S.R., Sorenson, J.A. and Phelps, M.E. *Physics in Nuclear Medicine*. 2003. 3rded, Saunders. ISBN: 0-7216-8341-X.

Cherry, P. and Duxbury, A. *Practical Radiotherapy: Physics and Equipment*. 2009.2nd ed. Wiley –Blackwell.ISBN: 9781405184267.

Ciraj, O., Markovic, S. and Kosutic, D. *Patientdosimetry in diagnostic radiology*.2003. Nuclear technology and radiation protection. 18:36-41.

www.ntpr.vinca.rs/2003_1/1_2003%20Ciraj.pdf

[www.jmpiasi.ro/2004/12\(3-4\)/4.pdf](http://www.jmpiasi.ro/2004/12(3-4)/4.pdf)

CEC, *Commission of the European Communities Quality Criteria for diagnostic radiography images in Paediatric Radiology*, a working document of the European Commission, Luxembourg (1993).

CEC. *European guidelines on quality criteria for diagnostic radiographic images in paediatrics, EUR 16261*. Luxembourg: Office for Official Publications of the European Communities, 1996.

<ftp://ftp.cordis.europa.eu/pub/fp5.../eur16261.pdf>

CEC. *European guidelines on quality criteria for diagnostic radiographic images*. EUR 16260: (Brussels EC).

<ftp://ftp.cordis.lu/pub/fp5-euratom/.../eur16260.pdf>

Connolly, J.R. *Interaction of X-ray with Matter and Radiation Safety, for EPS400-002, Introduction to X-ray Powder Diffraction*. 2007.

Cook, J.V., Shah, K., Pablot, S., et al. *Guidelines on best practice in the X-ray imaging of children; a manual for all X-ray departments*. Queen Mary's Hospital for Children, Carshalton, UK (1998).

Curry, T.S., Dowdey, J.E. and Murry, R.C. *Christensen's Physics of Diagnostic Radiology*. 1990. 4th ed, Lea & Febiger. ISBN: 0-8121-1310-1.

Dendy, P.P. and Heaton, B. *Physics for Radiologists*. 1987. Blackwell scientific Ltd publication. ISBN: 0-632-01351-6.

Dendy, P.P. and Heaton, B. *Physics for Diagnostic Radiology*. 1999. 2nd ed. Institute of Physics Publishing. ISBN: 0-7503-0591-6.

Dowsett, D.J., Kenny, P.A. and Johnston, R.E. *The Physics of Diagnostic Imaging*. 1998. 1st ed. Chapman & Hall Medical. ISBN: 0412460602.

EC. *The Health Protection of Individuals Against the Dangers of Ionizing Radiation in Relation to Medical Exposure*. L180/22, O. f. O. P. o. E. C., Ed European Commission: Luxemburg, 1997.

Farr, R.F. and Allisy-Roberts, P.J. *Physics for Medical Imaging*. 1997. Harcourt publishers limited. ISBN: 0702017701.

Feng, D.D. *Biomedical information technology (biomedical engineering)*. 2007. 1st ed. Academic press publisher. ISBN: 0123735831.

Fosbinder, R.A. and Orth, D. *Essentials of radiologic science*. 2011. Lippincott Williams Wilkins. ISBN: 078177554X.

Freitas, M.B., Yoshimura, E.M. *Diagnostic reference levels for the most frequent radiological examinations carried out in Brazil*. *Rev Panam Salud Publica*. 2009. 25(2):95–104.

www.scielosp.org/pdf/rpsp/v25n2/v25n2a01.pdf

Furlow, B. *Biological Effects of Diagnostic Imaging*. Radiologic Technology. 2004. 75(5): 355-63.

Graham, D.T. *Principles of Radiological Physics*. 1996. 3rd ed. Churchill Livingstone. ISBN: 0-443-04816-9.

Hall, E.J., Giaccia, E. *Radiobiology for the Radiologist*. 2006. 6th edition. J.B.Lippincott Company, Philadelphia, USA.

Hart, D., Hillier, M.C. and Wall, B.F. *Doses to patients from medical X-ray examinations in the UK-2000 review*. 2002. NRPB-W14 (Chilton, Didcot: NRPB).

Hart, D., Hillier, M.C. and Wall, B.F. 2009. *National reference doses for common radiographic, fluoroscopic and dental X-ray examinations in the UK*. *Br J Radiol*. 82(973): 1-12.

Hendee, W.R. and Ritenour, R. *Medical Imaging Physics*. 1992. 3rd ed. Mosby. ISBN: 015142412.

Hendee, W.R. and Ibbott, G.S. *Radiation Therapy Physics*. 1996. Mosby. ISBN: 0-8016-8099-9.

Hirshfeld, J.W., Balter, S., Brinker, J.A., et al. *ACCF/AHA/HRS/SCAI Clinical Competence Statement on Physician Knowledge to Optimize Patient Safety and Image Quality in Fluoroscopically Guided Invasive Cardiovascular Procedures*. 2004. *Journal of the American College of Cardiology*. Elsevier Inc pub. 44(11):2259-2282
<http://www.jaccjournaloftheacc.com/article/S0735-1097%2804%2901959-X/fulltext>

IAEA. *Radiological Protection for Medical Exposure to Ionizing Radiation*. IAEA: Vienna, 2002.

IAEA. *Dosimetry in diagnostic radiology: An international code of practice (Technical Reports Series No.457)*. 2007. IAEA Publisher. ISBN: 92-0-115406-2.

IAEA. *Radiation biology: A handbook for teachers and students*.2010. IAEA-TCS-42.Vienna, Austria. ISSN: 10185518.

www.pub.iaea.org/MTCD/publications/PDF/TCS-42_web.pdf

ICRP.*Recommendations of the International Commission on Radiological Protection*.ICRP Report no. 26. Annals of the ICRP 1 (3). Oxford, England: Pergamon, 1977.

ICRP. *Recommendations of the International Commission on Radiological Protection* ICRP Report no. 60. Annals of the ICRP 21 (1-3). Oxford, England: Pergamon, 1991.

ICRP.*Radiological protection and safety in medicine*. ICRP Publication 73. AnnICRP1996, 26 (2), 1-47.

ICRP Draft. *Diagnostic Reference Levels in Medical Imaging*. Draft (5 February 2001)ICRP Committee 3. www.ICRP.org/Newsand Drafts.

ICRP. *The 2007 Recommendations of the International Commission on Radiological Protection*. ICRP publication 103. Ann ICRP 2007; 37(2-4):1– 332.

ICRP. *Radiation protection in medicine*. ICRP Publication105. Ann ICRP 2007; 37 (6):1–63.

ICRP,2007b.*Quantities used in radiological protection. AnnexB to 2007Recommendations*.

ICRU, Report 74: *Patient dosimetry for X-rays used in medical imaging*. Journal of the ICRU, 2005. 5(2).

International Organization for Standardization. *Nuclear Power Plants – Quality Assurance*. International Standard ISO 6215-1980 (Geneva: ISO) (1980).

Kepler,K.,Filippova, I., Lintrop, M.andServomaa, A. *Paediatric patient dosimetry as a part of quality assurance program of radiology in Estonia*. College on Medical Physics, 2-27 September 2002, Trieste, Italy.

Kettunen, A. *Radiation dose and radiation risk to foetuses and newborns duringX-ray examinations*.2004.STUK-A204.Helsinki:Radiation and Nuclear Safety Authority. www.stuk.fi/julkaisut/stuk-a/stuk-a204.pdf

Khan, F.M. *The Physics of Radiation Therapy*.2003. 3rd ed. Lippincott Williams&Wilkins. ISBN: 0-7817-3065-1.

Lacerda, M.A.S., da Silva, T.A., Khoury, H.J., et al. *Radiation dose in paediatric patients undergoing chest X-ray examinations*. 2007. International Nuclear Atlantic Conference - INAC 2007. Santos, SP, Brazil, September 30 to October 5, 2007. Associação Brasileira DE Energia Nuclear – ABEN. ISBN: 978-85-99141-02-1.
www.ipen.br/biblioteca/cd/.../2007/.../E02_1105.pdf

Mahesh, M. *The AAPM/RSNA Physics Tutorial for Residents Fluoroscopy: Patient Radiation Exposure Issue*. 21(4). 2001

Martin CJ, Darragh CL, McKenzie GA, et al. *Implementation of a programme for reduction of radiographic doses and results achieved through increases in tube potential*. Br J Radiol 1993;66(783):228-33.

Martin, J.E. *Physics for Radiation Protection*. 2006. 2nd ed. Wiley-VCH Verlag GmbH & Co. KGaA. ISBN: 3527406115.

Miller, D.L, Balter, S., Schueler, B.A., et al. *Clinical radiation management for fluoroscopically guided interventional procedures*. 2010. 257(2).

Mohamadain, K.E.M. *Dosemetric survey in diagnostic radiology*. 2004.
www.twas.assaf.org.za:8080/.../Mohamadain_thesis.pdf?

Mohamadain, K.E.M., da Rosa, L. A. R., Azevedo, A.C.P., Guebel, M.R.N., et al. *Dose evaluation for paediatric chest X-ray examinations in Brazil and Sudan: low doses and reliable examinations can be achieved in developing countries*. 2004. Phys. Med. Biol. 49:1017–1031.
www.iopscience.iop.org/0031-9155/49/6/012/

Mohamadain, K.E.M., Azevedo, A.C.P., et al. *Dose Survey of pediatric and adult patients in Sudan*. 5th conference on nuclear and particle physics. 19-23 Nov. 2005 Cairo, Egypt.

Mohamadain, K. E. M., Azevedo, A. C. P. *Radiation dose Survey in conventional paediatric radiology*. J.Sc. Tech. 2009. 10(2):175-184.
http://jst.sustech.edu/content_details.php?id=277&chk=d9bbdf9dcefc3e2aa2a2126e3d190f19

Monaco, J.L., Bowen, K., Tadros, P.N. and Witt, P.D. *Iatrogenic deep musculocutaneous radiation injury following percutaneous coronary intervention*. J Invasive Cardiol 2003; 15 (8): 451 – 453.

Mooney, R. and Thomas, P.S. *Dose reduction in a paediatric X-ray department following optimization of radiographic technique*. Br J radiol. 1998. 71(848): 852-860.
www.bjr.birjournals.org/content/71/848/852.reprint

Mould, R. *Introductory Medical Statistics*. 1995. 3rd ed.; IoP: Bristol.

Nave, R (2009). X-rays.

<http://hyperphysics.phy-astr.gsu.edu/HBASE/quacon.html#quacon>, viewed 20/07/2009.

Nfaoui, K., Bentayeb, F., El Basraoui, O. and de Azevedo, A.C. *Evaluation of paediatric X-ray doses in Moroccan university hospitals*. 2010. *Radiation Protection Dosimetry* 142(2-4):238-243.

<http://rpd.oxfordjournals.org/content/142/2-4/238.short>

Nordic guidance levels for patient doses in diagnostic radiology: radiation protection and nuclear safety authorities in Denmark, Finland, Iceland, Norway and Sweden, report No. 5. 1996.

Ogundarea, F.O., Ajibola, C. L. and Balogun, F.A. *Survey of radiological techniques and doses of children undergoing some common X-ray examinations in three hospitals in Nigeria*. 2004. *Med. Phys.* 31(3):521–524.

<http://www.ncbi.nlm.nih.gov/pubmed/15070249>

Osibote, O.A., de Azevedo, A.C. *Estimation of adult patient doses for common diagnostic X-ray examinations in Rio de Janeiro, Brazil*. 2008. *Phys Med.* 24(1):21-28.

www.ukpmc.ac.uk/abstract/MED/18164640

Panichello, J.J. *X-ray Repair: A Comprehensive Guide to the Installation and Servicing of Radiographic Equipment*. 1998. Charles C. Thomas pub Ltd. ISBN: 0-398-06815-1.

Photodisintegration Pictures and Images - Zeably

www.zeably.com/Photodisintegration

Physical Principles of Medical Imaging Online, Resources for Learning and Teaching.

<http://www.sprawls.org/resources>

PTW: Radiation Therapy.

www.ptw.de/radiation_therapy.html

PTW: UNIDOS Universal Dosimeter.

www.ptw.de/unidos_dosemeter_ad0.html

Podgorsak, E.B. *Radiation oncology physics: A handbook for teachers and students*. 2005. IAEA Publisher. ISBN: 92-0-107304-6.

Podgorsak, E.B. *Radiation physics Handbook for medical physicists*. 2006. Springer, Berlin. ISBN: 3540250417.

Racz, G.B. and Noe, C.E . *Pain management – current issues and opinions*. 2012. In Tech publisher. ISBN: 9789533078137.

Ramanaidu, S., Sta Maria, R.B., Ng KH, George J, Kumar G. *Evaluation of radiation dose and image quality following changes to tube potential (kVp) in conventional paediatric chest radiography*. Biomed Imaging Interv J. 2006. 2(3):e35.
www.bij.org/2006/3/e35/e35.pdf

Rampado, O. and Ropolo, R.A *Method for a Real Time Estimation of Entrance Surface Dose Distribution in Interventional Neuroradiology*. 2004. American Association of Physicists in Medicine, Medical Physics. 31(8):2356-2361.

Schneider, K., Fendel, H., Bakowski, C., et al. *Results of a dosimetric study in the European Community on frequent X-ray examinations in infants*. 1992. Radiation Protection Dosimetry. 43: 31-36.

Seeram, E. and Brennan, P.C. *Diagnostic Reference Levels in Radiology*. 2006. *Radiological Technology*. 77 (5):376-384.

Seibert, J.A. and Boone, J.M. *X-ray Imaging Physics for Nuclear Medicine Technology. Part 2: X-ray Interactions and Image Formation*. 2005. Journal of Nuclear Medicine. 33(1):3-18.

Sorop, I. and Dadulescu, E. *Assessment of entrance surface doses for newborn babies within an intensive care unit*. Romanian Reports in Physics. 2011. 63(2):401-410.
www.infim.ro/rrp/2011_63_2/art08Sorop.pdf

Sprawls, P. *Physical Principles of Medical Imaging*. 1995. 2nd edition. Medical physics pub corp. ISBN: 0-944838-54-5.

Suliman, I.I. and Elshiekh, E.H.A. *Radiation doses from some common paediatric X-ray examinations in Sudan*. Radiation protection dosimetry. 2008. 132(1),64-72.
<http://rpd.oxfordjournals.org/content/132/1/64.short>

Thayalan, K. *Basic radiological physics*. 2001. 1st ed. Jaypee Brothers Medical Publishers, New Delhi. ISBN: 9788171798544.

Thompson, M.A., Hattaway, M.P., Hall, J.D. and Dowd, S.B. *Principle of Imaging Science and Protection*. 1994. W.B Saunders Company. ISBN: 721634281.

Toivonen, M. *Patient dosimetry protocols in digital and interventional radiology*. 2001. Radiat Prot Dosim. 94(1-2): 105-8

United Nation Scientific Committee on effect of Atomic Radiation. *Sources and effects of ionizing radiation*. Report to the General Assembly with Scientific Annex (United Nations, New York) (2000).

United Nations Scientific Committee on the Effects of Atomic Radiation Sources: (2000). *Effects and Risks of Ionizing Radiation*. UNSCEAR 2000 Report, vol. II: effects. New York, NY: United Nations.

United Nation Scientific Committee on effect of Atomic Radiation. *Sources and effects of ionizing radiation, UNSCEAR 2008 Report: Volume I : Sources – Report to the general assembly scientific annexes A and B*. 2010. ISBN: 9789211422740.

Wall, B.F. *How to assess the dose to the patient in diagnostic radiology*. NRPB Chilton, Didcot, Oxon. 1996.

Wall, B.F., Hart, D. *Revised radiation doses for typical X-ray examinations*. 1997. Br J Radiol 70: 437-439.

Webb, G.A.M and Wall, B.F. *Medical X-ray exposures in the UK*. National Radiological Protection Board, Chilton, UK.

Wolbarst, A.B. *Physics of Radiology*. 1993. Medical Physics Publishing. ISBN: 0-8385-5769-4.

Wraith CM, Martin CJ, Stockdale EJ, et al. *An investigation into techniques for reducing doses from neonatal radiographic examinations*. Br J Radiol 1995;68(814):1074-82.

APPENDIX A

The patient data and dose for Benghazi Children Hospital

Table (1A): The values of equivalent patient diameter (d), entrance surface dose (ESD)patient data for the age group (0-15)y. and

Examination	Age (y)	Weight (kg)	d (cm)	ESD (mGy)	Log ESD (mGy)
Abdomen AP	0.08	3.27	9.73	0.106	-0.973
Abdomen AP	0.42	5.4	11.18	0.124	-0.908
Abdomen AP	11.00	39.5	18.13	0.258	-0.589
Abdomen AP	0.08	5.05	10.53	0.235	-0.629
Abdomen AP	0.58	7	11.28	0.154	-0.812
Abdomen AP	5.00	17	14.03	0.146	-0.835
Chest AP	1.00	8	11.98	0.233	-0.633
Chest AP	0.08	3	9.32	0.239	-0.622
Chest AP	0.67	8.54	13.24	0.263	-0.580
Chest AP	1.00	10	12.78	0.245	-0.611
Chest AP	0.58	7.63	12.62	0.209	-0.680
Chest AP	0.08	3	9.02	0.225	-0.647
Chest AP	0.58	6	11.10	0.168	-0.774
Chest AP	0.33	7	11.28	0.229	-0.641
Chest AP	0.83	8.011	11.82	0.166	-0.779
Chest AP	0.25	5	10.86	0.168	-0.774
Chest AP	0.17	3.9	10.39	0.173	-0.761
Chest AP	1.00	11.5	13.05	0.233	-0.632
Chest AP	0.50	6.9	11.72	0.274	-0.562
Chest AP	1.00	9	12.20	0.196	-0.708
Chest AP	0.58	8.22	12.32	0.217	-0.664
Chest AP	0.42	5.4	11.18	0.171	-0.768
Chest AP	0.17	4.5	10.03	0.176	-0.755
Chest AP	0.33	5	10.30	0.181	-0.743
Chest AP	0.33	9	13.60	0.390	-0.409
Chest AP	0.17	5.42	11.30	0.373	-0.428
Chest AP	0.17	6.04	11.93	0.206	-0.685
Chest AP	2.00	13.5	13.52	0.265	-0.577
Chest AP	1.00	10	12.78	0.267	-0.574
Chest AP	1.00	8	11.73	0.233	-0.633
Chest AP	1.00	10	13.21	0.230	-0.639
Chest AP	2.00	14	13.56	0.232	-0.635

Chest AP	0.25	7	12.40	0.296	-0.529
Chest AP	0.42	7.52	12.33	0.242	-0.617
Chest AP	0.58	8.93	12.40	0.271	-0.567
Chest AP	0.75	10.2	13.34	0.275	-0.561
Chest AP	0.58	7	11.28	0.221	-0.656
Chest AP	1.00	8.5	12.26	0.313	-0.504
Chest AP	0.33	7.07	11.95	0.246	-0.609
Chest AP	0.42	8.25	13.34	0.235	-0.628
Chest AP	0.08	5.1	10.58	0.191	-0.720
Chest AP	1.00	10	12.86	0.234	-0.631
Chest AP	0.33	8.53	13.03	0.233	-0.632
Chest AP	0.08	5.32	11.20	0.220	-0.657
Chest AP	1.00	10.24	12.77	0.190	-0.720
Chest AP	0.25	6.33	12.00	0.228	-0.642
Chest AP	0.42	6	10.93	0.292	-0.535
Chest AP	1.00	6.65	11.08	0.269	-0.570
Chest AP	0.25	4.5	10.40	0.288	-0.541
Chest AP	0.33	7	11.71	0.252	-0.599
Chest AP	0.08	4.3	9.72	0.220	-0.657
Chest AP	0.42	5.2	10.42	0.314	-0.503
Chest AP	0.33	6.75	11.59	0.169	-0.772
Chest AP	0.33	6.5	10.80	0.195	-0.710
Chest AP	0.02	3.5	9.74	0.298	-0.526
Chest AP	0.42	5	10.05	0.220	-0.658
Chest AP	0.08	4.5	10.21	0.248	-0.606
Chest AP	1.00	8.6	12.69	0.252	-0.599
Chest AP	0.25	5	10.76	0.236	-0.627
Chest AP	1.00	9.5	13.75	0.185	-0.732
Chest AP	0.42	7.5	12.03	0.290	-0.538
Chest AP	0.42	7.32	11.79	0.403	-0.395
Chest AP	1.00	11	13.76	0.205	-0.688
Chest AP	0.08	8.04	11.92	0.242	-0.617
Chest AP	0.58	4	9.45	0.114	-0.943
Chest AP	0.33	7.25	12.01	0.249	-0.604
Chest AP	0.42	7.2	11.88	0.284	-0.547
Chest AP	2.00	12	13.18	0.304	-0.517
Chest AP	0.25	5	10.66	0.298	-0.526
Chest AP	0.75	9.26	13.17	0.228	-0.642
Chest AP	0.25	6.7	11.73	0.259	-0.587

Chest AP	0.25	5	10.76	0.410	-0.387
Chest AP	1.00	10	12.24	0.270	-0.568
Chest AP	0.25	5	10.66	0.320	-0.495
Chest AP	1.00	8	12.24	0.322	-0.493
Chest AP	0.17	6.14	11.82	0.299	-0.524
Chest AP	0.42	7.014	11.81	0.245	-0.611
Chest AP	0.50	7.5	11.85	0.260	-0.585
Chest AP	0.42	6.2	11.02	0.254	-0.595
Chest AP	1.00	11	13.07	0.221	-0.655
Chest AP	2.00	14	14.48	0.257	-0.589
Chest AP	0.58	7.5	11.52	0.251	-0.601
Chest AP	0.08	6	11.19	0.263	-0.581
Chest AP	0.92	10	13.21	0.312	-0.507
Chest AP	0.42	9	13.28	0.331	-0.480
Chest AP	0.33	8.16	12.95	0.309	-0.510
Chest AP	0.92	8	12.42	0.264	-0.578
Chest AP	0.08	5.57	11.06	0.303	-0.519
Chest AP	0.42	6.4	11.65	0.258	-0.588
Chest AP	0.50	7.5	12.62	0.357	-0.447
Chest AP	0.58	7	11.37	0.208	-0.682
Chest AP	0.75	7	11.28	0.248	-0.605
Chest AP	0.42	5	10.30	0.297	-0.528
Chest AP	1.00	7.73	12.03	0.285	-0.545
Chest AP	0.08	3	9.65	0.378	-0.423
Chest AP	0.42	6.5	11.65	0.438	-0.358
Chest AP	0.50	10	13.30	0.218	-0.662
Chest AP	0.17	3.2	8.94	0.253	-0.597
Chest AP	0.08	6	11.58	0.400	-0.398
Chest AP	0.92	9	12.36	0.376	-0.425
Chest AP	0.75	7	11.28	0.413	-0.384
Chest AP	0.03	3.64	9.63	0.213	-0.672
Chest AP	0.42	6.44	12.10	0.407	-0.391
Chest AP	0.42	9.1	13.15	0.335	-0.474
Chest AP	0.50	8.47	13.30	0.242	-0.617
Chest AP	0.50	7	11.71	0.251	-0.600
Chest AP	0.75	8.5	12.52	0.289	-0.539
Chest AP	0.17	4.18	9.84	0.252	-0.598
Chest AP	0.50	8.27	12.83	0.320	-0.495
Chest AP	0.58	8	11.98	0.254	-0.596

Chest AP	0.33	7	11.80	0.267	-0.573
Chest AP	0.25	2	7.14	0.235	-0.628
Chest AP	1.00	9	11.97	0.240	-0.619
Chest AP	1.00	9.09	12.51	0.305	-0.515
Chest AP	0.17	5.5	10.80	0.292	-0.535
Chest AP	0.92	8.8	12.65	0.266	-0.575
Chest AP	4.00	16	14.06	0.254	-0.594
Chest AP	5.00	15	13.68	0.298	-0.526
Chest AP	3.00	19	15.87	0.260	-0.585
Chest AP	7.00	22	14.79	0.297	-0.527
Chest AP	7.00	22	14.97	0.363	-0.440
Chest AP	3.00	18	15.37	0.262	-0.581
Chest AP	5.00	18	15.14	0.311	-0.507
Chest AP	4.00	17	14.09	0.402	-0.396
Chest AP	7.00	20	14.51	0.406	-0.391
Chest AP	4.00	16.5	14.49	0.298	-0.526
Chest AP	3.00	15.5	14.05	0.329	-0.483
Chest AP	3.00	15	13.75	0.336	-0.474
Chest AP	5.00	16.5	14.21	0.442	-0.355
Chest AP	3.00	12	13.03	0.379	-0.422
Chest Lat	0.83	6.8	11.20	0.081	-1.094
Chest Lat	1.00	9	12.53	0.288	-0.540
Chest Lat	0.58	7.6	12.02	0.281	-0.551
Chest Lat	0.50	7.5	12.62	0.280	-0.553
Chest PA	15.00	38	17.39	0.327	-0.486
Chest PA	11.00	34	17.10	0.195	-0.710
Chest PA	10.00	24.5	15.99	0.253	-0.597
Chest PA	8.00	35	19.03	0.301	-0.522
Chest PA	11.00	32	19.70	0.329	-0.483
Chest PA	9.00	25	15.19	0.295	-0.531
Chest PA	8.00	25	15.83	0.383	-0.417
Chest PA	8.00	27	16.08	0.234	-0.632
Chest PA	6.00	20	15.01	0.237	-0.625
Chest PA	7.00	22	14.85	0.286	-0.544
Skull Lat	11.00	33	17.58	0.654	-0.184
Cervical spine AP	8.00	25	16.57	0.167	-0.778

Table (2A): The values of equivalent patient diameter (d), entrance surface dose (ESD) and patient data for the group (0-1)y.

Examination	Age (y)	Weight (kg)	d (cm)	ESD (mGy)	Log ESD (mGy)
Abdomen AP	0.08	3.27	9.73	0.106	-0.973
Abdomen AP	0.42	5.4	11.18	0.124	-0.908
Abdomen AP	0.08	5.05	10.53	0.235	-0.629
Abdomen AP	0.58	7	11.28	0.154	-0.812
Chest AP	0.08	3	9.32	0.239	-0.622
Chest AP	0.67	8.54	13.24	0.263	-0.580
Chest AP	0.58	7.63	12.62	0.209	-0.680
Chest AP	0.08	3	9.02	0.225	-0.647
Chest AP	0.58	6	11.10	0.168	-0.774
Chest AP	0.33	7	11.28	0.229	-0.641
Chest AP	0.83	8.011	11.82	0.166	-0.779
Chest AP	0.25	5	10.86	0.168	-0.774
Chest AP	0.17	3.9	10.39	0.173	-0.761
Chest AP	0.50	6.9	11.72	0.274	-0.562
Chest AP	0.58	8.22	12.32	0.217	-0.664
Chest AP	0.42	5.4	11.18	0.171	-0.768
Chest AP	0.17	4.5	10.03	0.176	-0.755
Chest AP	0.33	5	10.30	0.181	-0.743
Chest AP	0.33	9	13.60	0.390	-0.409
Chest AP	0.17	5.42	11.30	0.373	-0.428
Chest AP	0.17	6.04	11.93	0.206	-0.685
Chest AP	0.25	7	12.40	0.296	-0.529
Chest AP	0.42	7.52	12.33	0.242	-0.617
Chest AP	0.58	8.93	12.40	0.271	-0.567
Chest AP	0.75	10.2	13.34	0.275	-0.561
Chest AP	0.58	7	11.28	0.221	-0.656
Chest AP	0.33	7.07	11.95	0.246	-0.609
Chest AP	0.42	8.25	13.34	0.235	-0.628
Chest AP	0.08	5.1	10.58	0.191	-0.720
Chest AP	0.33	8.53	13.03	0.233	-0.632
Chest AP	0.08	5.32	11.20	0.220	-0.657
Chest AP	0.25	6.33	12.00	0.228	-0.642
Chest AP	0.42	6	10.93	0.292	-0.535
Chest AP	0.25	4.5	10.40	0.288	-0.541
Chest AP	0.33	7	11.71	0.252	-0.599
Chest AP	0.08	4.3	9.72	0.220	-0.657

Chest AP	0.42	5.2	10.42	0.314	-0.503
Chest AP	0.33	6.75	11.59	0.169	-0.772
Chest AP	0.33	6.5	10.80	0.195	-0.710
Chest AP	0.02	3.5	9.74	0.298	-0.526
Chest AP	0.42	5	10.05	0.220	-0.658
Chest AP	0.08	4.5	10.21	0.248	-0.606
Chest AP	0.25	5	10.76	0.236	-0.627
Chest AP	0.42	7.5	12.03	0.290	-0.538
Chest AP	0.42	7.32	11.79	0.403	-0.395
Chest AP	0.08	8.04	11.92	0.242	-0.617
Chest AP	0.58	4	9.45	0.114	-0.943
Chest AP	0.33	7.25	12.01	0.249	-0.604
Chest AP	0.42	7.2	11.88	0.284	-0.547
Chest AP	0.25	5	10.66	0.298	-0.526
Chest AP	0.75	9.26	13.17	0.228	-0.642
Chest AP	0.25	6.7	11.73	0.259	-0.587
Chest AP	0.25	5	10.76	0.410	-0.387
Chest AP	0.25	5	10.66	0.320	-0.495
Chest AP	0.17	6.14	11.82	0.299	-0.524
Chest AP	0.42	7.014	11.81	0.245	-0.611
Chest AP	0.50	7.5	11.85	0.260	-0.585
Chest AP	0.42	6.2	11.02	0.254	-0.595
Chest AP	0.58	7.5	11.52	0.251	-0.601
Chest AP	0.08	6	11.19	0.263	-0.581
Chest AP	0.92	10	13.21	0.312	-0.507
Chest AP	0.42	9	13.28	0.331	-0.480
Chest AP	0.33	8.16	12.95	0.309	-0.510
Chest AP	0.92	8	12.42	0.264	-0.578
Chest AP	0.08	5.57	11.06	0.303	-0.519
Chest AP	0.42	6.4	11.65	0.258	-0.588
Chest AP	0.50	7.5	12.62	0.357	-0.447
Chest AP	0.58	7	11.37	0.208	-0.682
Chest AP	0.75	7	11.28	0.248	-0.605
Chest AP	0.42	5	10.30	0.297	-0.528
Chest AP	0.08	3	9.65	0.378	-0.423
Chest AP	0.42	6.5	11.65	0.438	-0.358
Chest AP	0.50	10	13.30	0.218	-0.662
Chest AP	0.17	3.2	8.94	0.253	-0.597
Chest AP	0.08	6	11.58	0.400	-0.398

Chest AP	0.92	9	12.36	0.376	-0.425
Chest AP	0.75	7	11.28	0.413	-0.384
Chest AP	0.03	3.64	9.63	0.213	-0.672
Chest AP	0.42	6.44	12.10	0.407	-0.391
Chest AP	0.42	9.1	13.15	0.335	-0.474
Chest AP	0.50	8.47	13.30	0.242	-0.617
Chest AP	0.50	7	11.71	0.251	-0.600
Chest AP	0.75	8.5	12.52	0.289	-0.539
Chest AP	0.17	4.18	9.84	0.252	-0.598
Chest AP	0.50	8.27	12.83	0.320	-0.495
Chest AP	0.58	8	11.98	0.254	-0.596
Chest AP	0.33	7	11.80	0.267	-0.573
Chest AP	0.25	2	7.14	0.235	-0.628
Chest AP	0.17	5.5	10.80	0.292	-0.535
Chest AP	0.92	8.8	12.65	0.266	-0.575
Chest Lat	0.83	6.8	11.20	0.081	-1.094
Chest Lat	0.58	7.6	12.02	0.281	-0.551
Chest Lat	0.50	7.5	12.62	0.280	-0.553
Chest AP	1.00	8	11.98	0.233	-0.633
Chest AP	1.00	10	12.78	0.245	-0.611
Chest AP	1.00	11.5	13.05	0.233	-0.632
Chest AP	1.00	9	12.20	0.196	-0.708
Chest AP	1.00	10	12.78	0.267	-0.574
Chest AP	1.00	8	11.73	0.233	-0.633
Chest AP	1.00	10	13.21	0.230	-0.639
Chest AP	1.00	8.5	12.26	0.313	-0.504
Chest AP	1.00	10	12.86	0.234	-0.631
Chest AP	1.00	10.24	12.77	0.190	-0.720
Chest AP	1.00	6.65	11.08	0.269	-0.570
Chest AP	1.00	8.6	12.69	0.252	-0.599
Chest AP	1.00	9.5	13.75	0.185	-0.732
Chest AP	1.00	11	13.76	0.205	-0.688
Chest AP	1.00	10	12.24	0.270	-0.568
Chest AP	1.00	8	12.24	0.322	-0.493
Chest AP	1.00	11	13.07	0.221	-0.655
Chest AP	1.00	7.73	12.03	0.285	-0.545
Chest AP	1.00	9	11.97	0.240	-0.619
Chest AP	1.00	9.09	12.51	0.305	-0.515
Chest Lat	1.00	9	12.53	0.288	-0.540

Table (3A): The values of equivalent patient diameter (d), entrance surface dose (ESD) and patient data for the age group (1-5)y.

Examination	Age (y)	Weight (kg)	d (cm)	ESD (mGy)	Log ESD (mGy)
Chest AP	2	13.5	13.52	0.265	-0.577
Chest AP	2	14	13.56	0.232	-0.635
Chest AP	2	12	13.18	0.304	-0.517
Chest AP	2	14	14.48	0.257	-0.589
Chest AP	3	19	15.87	0.260	-0.585
Chest AP	3	18	15.37	0.262	-0.581
Chest AP	3	15.5	14.05	0.329	-0.483
Chest AP	3	15	13.75	0.336	-0.474
Chest AP	3	12	13.03	0.379	-0.422
Chest AP	4	16	14.06	0.254	-0.594
Chest AP	4	17	14.09	0.402	-0.396
Chest AP	4	16.5	14.49	0.298	-0.526
Chest AP	5	15	13.68	0.298	-0.526
Chest AP	5	18	15.14	0.311	-0.507
Chest AP	5	16.5	14.21	0.442	-0.355
Abdomen AP	5	17	14.03	0.146	-0.835

Table (4A):The values of equivalent patient diameter (d), entrance surface dose(ESD) and;patient data for theage group (5-10)y.

Examination	Age (y)	Weight (kg)	d (cm)	ESD (mGy)	Log ESD (mGy)
Chest PA	6	20	15.01	0.237	-0.625
Chest AP	7	22	14.79	0.297	-0.527
Chest AP	7	22	14.97	0.363	-0.440
Chest AP	7	20	14.51	0.406	-0.391
Chest PA	7	22	14.85	0.286	-0.544
Chest PA	8	35	19.03	0.301	-0.522
Chest PA	8	25	15.83	0.383	-0.417
Chest PA	8	27	16.08	0.234	-0.632
Cervical spine AP	8	25	16.57	0.167	-0.778
Chest PA	9	25	15.19	0.295	-0.531

Table (5A): The values of equivalent patient diameter (d), entrance surface dose (ESD) and patient data for the age group (10-15)y.

Examination	Age (y)	Weight (kg)	d (cm)	ESD (mGy)	Log ESD (mGy)
Chest PA	10	24.5	15.99	0.253	-0.597
Abdomen AP	11	39.5	18.13	0.258	-0.589
Chest PA	11	34	17.10	0.195	-0.710
Chest PA	11	32	19.70	0.329	-0.483
Skull Lat	11	33	17.58	0.654	-0.184
Chest PA	15	38	17.39	0.327	-0.486

Table (6A): The values of entrance surface dose (ESD) and weight for paediatric patients with ages from (0-1)y undergoing chest AP.

Examination	Age (y)	Weight (kg)	ESD (mGy)	Log ESD (mGy)
chest AP	0.08	3	0.239	-0.622
chest AP	0.67	8.54	0.263	-0.58
chest AP	0.58	7.63	0.209	-0.68
chest AP	0.08	3	0.225	-0.647
chest AP	0.58	6	0.168	-0.774
chest AP	0.33	7	0.229	-0.641
chest AP	0.83	8.011	0.166	-0.779
chest AP	0.25	5	0.168	-0.774
chest AP	0.17	3.9	0.173	-0.761
chest AP	0.5	6.9	0.274	-0.562
chest AP	0.58	8.22	0.217	-0.664
chest AP	0.42	5.4	0.171	-0.768
chest AP	0.17	4.5	0.176	-0.755
chest AP	0.33	5	0.181	-0.743
chest AP	0.33	9	0.39	-0.409
chest AP	0.17	5.42	0.373	-0.428
chest AP	0.17	6.04	0.206	-0.685
chest AP	0.25	7	0.296	-0.529
chest AP	0.42	7.52	0.242	-0.617
chest AP	0.58	8.93	0.271	-0.567
chest AP	0.75	10.2	0.275	-0.561
chest AP	0.58	7	0.221	-0.656
chest AP	0.33	7.07	0.246	-0.609

chest AP	0.42	8.25	0.235	-0.628
chest AP	0.08	5.1	0.191	-0.72
chest AP	0.33	8.53	0.233	-0.632
chest AP	0.08	5.32	0.22	-0.657
chest AP	0.25	6.33	0.228	-0.642
chest AP	0.42	6	0.292	-0.535
chest AP	0.25	4.5	0.288	-0.541
chest AP	0.33	7	0.252	-0.599
chest AP	0.08	4.3	0.22	-0.657
chest AP	0.42	5.2	0.314	-0.503
chest AP	0.33	6.75	0.169	-0.772
chest AP	0.33	6.5	0.195	-0.71
chest AP	0.42	5	0.22	-0.658
chest AP	0.08	4.5	0.248	-0.606
chest AP	0.25	5	0.236	-0.627
chest AP	0.42	7.5	0.29	-0.538
chest AP	0.42	7.32	0.403	-0.395
chest AP	0.08	8.04	0.242	-0.617
chest AP	0.58	4	0.114	-0.943
chest AP	0.33	7.25	0.249	-0.604
chest AP	0.42	7.2	0.284	-0.547
chest AP	0.25	5	0.298	-0.526
chest AP	0.75	9.26	0.228	-0.642
chest AP	0.25	6.7	0.259	-0.587
chest AP	0.25	5	0.41	-0.387
chest AP	0.25	5	0.32	-0.495
chest AP	0.17	6.14	0.299	-0.524
chest AP	0.42	7.014	0.245	-0.611
chest AP	0.5	7.5	0.26	-0.585
chest AP	0.42	6.2	0.254	-0.595
chest AP	0.58	7.5	0.251	-0.601
chest AP	0.08	6	0.263	-0.581
chest AP	0.92	10	0.312	-0.507
chest AP	0.42	9	0.331	-0.48
chest AP	0.33	8.16	0.309	-0.51
chest AP	0.92	8	0.264	-0.578
chest AP	0.08	5.57	0.303	-0.519
chest AP	0.42	6.4	0.258	-0.588
chest AP	0.5	7.5	0.357	-0.447

chest AP	0.58	7	0.208	-0.682
chest AP	0.75	7	0.248	-0.605
chest AP	0.42	5	0.297	-0.528
chest AP	0.08	3	0.378	-0.423
chest AP	0.42	6.5	0.438	-0.358
chest AP	0.5	10	0.218	-0.662
chest AP	0.17	3.2	0.253	-0.597
chest AP	0.08	6	0.4	-0.398
chest AP	0.92	9	0.376	-0.425
chest AP	0.75	7	0.413	-0.384
chest AP	0.42	6.44	0.407	-0.391
chest AP	0.42	9.1	0.335	-0.474
chest AP	0.5	8.47	0.242	-0.617
chest AP	0.5	7	0.251	-0.6
chest AP	0.75	8.5	0.289	-0.539
chest AP	0.17	4.18	0.252	-0.598
chest AP	0.5	8.27	0.32	-0.495
chest AP	0.58	8	0.254	-0.596
chest AP	0.33	7	0.267	-0.573
chest AP	0.25	2	0.235	-0.628
chest AP	0.17	5.5	0.292	-0.535
chest AP	0.92	8.8	0.266	-0.575
chest AP	0.02	3.5	0.298	-0.526
chest AP	0.03	3.64	0.213	-0.672
chest AP	1	8	0.233	-0.633
chest AP	1	10	0.245	-0.611
chest AP	1	11.5	0.233	-0.632
chest AP	1	9	0.196	-0.708
chest AP	1	10	0.267	-0.574
chest AP	1	8	0.233	-0.633
chest AP	1	10	0.23	-0.639
chest AP	1	8.5	0.313	-0.504
chest AP	1	10	0.234	-0.631
chest AP	1	10.24	0.19	-0.72
chest AP	1	6.65	0.269	-0.57
chest AP	1	8.6	0.252	-0.599
chest AP	1	9.5	0.185	-0.732
chest AP	1	11	0.205	-0.688
chest AP	1	10	0.27	-0.568

chest AP	1	8	0.322	-0.493
chest AP	1	11	0.221	-0.655
chest AP	1	7.73	0.285	-0.545
chest AP	1	9	0.24	-0.619
chest AP	1	9.09	0.305	-0.515

Table (7A): The values of entrance surface dose (ESD) and weight for paediatric patients with ages from (1-5)y undergoing chest AP.

Examination	Age (y)	Weight (kg)	ESD (mGy)	Log ESD (mGy)
chest AP	2	13.5	0.265	-0.577
chest AP	2	14	0.232	-0.635
chest AP	2	12	0.304	-0.517
chest AP	2	14	0.257	-0.589
chest AP	3	19	0.26	-0.585
chest AP	3	18	0.262	-0.581
chest AP	3	15.5	0.329	-0.483
chest AP	3	15	0.336	-0.474
chest AP	3	12	0.379	-0.422
chest AP	4	16	0.254	-0.594
chest AP	4	17	0.402	-0.396
chest AP	4	16.5	0.298	-0.526
chest AP	5	15	0.298	-0.526
chest AP	5	18	0.311	-0.507
chest AP	5	16.5	0.442	-0.355

Table (8A): The values of entrance surface dose (ESD) and weight for paediatric patients with ages from (5-10)y undergoing chest PA

Examination	Age (y)	Weight (kg)	ESD (mGy)	Log ESD (mGy)
chest PA	6	20	0.237	-0.625
chest PA	7	22	0.286	-0.544
chest PA	8	35	0.301	-0.522
chest PA	8	25	0.383	-0.417
chest PA	8	27	0.234	-0.632
chest PA	9	25	0.295	-0.531

Table (9A): The values of entrance surface dose (ESD) and weight for paediatric patients with ages from (10-15)y undergoing chest PA.

Examination	Age (y)	Weight (kg)	ESD (mGy)	Log ESD (mGy)
chest PA	10	24.5	0.253	-0.597
chest PA	11	34	0.195	-0.710
chest PA	11	32	0.329	-0.483
chest PA	15	38	0.327	-0.485

Table (10 A): The values of entrance surface dose (ESD) and weight for paediatric patients with ages from (0-1)y undergoing chest lat.

Examination	Age (y)	Weight (kg)	ESD (mGy)	Log ESD (mGy)
chest lat	0.83	6.8	0.081	-1.092
chest lat	0.58	7.6	0.281	-0.551
chest lat	0.5	7.5	0.28	-0.553
chest lat	1	9	0.288	-0.541

Table (11 A): The values of entrance surface dose (ESD) and weight for paediatric patients with ages under 15 undergoing abdomen AP.

Examination	Age (y)	Weight (kg)	ESD (mGy)	Log ESD (mGy)
abdomen AP	0.08	3.27	0.106	-0.973
abdomen AP	0.42	5.4	0.124	-0.908
abdomen AP	0.08	5.05	0.235	-0.629
abdomen AP	0.58	7	0.154	-0.812
abdomen AP	11	39.5	0.258	-0.589
abdomen AP	5	17	0.146	-0.835

APPENDIX B

The patient data and dose for Alhawari General Hospital

Table (1B): The values of effective dose (ED) calculated using dosecal software and dose area product (DAP) for adult patients undergoing abdomen AP.

Examination	Age (y)	Weight (kg)	ED (mSv)	DAP (Gycm ²)
abdomen AP	25	77	0.119	0.64
abdomen AP	41	85	0.394	2.12
abdomen AP	29	80	0.155	0.83
abdomen AP	75	57	0.155	0.84
abdomen AP	34	62	0.106	0.57

Table (2B): The values of effective dose (ED) calculated using dosecal software and dosearea product(DAP) for adult patients undergoing chest PA.

Examination	Age (y)	Weight (kg)	ED (mSv)	DAP (Gycm ²)
chest PA	75	76	0.016	0.08
chest PA	26	62	0.020	0.11
chest PA	36	59	0.007	0.04
chest PA	36	59	0.004	0.02
chest PA	65	101	0.033	0.17
chest PA	50	91	0.024	0.13
chest PA	62	75	0.022	0.12
chest PA	64	98	0.021	0.11
chest PA	43	100	0.026	0.14
chest PA	49	88	0.024	0.13
chest PA	34	75	0.012	0.06
chest PA	17	90	0.027	0.14
chest PA	40	112	0.029	0.16
chest PA	25	58	0.010	0.05
chest PA	27	60	0.051	0.27
chest PA	70	88	0.020	0.10
chest PA	37	100	0.052	0.28
chest PA	15	64	0.016	0.08
chest PA	53	118	0.047	0.25
chest PA	60	75	0.016	0.09
chest PA	54	62	0.011	0.06

chest PA	52	91	0.041	0.22
chest PA	77	57	0.038	0.20
chest PA	53	83	0.028	0.15
chest PA	27	82	0.033	0.17
chest PA	31	99	0.021	0.11
chest PA	48	75	0.017	0.09
chest PA	79	87	0.028	0.15
chest PA	36	105	0.015	0.08
chest PA	51	73	0.041	0.22
chest PA	55	55	0.013	0.07
chest PA	52	95	0.015	0.08
chest PA	58	106	0.040	0.21
chest PA	24	101	0.017	0.09
chest PA	33	90	0.024	0.13
chest PA	42	66	0.013	0.07
chest PA	43	65	0.010	0.05
chest PA	70	95	0.021	0.11
chest PA	60	57	0.011	0.06
chest PA	32	102	0.029	0.15
chest PA	49	99	0.011	0.06
chest PA	35	80	0.015	0.08
chest PA	50	75	0.011	0.06
chest PA	70	86	0.015	0.08
chest PA	75	72	0.013	0.07
chest PA	71	52	0.012	0.07
chest PA	30	82	0.020	0.11
chest PA	25	73	0.012	0.06
chest PA	36	105	0.046	0.24
chest PA	33	85	0.141	0.75
chest PA	60	101	0.027	0.14
chest PA	18	65	0.014	0.07
chest PA	26	85	0.049	0.26
chest PA	20	115	0.098	0.82
chest PA	44	68	0.020	0.11
chest PA	31	93	0.013	0.07
chest PA	26	66	0.021	0.11
chest PA	32	67	0.019	0.10
chest PA	59	95	0.018	0.09
chest PA	28	67	0.014	0.07

chest PA	24	83	0.010	0.05
chest PA	38	90	0.019	0.10
chest PA	59	73	0.020	0.11
chest PA	65	52	0.010	0.05
chest PA	56	115	0.039	0.21
chest PA	20	80	0.053	0.28
chest PA	61	107	0.031	0.16
chest PA	40	65	0.012	0.06
chest PA	30	54	0.008	0.04
chest PA	65	107	0.036	0.19
chest PA	37	77	0.013	0.07
chest PA	75	113	0.039	0.21
chest PA	26	60	0.024	0.13
chest PA	34	62	0.012	0.06
chest PA	70	95	0.028	0.15
chest PA	47	67	0.012	0.06
chest PA	55	71	0.015	0.08

Table (3B): The values of effective dose (ED) calculated using dosecal software and dosearea product (DAP) for adult patients undergoing cervical spine AP.

Examination	Age (y)	Weight (kg)	ED (mSv)	DAP (Gycm ²)
cervical spine AP	37	66	0.087	0.41
cervical spine AP	38	55	0.008	0.04
cervical spine AP	37	100	0.041	0.20
cervical spine AP	43	78	0.014	0.07
cervical spine AP	42	99	0.049	0.23

Table (4B): The values of effective dose (ED) calculated using dosecal software and dose area product(DAP) for adult patients undergoing pelvis AP .

Examination	Age (y)	Weight (kg)	ED (mSv)	DAP (Gycm ²)
pelvis AP	52	91	0.820	3.66
pelvis AP	79	97	0.853	3.81
pelvis AP	27	67	0.124	0.56
pelvis AP	34	72	0.402	1.80
pelvis AP	63	70	0.499	2.23

Table (5B): The values of effective dose (ED) calculated using dosecal software and dosearea product (DAP) for adult patients undergoing lumbar spine AP.

Examination	Age (y)	Weight (kg)	ED (mSv)	DAP (Gycm ²)
lumbar spine AP	79	97	0.615	2.49
lumbar spine AP	41	73	0.392	1.88
lumbar spine AP	57	88	0.832	3.99
lumbar spine AP	71	52	0.119	0.57
lumbar spine AP	20	115	0.819	3.93
lumbar spine AP	55	95	0.790	3.79
lumbar spine AP	58	81	0.688	2.79
lumbar spine AP	48	76	0.076	0.36
lumbar spine AP	54	86	0.179	0.86

APPENDIX C

Descriptive Statistics

The statistical analyses in practice usually include two parts: statistical description and statistical inference. Statistical description is a kind of fundamental work for statistical inference, which describes the feature of the sample. The main forms for description are tables (such as frequency table), plots (such as scatter diagram, histogram) and numerical indexes (such as mean, standard deviation). There are many descriptive statistics, but not all are used regularly. The most commonly used descriptive statistics include frequency, sample mean, median, minimum, maximum, range, mode, variance, standard deviation.

- **Mean**

The average value is usually represented by the arithmetic mean. The mean is simply the sum of the values divided by the number of values.

$$\text{Mean } (\bar{x}) = \frac{\sum x}{n}$$

Where x denotes the values of the variable and n is the number of observations. The mean is denoted by \bar{x} .

- **Median**

It is the statistic most commonly used as a measure of central tendency. The median of a set of observations arranged in an increasing or decreasing order of magnitude is the middle value when the number of observations is odd or the arithmetic mean of the two middle values when the number of observations is even.

- **Range**

The range is defined as the difference between the maximal value and minimal value in the sample.

- **Quartiles**

Quartiles are values that divide a set of observations into 4 equal parts. These values, denoted by Q_1 , Q_2 and Q_3 , are such that 25% of the data falls below Q_1 , 50% falls below Q_2 and 75% falls below Q_3 .

- **Standard deviation (S.D)**

The standard deviation is square root of the arithmetic mean of the squared deviations of the individual observations from their mean (positive square root of the variance S^2). The Sample standard deviation is calculated using the following formula:

$$S.D = \sqrt{\frac{1}{N-1} \sum_{i=1}^N (X_i - \bar{X})^2}$$

Where $X_1, X_2, X_3, \dots, X_N$ are the sample data set, \bar{X} is the mean value of the sample data set and N is size of the sample data set.

- **Coefficient of Variation (C.V)**

The coefficient of variation expresses the standard deviation as a percentage of the sample mean. The coefficient of variation for any variable is given by:

$$C.V = \frac{SD}{Mean} \times 100$$